Quantifying the effects of offshore infrastructure on shelf sediment blue carbon dynamics

H. N. Woodward – Rowe

A thesis submitted for the degree of Doctor of Philosophy in Marine Biology.

School of Life Sciences

University of Essex

October 2025

Abstract

The effect of offshore infrastructure on shelf sediment blue carbon dynamics, is a key knowledge gap for blue carbon science, and shelf systems' ability to mitigate climate change. This thesis addresses this research gap, by quantifying sediment type, organic carbon stocks, accumulation rate, source and vulnerability in sediments surrounding two decommissioned oil and gas platforms (North West Hutton and Miller) in the North Sea. Overall, organic carbon stocks and sediment type varied distinctly between sites, with higher carbon stocks closer to Miller, but no relationship with distance at North West Hutton. Accumulation rates were refined to account for heavy metal contamination, which provides a new methodological framework of correcting for this issue in future blue carbon assessments. Using a novel binary mixing model application and hydrocarbon analysis, both sites presented organic carbon enrichment from anthropogenic sources, namely hydrocarbons, within close proximity (50 m) to the decommissioned sites. This highlights that sources of organic carbon other than marine may be present within shelf sediment stocks. A key recommendation from these studies is to take these measurements throughout the lifecycle of infrastructure; from pre and post construction, during operation, and pre and post decommissioning to better assess the varying impact of infrastructure. Finally, this thesis presents a methodological exploration to determine organic carbon mineralisation rates from acute disturbance events in sediments using oxygen consumption rates as a proxy. This provides a baseline for addressing the key question of carbon vulnerability from increasing infrastructure induced disturbance in a warming climate.

Acknowledgements

Firstly, thank you to the NERC-INSITE in partnership with the University of Essex and the UK National Decommissioning Centre as well as a case studentship from Shell for funding this work.

A huge thank you to the technicians at the University of Essex, namely John Green and Russell Smart, for tolerating my mess and my uncanny knack for breaking pieces of equipment. Also, I want to acknowledge the technical staff at Cefas, Terri and Lauren, for their huge effort in preparing many of my samples for radiochemical analysis. I also want to thank Clare Hynes, at Cefas, for running some of my samples to determine total hydrocarbon content.

To Natalie Hicks, Ruth Parker and Frank Dal-Molin, thank you for your understanding, support and ability to enlighten me through the course of this project. Also, a special mention to Ben Gregson for his wonderful mentorship.

To David Hughes for being a great research cruise partner and for helping me during fieldwork, lab work. Also thank you to Two Brews and my associated friends for their comradery which gave me many much needed breaks throughout writing my thesis.

To the other PGR's that have helped me throughout, from distracting office chats to witnessing all the trials a PhD student must go through. You made coming into the office more than just work but a real joy especially during the difficult times. A special mention to Alice Malcolm-McKay for her unwavering support and ability to pull off a chicken costume.

Finally, to my parents and my siblings, Bertie and Sophie for their ideas, support and love.

Table of Contents

Abbreviations

ANOVA	Analysis of variance
Ba	Barium
BC	Blue carbon
$CaCO_3$	Calcium carbonate
CF-CS	Constant flux constant sedimentation
CO_2	Carbon dioxide
CRI	Carbon reactivity index
DBD	Dry bulk density
DIC	Dissolved inorganic carbon
EEZ	Exclusive economic zone
GC-MS	Gas chromatography mass spectrometry
IC	Inorganic carbon
ICP-MS	Inductively coupled mass spectrometry
LSR	Linear sedimentation rate
MAR	Mass accumulation rate
MMS	Man-made structures
MPA	Marine protected area
NORM	Naturally occurring radioactive material
O&G	Oil and gas
OC	Organic carbon
OCAR	Organic carbon accumulation rate
OPSAR	Oslo and Paris commission
PAH	Polyaromatic hydrocarbons

Pb	Lead
PIC	Particulate inorganic carbon
PSA	Particle size analysis
SAR	Sediment accumulation rate
Sr	Strontium
TGA	Thermogravimetric analysis
THC	Total hydrocarbon content
TOC	Total organic carbon
UVF	Ultra-violet fluorescence spectrometry
^{137}Cs	Caesium-137
^{210}Pb	Lead-210
^{226}Ra	Radium-226
^{226}Rn	Radon-226

Chapter 1: The biogeochemistry of North Sea shelf sediments: quantifying carbon stocks and assessing the impacts of anthropogenic activities

1.1 Introduction to Blue Carbon

Blue Carbon refers to the organic carbon (OC) that is captured and stored in marine and coastal ecosystems (Alongi, 2020; Lovelock & Duarte, 2019; Macreadie et al., 2019), and is stored for long timescales (decades to geological) (Howard et al., 2023). The term 'Blue Carbon' was first used to describe the ability of coastal ecosystems to sequester significantly higher rates of carbon than terrestrial forests per unit area (Nellemann et al., 2009), highlighting its potential for climate mitigation (Duarte et al., 2013; McLeod et al., 2011). Initially the definition was restricted to three vegetated coastal ecosystems identified as major carbon sinks: mangrove forests (Alongi, 2012, 2020; Lovelock & Duarte, 2019; Moritsch et al., 2021),; seagrass meadows (Duarte et al., 2013; Greiner et al., 2013; Moritsch et al., 2025); and saltmarshes (Gore et al., 2024; McMahon et al., 2023; Perera et al., 2022). More recently, shelf sediments ecosystems (Luisetti et al., 2020), a non-vegetated habitat, have been highlighted as a store of OC due to their vast spatial extent and depositional environments (Diesing et al., 2017; Diesing et al., 2024; Legge et al., 2020), alongside other 'emerging' habitats such as intertidal sediments (Howard et al., 2023).

Blue Carbon (BC) is a relatively new research topic, which has led to varied definitions, from the initial definition of marine habitats that take up and store carbon (Nellemann et al., 2009), to the current emphasis on the long-term storage of carbon (Lovelock & Duarte, 2019). For the purpose of this thesis, the definition of Blue Carbon will be aligned with the IPCC (2021) and Howard et al. (2023), which is organic carbon that is stored in the marine environment on a long term basis, and that is amenable to management.

1.1.1. Global carbon stocks within marine sediment

Marine sediments represent the largest global stores of OC due to their vast spatial extent and high concentration of carbon stocks (Atwood et al., 2020; Mariani et al., 2020). Global marine sedimentary carbon stocks store an estimated 2,322 ± 83 petagrams of carbon (Pg C) in the top metre of sediment, with highest carbon stocks located in abyssal/basin zones (177-1898 Pg C) followed by continental slopes (164 - 175 Pg C) (Atwood et al., 2020). It is important to note, that these estimates however do vary largely depending on the sediment depths to which carbon is measured or calculated; these range from 0-2 cm (Smeaton, Hunt, et al., 2021), 0-5 cm (Lee et al., 2019), 0-10 cm, to 1 m (Atwood et al., 2020). Consequently, carbon stock estimates are frequently derived from carbon content only determined from surface layers and extrapolated to the desired depth (Smeaton, Hunt, et al., 2021). If left undisturbed, these OC stocks buried deep within marine sediment can persist for 1000's of years (Middelburg, 2018).

Carbon storage "hotspots" can be found throughout the ocean, including on coastal margins due to high primary productivity from both terrestrial and oceanic sources (Ausín et al., 2021; Bianchi et al., 2018). Glacial troughs also serve as hotspots due to high deposition and low temperatures (Diesing et al., 2024), as do areas of deposition in continental shelves such as mud depocenters (Porz et al., 2021) including the Western Irish Sea Mud Belt (Ward et al., 2025). Continental shelf sediments are particularly important as these areas contain an estimated 80% of all OC buried in marine sediment (Burdige, 2007). This is attributed to their proximity to large river systems which input a vast amount of terrestrial carbon. Despite their importance, global annual burial within continental shelf sediment (0.12 – 0.35 Gt OC $year^{-1}$) remain poorly constrained (Burdige, 2007; Hedges & Keil, 1995; Lee et al., 2019). Although the North Sea has high levels of uncertainty for carbon stock estimates (Atwood et al., 2020), it is the largest carbon stock in the North West European Shelf (Legge et al, 2020).

1.1.2. Economic value of blue carbon

The potential for using blue carbon ecosystems for climate mitigation has also gained significant interest from outside the scientific community, such as the private sector (through carbon credit schemes and net zero targets), conservation non-government organisations, international bodies, and governments all of whom recognise the potential to offset carbon emissions through the protection or restoration of BC habitats (Lovelock & Duarte, 2019; Macreadie et al., 2019). This increasing interest has led to the monetisation of blue carbon wealth as a tool to highlight its importance and drive policy change (Luisetti et al., 2019). The three traditional Blue Carbon coastal ecosystems, (mangroves, seagrass meadows, and saltmarshes) contribute $190.67 +/- 30 billion per year to global blue carbon wealth (Bertram et al., 2021) with nations such as Australia, Indonesia, and Cuba having the highest contributions. The economic impact of carbon loss can be substantial; for example, damage to UK coastal and shelf sediment ecosystems over a 25 year period through human pressures could have a cost as high as $12.5 billion for carbon storage loss (Luisetti et al., 2019). However, there are significant gaps in blue carbon accounting, as systems like continental shelf sediments are difficult to manage due to their transboundary nature, and the scientific knowledge required to robustly assess their carbon sequestration and storage potential is often lacking (Luisetti et al., 2020).

1.1.3. Climate mitigation and policy

Blue carbon ecosystems provide a climate change mitigation solution through two management pathways. Firstly, through conservation to reduce the potential greenhouse gas emissions associated with the loss and degradation of systems and secondly, through restoration to increase their carbon sequestration potential (Williamson & Gattuso, 2022). Therefore, blue carbon ecosystems can provide a nature based solution to climate change if managed correctly as significant OC sinks (Nellemann et al., 2009). These benefits could

contribute to global initiatives and agreements which have set ambitious goals to limit emissions. In 2015, under the Paris Climate Agreement, a target was set to limit global warming to 2 degrees Celsius (˚C) by 2050 (Glanemann et al., 2020). Crucially, the agreement explicitly noted the importance of "ensuring the integrity of all ecosystems, including oceans, and the protection of biodiversity" (Herr et al., 2017). The Paris Agreement also requires participating nations to work towards Nationally Determined Contributions, which can include restoration or enhancement of carbon sequestering marine ecosystems (Williamson & Gattuso, 2022). While this framework has the scope to include blue carbon ecosystems, significant uncertainties remain regarding their carbon burial rates, transport and vulnerability to future climate change for many systems (Williamson & Gattuso, 2022).

For coastal systems, where the carbon storage capacity is better defined, there have been restoration and conservation efforts of these blue carbon ecosystems across the world, particularly in Australia where the Emission Reduction Fund, and the research agenda on Negative Emissions Technologies and Reliable Sequestration have been recently launched (Bertram et al., 2021). However, for shelf sediments, carbon dynamics are less understood with even greater degrees of uncertainty for burial terms (Graves et al., 2022). Shelf seas should not only be valued for their potential carbon storage, they also provide a variety of valuable ecosystems services including biodiversity enhancement (Ellingsen, 2001), fisheries provisioning (Branch et al., 2011), and offshore energy production from oil and gas to renewables (Bailey et al., 2014; Martins et al., 2023). These services highlight the intensity of human induced pressure on shelf sediments, therefore determining these potential pressures effect on sediment blue carbon dynamics is critical and timely.

1.2 Shelf sediment biogeochemistry

The continental shelf is a submerged gently sloping landmass that extends from a continent's coastline to a point known as the shelf break, where the seafloor begins to descend more steeply into the deep ocean (Emery, 1969). Despite only accounting for 10% of the global ocean area, continental shelf seas contribute 50% and 80% of the OC delivery to the deep ocean and burial in sediments respectively (Bauer et al., 2013; Laruelle et al., 2018). Organic carbon captured through oceanic photosynthesis (e.g. phytoplankton) is usually remineralised in the water column or sediment surface, with less than 99.5% ending in burial in sediments (Burdige, 2007). OC in sediments is derived from both organic marine sources such as phytoplankton as well as terrestrially derived sources (LaRowe et al., 2020), depending on proximity to the coast. When OC reaches the sediment surface, at the sediment-water interface, diagenetic processes (breakdown and remineralisation of carbon) begins, driven by the microbial communities (Azam et al., 1993; Hoshino et al., 2020; Legendre et al., 2015). Despite the ubiquitous presence of a sediment-water interface across much of the global ocean, where there is a sedimentary seabed, the early diagenetic processes that occur remain poorly understood and are associated with high uncertainty (Soetaert et al., 1996; Soetaert et al., 2000).

The sediment-water interface is one of the largest interfaces in the world (Middelburg, 2018) and processes at this boundary determine whether the remains from organisms are remineralised and returned to the short-term biosphere or are stored within the long-term geosphere (Middelburg, 2018).

1.2.1. Vertical ocean carbon pumps

Carbon is transported to the sediment through multiple mechanisms, including the biological carbon pump (also known as the continental shelf pump) (Thomas et al., 2004), the oceanic carbonate pump (Mitchell et al., 2017) and the solubility pump (Legendre et al., 2015).

The biological carbon pump is the mechanism of shelf seas taking up atmospheric CO_2 through high biological activity (photosynthesis) and subsequent drawdown to the subsurface layer (De La Rocha & Passow, 2007). The outflow of this CO_2 rich layer is transferred to intermediate layers of the ocean (through consumption through grazing or ingestion) and eventually a small portion is exported to the sediment (in the form of detritus or faecal particles) (Burdige, 2007). As the OC moves through these processes in the water column, much of this is converted back into CO_2 through bacterial oxidation (Mucci et al., 2000). Finally, between 1 and 10% of this primary production from the surface layer is received by shelf sediments (Hedges & Keil, 1995) and this carbon is either recycled, remineralised or buried (Soetaert et al., 1996).

The oceanic carbonate pump is the mechanism by which particulate inorganic carbon (PIC) is transported to the seafloor (Mitchell et al., 2017). This is also known as the carbonate counter pump as the precipitation of $CaCO_3$ is followed by the release of CO_2 (Legendre et al., 2015). PIC primarily comes from shell and skeletal growing organisms such as coccolithophores and diatoms within the plankton; following mortality of these organisms, these hard parts aid faster sinking through the water column to the seafloor (Mitchell et al., 2017). During this process, $CaCO_3$ is partially dissolved, and releases CO_2 back to the surrounding water and then may eventually release this to the atmosphere (Legendre et al., 2015). The remainder of the $CaCO_3$ is deposited on the seafloor where it may be stored (Mitchell et al., 2017).

The solubility pump transports dissolved atmospheric CO_2 to the deep ocean. This process begins with the natural diffusion of CO_2 from the atmosphere into the surface waters (Falkowski et al., 2000). Once dissolved, atmospheric CO_2 combines with water molecules to produce carbonate and bicarbonate ions as well as protons (Falkowski et al., 2000). At this point, dissolved CO_2 may be released to the atmosphere if there is higher CO_2 in the surface waters than in the overlying atmosphere. However, currently, atmospheric CO_2 is higher than in surface waters, causing uptake into the ocean (Sabine et al., 2004). The effectiveness of the

solubility pump relies upon global thermohaline circulation and fluctuations in ocean ventilation (Lynch-Stieglitz et al., 1995). Seasonal changes alter the solubility of CO_2 as colder and less saline waters cause CO_2 to become more soluble. Hence, atmospheric CO_2 sequestration is controlled by the formation of high latitude cold, dense, water masses which sink dissolved CO_2 laterally, essentially preventing re-equilibrium at surface water to atmospheric inferences for hundreds of years (Falkowski et al., 2000; Legendre et al., 2015).

All three of the oceanic carbon pumps transfer carbon from the surface layer to deep waters below the maximum depth of the permanent pycnocline (in open ocean) and finally to the sediment surface.

1.2.2. Carbon dynamics, composition and interactions in shelf sediment

Continental shelf sediments rapidly accumulate and turn over OC (Diesing et al., 2021; Legge et al., 2020). Organic matter composition and content in marine sediment are determined by a variety of abiotic and biotic factors such as utilisation and degradation rates, oxygen availability (Glud et al., 2016; Hartnett et al., 1998), temperature (Ausín et al., 2021; De Haas, 1997), in situ production, lateral advection, allochthonous input (Mucci et al., 2000), sediment type (Bianchi et al., 2018), and interactions with minerals (Mayer, 1994). .

When particulate OC (POC) settles on the seafloor, any portion that is not consumed on the sediment surface is entrained in the sediment through bioturbation and burial (Bianchi et al., 2021; Epstein et al., 2022). The more easily degradable organic compounds within the settling POC are mineralised into inorganic solutes (usually dissolved inorganic carbon, DIC), which causes a decrease in PIC content over time (Burdige, 2007). Overall, the accumulation rate of POC in marine sediment is subject to the balance of the supply of POC from the water column and the benthic remineralisation rate (Diesing et al., 2017). The seabed is heterogenous, so different areas have varying abilities to accumulate and cycle carbon depending on multiple

factors (including sediment type). This can be used to inform the modelling of carbon stocks in continental shelves. Previous modelling work considered different variables for organic carbon content, such as mud content in sediment, distance to closest shoreline and bottom water temperature (Diesing et al., 2017). However, using limited data to extrapolate carbon content across vast areas can lead to inaccuracies.

Carbon stocks or 'storage' represent a snapshot of OC to a given sediment depth (Graves et al., 2022), however, determining how these will change temporally relies on determining rates of accumulation and burial (Ausín et al., 2021; Bianchi et al., 2018). OC accumulation rates are how much organic carbon is deposited on the sediment through sedimentation of OC attached particles (Arias-Ortiz et al., 2018). This is distinct from sequestration or burial which requires OC to reach a depth where it is unlikely to be disturbed, representing climate relevant OC (Graves et al., 2022) (Figure 1). Determining these differences is vital, especially when interpreting the consequences of impact. For example, if a carbon stock is disturbed this does not necessarily infer carbon impact. If the mechanisms which create these carbon stocks (input terms) or deep, previously buried or sequestered stocks are impacted this would have greater long-term effect on sediment ability to mitigate climate change.

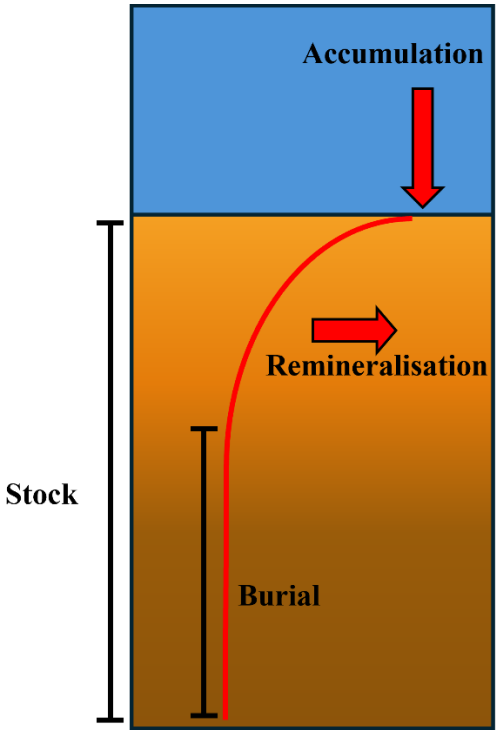

Figure 1: A conceptual model describing key terms of organic carbon dynamics on the seafloor. Accumulation indicates the sedimentation of organic carbon onto sediments (typically from marine snow), the red line shows typical OC content (%), remineralisation is organic carbon that is broken down into CO_2. The burial (sequestration) is organic carbon that is as deep as to not be disturbed, and stock indicates the total amount of OC within a given depth range.

Burial efficiency of carbon is strongly linked to benthic oxygen concentrations and the sum of diffusive and faunal mediated uptake (Glud et al., 2016; Soetaert et al., 2000). OC is mineralised aerobically when oxygen penetrates sediment (Epstein et al., 2022; Porz et al., 2024). Oxygen's ability to permeate into porewater spaces decreases within increasing depth in the sediment (strongly linked to sediment type, or grain size), so there is a vertical gradient of varying mineralization pathways linked to oxygen availability (Soetaert, Herman and Middelburg, 1996). This is coupled to the carbon storage capacity through the physical characteristics of sediment. Surface sediments (mm to cm's, depending on sediment type) are typically oxic, so much of the carbon in these oxic layers is quickly remineralised by microbial processes.

Shelf sediments are a mixture of coarser permeable sandy sediment and fine-grained muddy sediment, with sandy sediments making up an estimated 70% of coastal shelves (Huettel et al., 2014). The high permeability of these sediments causes them to be susceptible to biological and hydrodynamic pressures which in turn, causes circulation of water throughout the sediment profile (Rusch et al., 2006). This circulation increases oxygen availability and therefore carbon mineralisation, as these sediments are well flushed and oxic (D'Hondt et al., 2015; Hulthe et al., 1998; Kristensen, 2000). Permeable sandy sediment characteristically has higher inorganic carbon (IC) and lower OC concentrations compared to muddy cohesive sediment (Legge et al., 2020). Cohesive muddy sediment has higher oxygen uptake rates (greater oxygen demand for microbial processes) when compared to permeable sediment (Diesing et al., 2017). As cohesive sediments have less space for water to flow through, less oxygen can penetrate at depth within the sediments, decreasing the oxidation and subsequent mineralisation of organic matter (Smeaton, Hunt, et al., 2021). This causes finer sediments to store, on average, more OC due to lower mineralisation rates in the much smaller oxic layers, and slower mineralisation through anaerobic pathways (Leipe et al., 2011). For example, Leipe et al (2011) found notably higher POC concentrations (10-17 $mg.cm^{-3}$) in sediment with 60 - 100% mud content when compared to sandier sediments in the Baltic Sea. The oxic status of sediments can also be influenced with the presence of macrofauna, when bioirrigation and bioturbation may alter the area of oxic mineralisation by introducing oxygen deeper into the sediment (Middelburg, 2019).

1.2.3. Depth profiles and accumulation rates

The distribution of OC content at varying depths of shelf sediment is a relatively well-researched topic, often through measuring carbon content at regular depths from sediment cores. Generally, global continental shelf sediment show a loss of OC with increasing depth due to a relationship with sediment surface area (Figure 1) (Burdige, 2007). Mayer (1994)

hypothesised that the observed OC concentration decrease within sediment occurs as saturation of adsorption sites within small pores of sediment exclude hydrolytic enzymes which stops the mineralisation of organic matter (Mayer, 1994). However, deeper in sediments, OC which is not oxidised can still be microbially reduced, for example the process of methanogenesis which converts this into methane (CH_4) and fuels the slow build-up of methane hydrates under some conditions (LaRowe et al., 2020). For example, Masqué et al. (2002) found that mixing at the sediment water interface influences deeper OC concentration, which then stabilised to consistent low OC concentrations at depth (Figure 2). Similarly, Mucci et al. found OC content decreases with depth within sediment cores taken from eastern Canada. However, within these same cores, inorganic carbon content varied slightly with increasing levels at depths due to precipitation from the initial loss at the surface interface (Mucci et al., 2000).

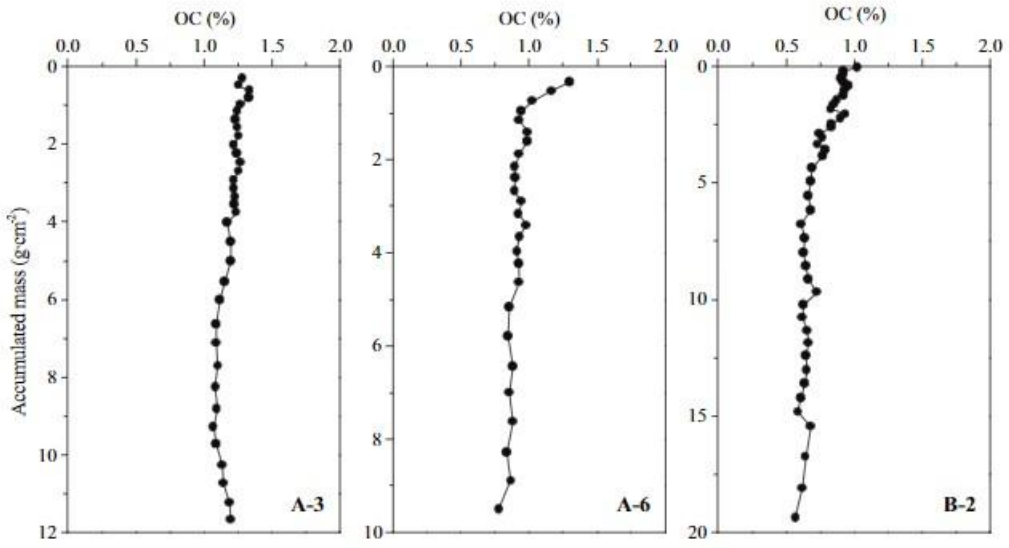

Figure 2. OC profiles in relation to mass accumulation in three core samples taken from the western Bransfield Strait, Antarctica, showing the relative stability in OC concentration in deeper sediment layers (Masque et al., 2002).

OC accumulation rates (OCARs) are used to determine how carbon stocks will vary temporally (Arias-Ortiz et al., 2018) throughout marine systems. In shelf sediments these rates are typically low due to high rates of lateral transport, permeable sediments and high POC turnover in the water column (Dunne et al., 2007). However there are sites in shelf seas which

exhibit higher than average carbon accumulation including depositional areas such as glacial troughs and trenches (Diesing et al., 2024) and muddy depocenters such as the Western Irish Sea Mud Belt (Ward et al., 2025) .

1.2.4. The effect of anthropogenic disturbance on carbon storage in shelf sediment

Continental shelf sediments face degradation from anthropogenic sources, including bottom trawling (Eigaard et al., 2017); oil, gas and mining exploration and drilling (Bull & Love, 2019; Jagerroos & Krause, 2016); as well as development for offshore energy from wind farms (Bailey et al., 2014) to oil and gas platforms (Bull & Love, 2019). These disturbances may potentially resuspend surface sediment, mixing it into the water column, which could expose organic matter to higher concentrations of oxygen and heterotrophic metabolism (Black et al., 2022) causing re-mineralisation of carbon stored in sediment into CO_2 (Sciberras et al., 2016). A recent study suggested this could contribute to carbon emissions and ocean acidification (Sala et al., 2021). This hypothesis has met widespread criticism, as water column re-mineralisation of carbon will not automatically link to increases in the atmosphere, and the majority of this will be absorbed into the carbonate system within the water column relatively quickly (Mitchell et al., 2017). Additionally, the degradation factors of organic matter within sediments used with these modelling estimations in the Sala et al 2021 study, and the following Atwood et al 2024 study, are likely overestimated (Hiddink et al., 2023). However, long term degradation of marine ecosystems has caused concern that these habitats could eventually lead to these systems becoming a source of emitted CO_2 (Atwood et al., 2024; Mariani et al., 2020).

1.2.4.1. Trawling effect on carbon storage

Surface sediment in shelf systems that experiences rapid oxygen depletion at depth and high sedimentation rates are also the same sediments subject to anthropogenic disturbance such as bottom trawling for commercial fisheries (Sala et al., 2021). Bottom trawling fisheries are widespread within coastal shelf seas and provide 23% of global fish landings (De Borger,

Tiano, et al., 2021). These involve the dragging of nets and attached weights along the seabed to trap fish within (Depestele et al., 2016). Trawling impacts on mineralisation of OC within shelf sediment are not well constrained (Black et al., 2022; De Borger, Tiano, et al., 2021; Palanques et al., 2014) with mixed results in various studies (J. Tiano et al., 2024). There are two sides of this debate, some studies have found that trawling can increase carbon content in sediment (O'Neill & Summerbell, 2011; Pusceddu et al., 2005) whereas others have found contrasting results (De Borger, Tiano, et al., 2021; Paradis et al., 2021). A review by Epstein et al. (2022) observed that 51% of studies found no significant effect of demersal fishing on OC content within sediment, 41% reported lower OC content and 8% reported higher OC content.

Trawling can affect benthic metabolism by resuspending organic matter, causing mortality of macrofauna, and changing physical sediment structure (Dounas et al., 2007; Eigaard et al., 2017). Using modelling, de Borger *et al.* (2021) demonstrated in five sedimentary environments with different gear intensities that trawling events caused significantly lower OC in the top 10 cm of sediment (62-96% reduction). Simulated trawling in this study depleted and redistributed OC near the sediment-water interface and increased oxygen availability in the sediment provoking higher rates of mineralisation (De Borger, Tiano, et al., 2021). These results highlight that sediment mixing alone could increase OC content at the mixing zone, however continuous trawling events causing the removal and mortality of bioturbators would redistribute OC towards the sediment water interface allowing increased remineralisation by oxidized reactants (O_2 and NO_3^-) (De Borger, Tiano, et al., 2021). Similarly, sediment cores from the Gulf of Castellammare in the southwestern Mediterranean analysed by Paradis et al (2019) showed that trawled sites had organic matter which were between 20 % and 60 % lower than untrawled sites. However, this was due to trawling enhanced remineralisation and sedimentation rates due to the arrival of fresh particles in a

sedimentary system which was previously deprived of OC. This study, similar, to de Borger *et al*, concluded that the effect of trawling can initially be lessened by the sedimentation of nutrient rich organic matter but are quickly eroded when continuously trawled (Paradis et al., 2019).

Conversely, several studies have concluded that bottom trawling may increase OC content of sediment. For example, Palanques et al (2014) sampled sediment cores at the Ebroi prodeltaic mud belt fishing ground (NW Mediterranean) and found OC showed an upward increasing gradient and higher values at trawled sites. A hypothesised cause of this trend is that trawling gears cause entrainment of sediment in their wake which releases significant amount of previously trapped bottom nutrients which contributes to primary production of phytoplankton and subsequent carbon pump (O'Neill & Summerbell, 2011). Similarly, Pusceddu et al. (2005) found total OC concentrations within sediment increased significantly following trawling events in the Thermaikos Guld in the Aegean Sea compared to control sites. Sediment properties did not vary significantly during this study so changes in OC content were attributed to organic matter uplift by physical disturbance of sediment from deeper sediment layers (Pusceddu et al., 2005). However, there is still a large uncertainty regarding trawling effects on OC content within sediment, particularly depending on gear type and frequency of trawling activities (Epstein et al., 2022).

Nevertheless, recent attention is being paid to the potential protection of sedimentary shelf sediment (Burrows et al., 2021; Epstein & Roberts, 2022). For example, Epstein and Roberts (2022) identified priority seabed areas within the UK Exclusive Economic Zone (EEZ) to be targeted for precautionary carbon management which could reduce carbon disturbance by a minimum of 27% and up to 67% by ceasing all mobile bottom fishing. However, the effect of bottom trawling on sedimentary carbon stocks and subsequent emissions is still relatively unknown (Epstein et al., 2022; Hiddink et al., 2023).

Further than just changing in sediment OC content, a rising concern by scientists and governments is the potential emission of stored CO_2 from the seabed back to the atmosphere (Atwood et al., 2024). This potential for mineralisation and subsequent emissions is fundamentally linked to the vulnerability (reactivity or lability) of OC within sediments (Figure 1). The majority of the OC within shelf sediments is thought to be unreactive, based on current measuring techniques (Smeaton & Austin, 2022a). Therefore, sequential resuspension is unlikely to cause the mineralisation of this 'inactive' POC to DIC. However, this carbon vulnerability remains a large research gap, as does how to accurately determine carbon reactivity, or *in situ* mineralisation rates of OC within different sediment types.

1.2.5. The North Sea

The North Sea has historically experienced widespread anthropogenic influences (Ducrotoy et al., 2000) from food production (Eigaard et al., 2017; Roberts, 2007) to the introduction of energy infrastructure (Martins et al., 2023). The North Sea provides economic, cultural and social services which are important to not only the UK but also the six other European countries that have exclusive economic zones within its borders. This poses management obstacles, more recently due to the UK's departure from the European Union causing policy disagreements between stakeholder countries regarding future fishing rights (Phillipson & Symes, 2018). There are other legislative guidelines that do certain the North Sea such as the Oslo and Paris commission (OSPAR) (see section 3.2 for further details). Nevertheless an integrated management strategy my be vital for climate mitigation through effective seabed carbon management.

1.2.5.1. Physical and biological characteristics

The North Sea has an open boundary to the North Atlantic Shelf and is located on the northwest European continental shelf (Thomas et al., 2005). In the southern part of the North Sea, the English Channel is another connection to the North Atlantic Ocean. The North Sea

borders seven countries including: the United Kingdom, France, Belgium, Netherlands, Germany, Denmark, and Norway (Figure 3). It is characterised as being a tidally dominated marginal shelf sea, a surface area of 575,300 km^2, with a shallow average depth of 74 m and a volume of 42,294 km^3 (Otto et al., 1990). Water circulation is dominated by an anticlockwise 'u-shape' of North Atlantic Ocean water due to currents from the Shetland Channel and the Faire Island Channel and flowing up through the Norwegian trench boundary (Thomas et al., 2004). In winter, the water column is completely mixed by waves and during the summer it is stratified in the northern regions by rising surface temperatures (Thompson et al., 2011).

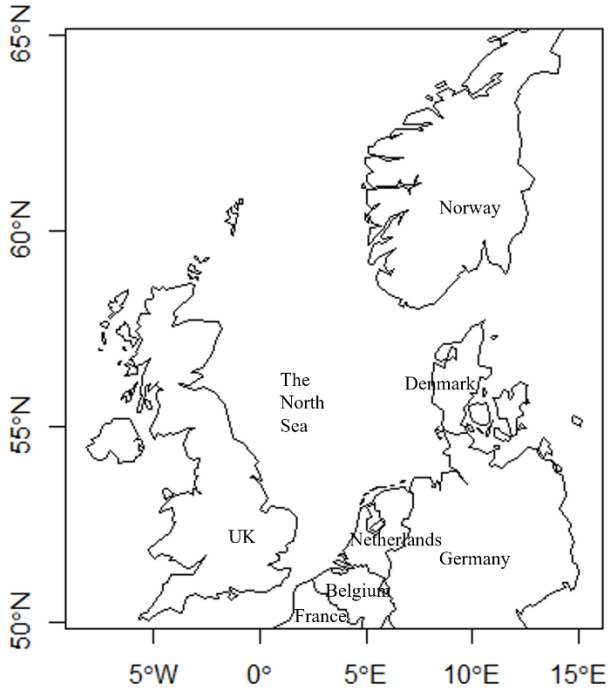

Figure 3: The North Sea and bordering nations, United Kingdom, France, Belgium, Netherlands, Germany, Denmark, and Norway.

The benthic environment of the North Sea is a mix of different sediment types, predominantly sand/muddy sand but also coarse sediment and muddy/sandy mud (Stephens & Diesing, 2015) which plays host to between three to five thousand species (Heip & Craeymeersch, 1995; Hiddink et al., 2015). This habitat has vertical gradients over scaling

millimetres to centimetres (Heip & Craeymeersch, 1995). In deeper waters, sediments are predominantly fine-grain beds compared to shallower areas which consist of gravel and sandbanks (Thompson et al., 2011). Sediment turnover is dominated by waves in the deeper areas of the North Sea and by tidal forcing in the Southern Bight (Thompson et al., 2011). Oxygen profiles within North Sea sediment vary with sediment type. In sandy sediment, oxygen profiles indicate enhanced diffusion with highest effective diffusion coefficients reported at non-depositional environments with low diffusive oxygen fluxes and deeper penetration depths of oxygen (Lohse et al., 1996).

1.2.5.2. Quantification of carbon stocks

Several benthic, pelagic, and coastal carbon stock estimations have been made for the North Sea (Diesing et al., 2021), the Northwest European continental shelf zone (Diesing et al., 2017; Legge et al., 2020) and the UK economic exclusion zone (EEZ) (Burrows et al., 2021; Luisetti et al., 2019; Smeaton, Hunt, et al., 2021). Overall, sediments in the North Sea primarily are depleted in OC due to having a high sand content (Diesing et al., 2021). Using a Random Forest model, and predictor variables, Diesing et al. (2017) predicted the mass of POC stored in the top 10cm of shelf sediment of the Northwest European continental shelf area to be between 230-882 Mt with the most likely estimate to be on the order of 476 Mt. This estimate found the largest POC stock was related to the widespread occurrence of coarse grained sediment with high dry bulk densities (Diesing et al., 2017). Similarly, Legge et al (2020) estimated that the Northwest European continental shelf sediment stored between 520 – 1600 10^{12}mol of carbon in the top 10cm of sediment, which was the largest stock of carbon when compared to coastal and pelagic due to its larger spatial extent. Focusing on the UK's EEZ, Smeaton et al (2021) estimated that the top 10cm of sediment contained 524 ± 68 Mt of OC and 2582 ± 168 Mt of IC (extrapolated from 2cm depth measurements). Sediment maps are often created to visually show the distribution of carbon stocks, highlighting OC hotspots

within coastal muds, fjords and estuaries and high IC accumulation zones around Shetland, Orkney, and the Southwest of England due to tidal sweeping (Smeaton et al., 2021). Finally, Diesing et al (2021) estimated OC densities of the North Sea and Skagerrak (Figure 4) to be 230.5 ± 134.5 10^{12}g C of which, 26% came from the Norwegian trough.

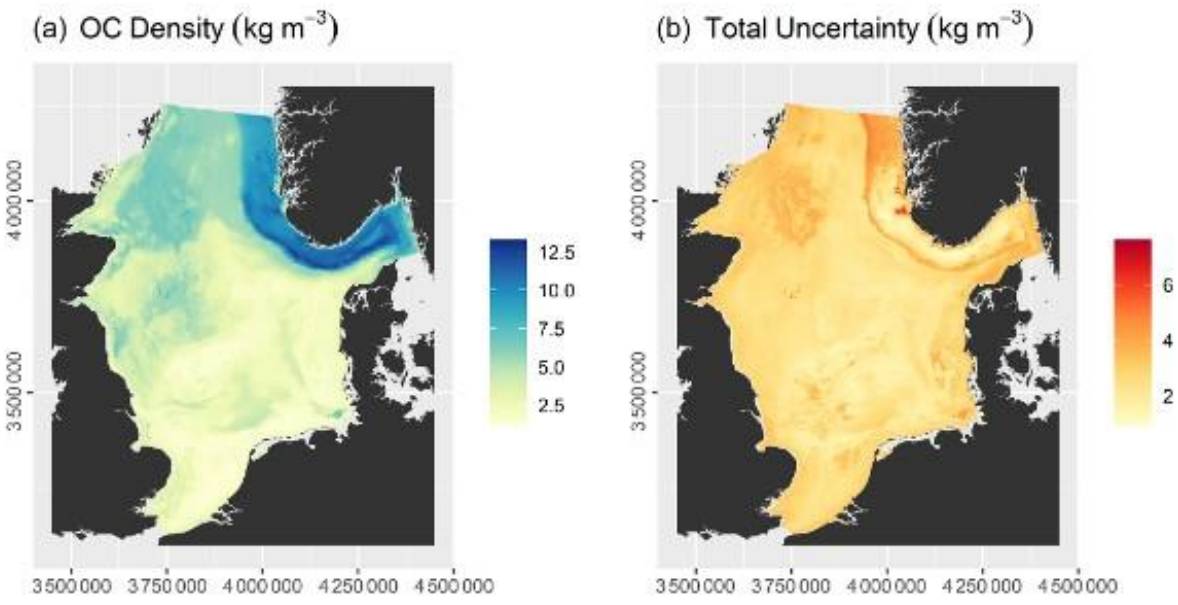

Figure 4. Predicted a) OC density (kg m^{-3}) with b) total uncertainty (kg m^{-3}) of the North Sea and Skagerrak (Diesing et al., 2021).

1.2.5.3. Anthropogenic activity

The North Sea has been subject to intensive anthropogenic activity over the past century, including fishing activities (Eigaard et al., 2017; Engelhard et al., 2014), extractive uses (Birchenough & Degraer, 2020; Fortune & Paterson, 2020) and climate change pressure (Weinert et al., 2021). For example, Atlantic cod stocks within the North Sea have seen reductions in size to historically low levels since the 1960's (Engelhard et al., 2014) attributed to extensive overfishing and rising sea surface temperatures (Thurstan, Brockington and Roberts, 2010). This long-term pressure is evidenced by a 94% reduction in landings per unit of fishing power in UK bottom trawling fisheries over the last 118 years indicating dramatic changes in seabed ecosystems, benthic habitat and biogeochemistry (Thurstan et al., 2010).

Recently, it has been highlighted that bottom trawling of shelf sediment seas in the North Sea can occur more than 10 times per year over the same seabed (De Borger, Tiano, et al., 2021; Eigaard et al., 2017).

In addition to fishing, the North Sea has been heavily developed by infrastructure with over 1350 current oil and gas platforms (Fortune & Paterson, 2020) and rapidly expanding number of offshore wind farms (De Borger, Ivanov, et al., 2021; G.W.E.C, 2023) due to rising energy demands (Putuhena et al., 2023). These man-made structures can have varied effects on the environment, including reducing invertebrate diversity (Chen et al., 2024), increasing larval migration (Coolen, Boon, et al., 2020; Coolen, Van Der Weide, et al., 2020) and altering fouling assemblages (Van Der Stap et al., 2016).

1.2.5.4.Effects of climate change

Sea surface temperatures have increased above global averages with an increase of ~0.06 ˚C.yr^{-1} compared to the global average of 0.017 ± 0.005 ˚C.yr^{-1} (Weinert et al., 2021). Benthic communities and habitats are key indicators of climate induced change due to these organisms being sessile, having low mobility and long lifespans (Ellingsen, 2002), allowing changes to be seen with relative ease (Hiddink et al., 2015). The North Sea's benthic environment is under heightened pressure due to a 1.6 °C increase in near-bottom temperature between 1980 and 2004 (Weinert et al., 2021). As a result, 65 benthic species showed a distribution centroid shift between 3.8 and 7.3 km yr^{-1} northwest during temperature changes from 1986 to 2000 in the North Sea (Hiddink et al., 2015). Furthermore, temperature also drives many microbial process, including those which turnover organic carbon (Malinverno & Martinez, 2015). For example, changes in bottom temperatures in sediments have been found to alter microbial community structures and subsequent biogeochemical processes (Hicks et al., 2017). These rapid temperature shifts and the resulting redistribution of benthic species

underscore how climate change could alter the biogeochemical cycling in North Sea shelf sediments.

1.3 Man-Made Structures

Man-Made Structures (MMS's) are artificial structures present in the marine environment, this includes artificial reefs, piers, jetties, shipwrecks, oil and gas infrastructure and renewable energy structures (Elrick-Barr et al., 2022). Coastal MMS's including dikes, groynes, aquaculture constructions and buoys have been present for centuries (Birchenough & Degraer, 2020). However, continued growth in blue economy has led to a rise in offshore renewable energy installation and aquaculture, and there is a predicted rise of global spatial coverage of MMS's from 32,000 km^2 in 2018 to 39,400 km^2 by 2028 (Bugnot et al., 2021). Coastal and marine developments have been increasing in the face of rising energy demands causing the construction of both renewable energy structures (offshore windfarms) and extraction platforms (oil and gas) (Birchenough & Degraer, 2020) (Figure 5). Specifically, the offshore wind energy sector has increased worldwide with an annual growth rate of 24% between 2013 to 2019 (The Crown Estate, 2022). Offshore MMS's are composed of a substructure which are either concrete that persists on the seabed through its own weight (and subsequent gravity) (Wu et al., 2019) or steel jackets which have footing adhered to the seafloor (Techera & Chandler, 2015). Additionally, these usually are constructed with a topside structure above the water level such as an oil or gas platform or wind turbine (Techera and Chandler, 2015).

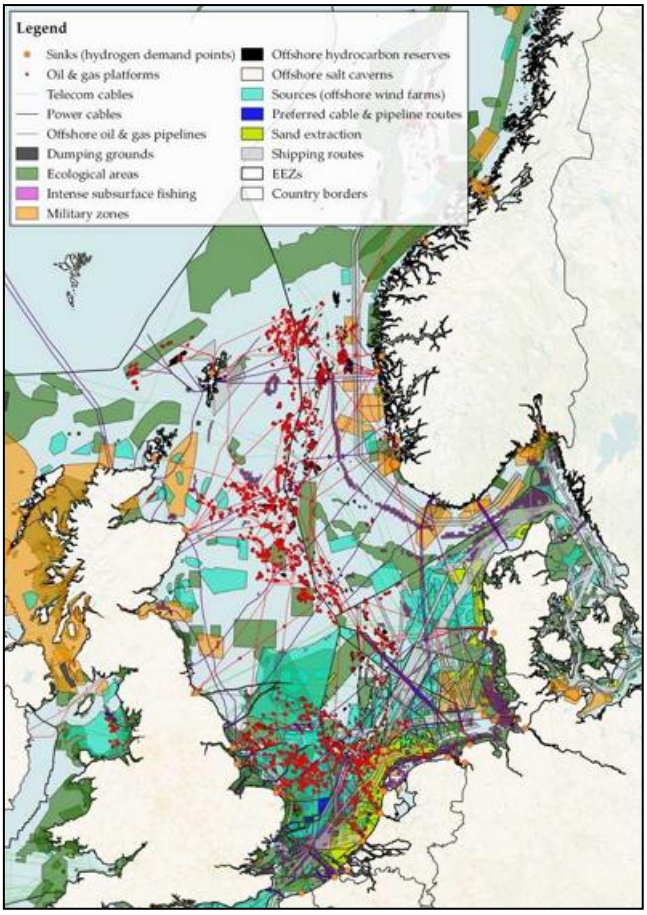

Figure 5: Anthropogenic activity and uses throughout the North Sea, including different offshore infrastructure. Taken from (Brosschot, 2022)

1.3.1. Effect of Man-Made Structures on the marine environment

Subsea MMS's in usually featureless soft sediment dominated environments introduce habitat heterogeneity by providing hard substrate throughout the whole water column (Todd et al., 2018). Offshore structures can support and develop significant diverse and abundant marine communities (Coolen, Van Der Weide, et al., 2020; Fowler et al., 2020; Schutter et al., 2019) which can include fish assemblages (Patterson & Tarnecki, 2016), fouling organisms (Coolen, Van Der Weide, et al., 2020), top level predators such as marine mammals, and soft and hard corals (Todd et al., 2018). MMS's can also impact the behaviour of fish assemblages by providing foraging and refuge areas (Paxton et al., 2020; Wright et al., 2020). For example, Wright et al (2020) demonstrated using fisheries surveys and electronic tagging that artificial

structures (O&G platforms and offshore wind) in the North Sea increase seasonal abundance of three fish species: cod (*Gadus morhua),* thornback ray (*Raja clavate)* and plaice (*Pleuronectes platessa)*. Atlantic cod showed increased abundance near cables, oil and gas platforms, wrecks and windfarm artificial reefs during intensive feeding periods higher prey abundance near these structures (Wright et al., 2020). While there is strong evidence that fish aggregate around these structures (Fujii & Jamieson, 2016), there is still debate as to whether this is a result of increased production (more fish being born) or simply attraction (fish being drawn to the structures from other areas) (Brickhill et al., 2005; Pickering & Whitmarsh, 1997). However, using remotely operated vehicle footage of oil and gas platforms in the North Sea, Todd et al (2018) found both cod and lumpsucker fish (*Cyclopterus lumpus)* use these structures for different stages of reproduction. This indicates that these structures can provide areas of fish production which has ecological and fisheries-related implications.

MMS's also provide increased connectivity for hard substrate adhering flora and fauna (Coolen, Boon, et al., 2020). These previously unavailable settlement areas provide 'stepping-stones' which connect habitats through migration of two or more generations (Fowler et al., 2020). The specific benthic and epifouling communities which are connected by these structures do not vary significantly between offshore windfarms and oil and gas platforms, with similar fauna being found at both sites (Coolen, Van Der Weide, et al., 2020). Most non sessile species do not inhabit MMS's for their whole life cycle but use the surrounding regions during different life stages (Fortune & Paterson, 2020). Also, species can use MMS's as spawning and setting locations to disperse larvae further beyond their previously limited range (Coolen, 2017). For example, Coolen et al. (2020) showed *Mytilus* spp. were able to reach locations 181 km from the nearest coastline after predictions that without MMS stepping-stones larvae could not migrate past 85 km from the coastline. However, this increased connectivity can have negative consequences, as MMS's can spread the distribution invasive non-native species

(Fortune & Paterson, 2020). For example, the invasive species *Caprella mutica* have been found on wind farm foundations in the North Sea alongside native species *Caprella linearis* (Coolen et al., 2016).

1.3.2. Effect of Man-Made Structures on the sedimentary blue carbon

The effect of MMS's on surrounding sediment carbon storage is a considerable research gap and refining knowledge in this area could provide evidence to support changes in their operational lifecycles. This includes construction of structures, their operation and their final decommissioning.

The construction of MMS's in the marine environment is likely to cause significant disturbance of sediment and the resuspension of stored carbon. Building offshore structures requires often extensive sediment movement from dredging for foundations (Schneider & Senders, 2010; Wu et al., 2019) to pile driving for monopiles (Hinzmann et al., 2018). As previously mentioned, OC disturbance might not directly cause remineralisation depending on the carbon's vulnerability (Smeaton & Austin, 2022a); however, this (potentially deep) excavation is likely to increase the chance of OC degradation of previously buried stocks. Conversely, during the operational period of offshore infrastructure, often these sites create *de facto* Marine Protected Areas (MPA's) with low levels of disturbance, often within an exclusion zone around the MMS, which can enhance biodiversity, particularly from attached fouling organisms (Heinatz & Scheffold, 2023). Fouling organisms can potentially enhance carbon flux from the water column to the sediment through the sinking of faeces or detritus (Krone et al., 2013). This extra fresh marine OC will promote higher levels of mineralisation (De Borger, Ivanov, et al., 2021) however, due to the vast quantity, some will likely be buried long term (Heinatz & Scheffold, 2023). This *de facto* MPA status around MMS's provides a potential to study the baseline carbon dynamics in the surrounding sediment, which has not been disturbed through trawling or other anthropogenic activities. Finally, decommissioning of

MMS's can cause additional disturbance with some techniques involving total removal of foundations and steel jackets (Birchenough & Degraer, 2020). Similar to construction, this decommissioning will likely disturb the accumulated carbon and potentially decrease stocks around these sites.

1.3.2.1. Oil and gas platforms

Oil and gas platforms in the North Sea provide artificial reefs with attachment opportunities for fouling organisms, particularly sessile epifauna in predominantly a soft sediment environment (Klunder et al., 2018; Maar et al., 2009). This epifauna (largely filter feeders) creates a "shadow" over the soft sediment habitat as the water column dynamics are changed by reducing food availability in the water column (Coates et al., 2014). The impact of these structures on sedimentary OC varies. Klunder et al (2018) found less OC in the sediment in the vicinity of the oil and gas platform L7A in the southern part of the North Sea either caused by the biofilter effect which depletes the organic content of the water or scouring of the sediment due to acceleration of the water flow. Conversely, the Ninian northern platform, in the North Sea, showed contrasting results of sedimentary OC content. The innermost sites to the platform had higher organic matter with percentages of 5.5 and 4.9% compared to sites at greater distance which ranged from 0.9 to 3.8% (CNR International, 2017). Similarly, sediment surrounding the Murchison platform, also in the North Sea, had higher OC at 250m and 500m sampling sites (3 and 4% respectively) when compared to all other sites to a distance of 8000m where all were below 1% (CNR International, 2013). Hypothesised causation of this was attributed to drilling activity at the platform which elevated the proportion of fine-grained sediment and organic matter content (CNR International, 2017).

1.3.2.2.Offshore wind farms

Conversely, the presence of MMS's such as offshore wind farms can increase organic matter content in surrounding sediment through the structures lifecycle and even following decommissioning (Heinatz & Scheffold, 2023). For example, Coates et al (2014) found organic matter content increased from 0.4 ± 0.01% at 100m to 2.5 ± 0.9% at 15m from turbine foundation. This increase is likely due to two factors. First, the epifauna that attach to the turbine foundations contribute organic matter through the sedimentation of detritus and faeces (Maar et al., 2009). Second, is the physical presence of the windfarm can increase mixing of seasonally stratified seas which can enhance sea surface primary productivity (Dorrell et al., 2022). Phytoplankton growth requires sunlight, CO_2, and nutrients (Falkowski et al., 2004). In naturally stratified seas, phytoplankton can grow into blooms in the well-lit surface waters, which are separated from the nutrient-rich bottom waters by a thermocline (Huppert et al., 2002). With increased offshore wind infrastructure, the wake enhancement can mix cold nutrient rich bottom water with warm surface water which is low in nutrients, creating an ideal layer for phytoplankton growth (Dorrell et al., 2022). Wind farms can also increase pelagic primary productivity due to the presence of epifauna such as *Mytilus edulis* (Slavik et al., 2017). With enhanced primary production, this could have some knock on effects on benthic carbon storage as more OC would sink through the water column and a percentage of this would be deposited on shelf sediment. While these pathways for enhanced OC storage would be present during the operational phase, the subsequent decommissioning could disturb this elevation OC stock. However, models from Heinatz and Scheffold (2023) demonstrate that due to the specific size of disturbance from decommissioning there could be up to 4.6 ± 1.4 times more OC in sediments following the entire lifecycle of these sites.

1.3.3. Decommissioning man-made structures in the North Sea

Many MMS's in the marine environment, including oil rigs and offshore wind farms, are in use for a specified operational period, after which they are required to be decommissioned (Fortune & Paterson, 2020). Currently, in the North Sea and the Northeast Atlantic, under the Oslo and Paris Commission (OSPAR), these have to be fully removed when being decommissioned, as decision 98/3 prohibits the 'dumping' of these structures at sea (OSPAR, 1998). The rationale behind complete removal of MMS's was heavily influenced by the 'Brent Spar' event in 1995, in which Greenpeace protesters occupied the oil and gas installation for 24 days after plans to dispose of the facility in a deep-water trench were announced (Ounanian et al., 2020). These actions captured significant media attention and caused the boycotting of Shell gas stations. This was seen as the turning point in the North Sea decommissioning policy with commitments to processing these structures on land rather than 'dumping' the structures (Jørgensen, 2012). Decommissioning North Sea installations is estimated to cost between €80 and €100 bn for over 10,000 km of pipeline, 5000 wells, and 500 platforms (Ahiaga-Dagbui et al., 2017). Therefore, stakeholders in countries invested in MMS's in the North Sea such as the United Kingdom, Norway, and the Netherlands, are still debating re-purposing and extending the life of these installations, not only to save money but also to promote potential marine habitat benefits (Ounanian et al., 2020).

1.3.3.1 Rigs to Reefs approach

A potential decommissioning approach is Rigs to Reefs which converts decommissioned platforms and rigs into artificial reefs (Bull & Love, 2019; Elrick-Barr et al., 2022; Fowler et al., 2014; Hatcher et al., 2021). For the past twenty years, OSPAR's policy regarding the rigs to reefs approach to decommissioning in the North Sea has been unfavourable (Ounanian et al., 2020). However, this approach has had reasonable success in the Gulf of Mexico, which has enhanced fisheries resources and provided savings for oil and

gas companies (Macreadie et al., 2011). Recently, emerging calls for changes and flexibility in the decommissioning policy in the North Sea have increased, most recommending a case by case approach rather than blanket regulations which might not provide optimal economic, environmental, and social benefits (Fortune & Paterson, 2020; Fowler et al., 2020). MMS's as artificial habitats within the UK coastal seas are not included in the European habitats Directive despite hosting potential rare or valuable species (Fortune & Paterson, 2020). Using a science-based evidence approach to play a role in decision making around decommissioning of these sites could provide greater ecosystem benefits rather than keeping existing regulations (Birchenough & Degraer, 2020).

The 500 m exclusion zones surrounding oil and gas platforms in the North Sea effectively act as a small scale MPA without destructive effects such as trawling and dredging (Todd et al., 2018). MPAs provide a wide array of ecosystem services including fish stock spill over (Harmelin-Vivien et al., 2008), habitat restoration (McLeod et al., 2009) and climate change mitigation (Salm et al., 2011). Likewise, offshore winds farms have been proposed as *de facto* MPAs by providing artificial substrate for reefs, fish aggregating devices and small-scale exclusion zones from fishing efforts (Ashley et al., 2014). Specifically for O&G platforms, this rationale has led to the argument of keeping these sites intact to maintain the benefits of the exclusion zones after the MMS is operational.

Conversely, there is also evidence to suggest that the rigs to reefs approach is not always ecologically beneficial (Perkol-Finkel et al., 2006). Obstacles in opposition to the rigs to reefs approach are associated costs (partial removal, cleaning, maintenance and monitoring, local pollution levels near remaining installations) (Jagerroos & Krause, 2016), liability issues (well leakage and safety risks for navigation) (Rastelli et al., 2016) and finally the heightened risk of spreading marine invasive species (Coolen et al., 2016). Converting platforms to reefs can change water circulation and quality (Elrick-Barr et al., 2022), seabed ecology (Chen et al.,

2024), wave action and sedimentation rate which have yet to be wholly assessed (Jagerroos and R Krause, 2016). Similarly, there are legal issues regarding the responsibility of the decommissioned structures to ensure further upkeep and maintenance to reduce the potential impact to the surrounding marine environment (Hatcher et al., 2021). For example, in the Gulf of Mexico, the operators are required by law to assume liability and contribute half of the cost savings of non-decommissioning to implementation a rigs to reefs decommissioning strategy; this money is then used to create a fund which goes towards maintenance costs (Hatcher et al., 2021).

1.4 Thesis Aims

This thesis aims to fill key knowledge gaps in how offshore infrastructure in shelf sea systems, particularly decommissioned oil and gas (O&G) platforms in the North Sea, will impact sedimentary carbon dynamics. This includes assessing carbon stocks, sediment type, carbon accumulation rates, carbon provenance and vulnerability. Chapter two determines the baseline carbon dynamics around decommissioned O&G platforms, including sediment type, organic carbon stock and initial organic carbon accumulation rates. Chapter three refines these initial organic carbon accumulation rates to correct for local contamination from the O&G platform during operation. Chapter four determines the source of the organic carbon stock at each site, with increasing distance from the decommissioned sites. Finally, chapter 5 is a methodological exploration of the effect of disturbance (such as those from offshore infrastructure) on mineralisation rates of organic carbon. The specific aims of each data chapter are outlined here:

- **Chapter two**: *To describe carbon dynamics around two decommissioned oil and gas platforms in the North Sea including determining OC stock, sediment*

type and a first attempt at calculating organic carbon accumulation rates (OCAR).

- **Chapter three**: *To refine previous OCARs at impacted sites by quantifying attenuation causing heavy metal contamination and using alpha spectrometric techniques*.
- **Chapter four**: *To quantify the primary OC source and vulnerability around these decommissioned platforms and how this changes with increasing distance.*
- **Chapter five**: *To trial an experimental protocol for determining OC reactivity of disturbed shelf sediment, such as those caused by construction or decommissioning of man-made structures.*

Chapter 2: Sedimentary blue carbon around decommissioned oil and gas platforms in the North Sea

Please note, this chapter has been published in the Marine Pollution Bulletin in June 2025: https://doi.org/10.1016/j.marpolbul.2025.118250

2.1. Introduction

The North Sea has been extensively modified by anthropogenic activities including the introduction of man-made structures (Dannheim et al., 2018; Fowler et al., 2020). The global footprint of MMS, such as oil and gas platforms and offshore wind farms, is growing rapidly with projected expansion from 32,000 km^2 in 2018 to 39,400 km^2 by 2028 (Bugnot et al., 2021), driven by a rising demand for fossil fuels and renewable energy (Birchenough & Degraer, 2020). Within the Oslo and Paris Convention (OSPAR) maritime area alone there are over 1,350 offshore oil and gas installations that require decommissioning in the coming decades (Fortune & Paterson, 2020). By 2040, it is estimated that 2000 offshore oil and gas platforms will have to be decommissioned worldwide (Vidal et al., 2022; Wei & Zhou, 2024).

The effect of O&G platforms on the marine environment is still an expanding area of research, which has primarily focused on changes to marine biology, such as food webs (Fowler et al., 2020; Fujii & Jamieson, 2016; Todd et al., 2018; Wright et al., 2020), connectivity and

invasive species (Coolen, Boon, et al., 2020; Molen et al., 2018; Tidbury et al., 2020), fish attraction versus production (Brickhill et al., 2005; Grossman et al., 1997; Pickering & Whitmarsh, 1997; Todd et al., 2018) and seabird interaction (Ronconi et al., 2015). However, the effect of MMS on the seabed around these structures, and particularly on benthic carbon stocks, is poorly understood.

Shelf seas and the sediments therein play a key role in maintaining marine carbon stocks (Burdige, 2007; Legge et al., 2020; Smeaton, Hunt, et al., 2021) and supporting organic carbon sequestration potential (Atwood et al., 2020; Graves et al., 2022; LaRowe et al., 2020). Blue Carbon refers to organic carbon that is captured and sequestered in marine ecosystems, including coastal and ocean environments (Nellemann et al., 2009). This organic carbon is modified and remineralised while it descends through the water column (Soetaert et al., 2000). However, a proportion is stored within shelf sediment where it is further remineralised through diagenetic processes (Soetaert et al., 1996; Talin et al., 2002) or eventually, buried (Burdige, 2007). Despite covering only 7-10% of worldwide ocean area, shelf seas contribute 80% of organic carbon in sediments (Bauer et al., 2013), making them vital for climate change mitigation (Luisetti et al., 2020). It is estimated that global sedimentary blue carbon stocks are 2322 Pg C in the top 1 m of sediment (Atwood et al., 2020). Furthermore, the North-West European continental shelf area is estimated to have a standing organic carbon stock of between 230 – 882 Mt of POC in the upper 10 cm of sediment (Diesing et al., 2017).

Previous blue carbon research has largely focused on vegetated coastal habitats as these sequester significantly more carbon than other terrestrial habitats (Lovelock & Duarte, 2019; Macreadie et al., 2017; McLeod et al., 2011). More recently, shelf sediment ecosystems are increasingly recognised for their significant storage of blue carbon due to their large spatial extent (Diesing et al., 2017; Legge et al., 2020; Luisetti et al., 2019; Thomas et al., 2004). However, shelf sediment is subject to substantial disturbance from activities such as trawling

(Dounas et al., 2007; Epstein et al., 2022; Palanques et al., 2014) and construction and decommissioning of offshore MMS (Birchenough & Degraer, 2020; Dannheim et al., 2020; Fortune & Paterson, 2020). While the effect of disturbance on carbon stocks remains unclear (Epstein et al., 2022), it is essential to determine potential impacts of anthropogenic activity, such as decommissioning of MMS, on shelf sedimentary carbon stocks.

Currently under OSPAR Decision 98/3, MMS in the North Sea are required by law to be fully removed from the sea at the end of its active life cycle, and the marine environment to be returned to its natural state prior to construction (Bull & Love, 2019; Fortune & Paterson, 2020; Fowler et al., 2020; Fowler et al., 2014). Recent literature has started to explore the effect of disturbance to benthic carbon stocks, with an emphasis on trawling (De Borger, Tiano, et al., 2021; Epstein et al., 2022; Paradis et al., 2019; Porz et al., 2024). Any pressure which changes the degradation rates within upper sediment depth, or input of carbon to the seabed will likely disrupt the overall carbon stock and sequestration rates (Legge et al., 2020). Decommissioning of MMS, especially 'whole removal' which is preferred by OSPAR commission regulations (OSPAR, 1998) is a significant form of marine disturbance (Sommer et al., 2019).

Removing oil and gas structures typically involves abrasive water jetting, diamond wire cutting, hydraulic shears or explosives (Sommer et al., 2019). These methods not only cause complete mortality of attached invertebrates and nearby fish but likely impact the benthic environment during the removal of the steel jackets and concrete foundations (Jagerroos & Krause, 2016). With the mandatory decommissioning of many platforms approaching rapidly, it is vital to determine how these activities affect sedimentary organic carbon storage and sequestration rates. Exclusion zones, particularly the 500 m zones around active O&G platforms, provide an area free from disturbance by trawling and other extractive uses. These undisturbed zones could potentially safeguard carbon stocks and facilitate recovery (Epstein & Roberts, 2022). Moreover, decommissioned O&G platforms are often surrounded by drill

cuttings piles (Breuer et al., 2004). These piles, produced during offshore hydrocarbon drilling operations, are composed of subsurface rock coated with hydrocarbons and drilling fluids (Bakke et al., 2013; Haanes et al., 2023) could influence seabed carbon stocks. Including carbon stock considerations, alongside other factors such as expense and environmental impact (Hall et al., 2022; Sommer et al., 2019) into cost-benefit analysis of decommissioning methods (Fowler et al., 2014) could provide managers with more information to determine best practices (Fortune & Paterson, 2020; Zawawi et al., 2012). This is the first study to investigate the benthic carbon dynamics around decommissioned O&G structures in the North Sea, and with samples taken as close as 50 m. The overall aim of this study is to determine the effect of decommissioned O&G platforms on organic sedimentary carbon stocks and sedimentation/carbon accumulation rates, compared to areas which have not been excluded from anthropogenic extraction activities.

2.2 Methods

2.2.1. Study sites

Sediments at two decommissioned O&G platforms, North West Hutton (61°6' 23.9508", 1°18'32.9724") and Miller (58° 43' 19.7004", 1° 24' 7.4016"), were sampled between 24th and the 30th of June 2021, during a research cruise on the MRV *Scotia* (Figure 6). Details of sampling depth are displayed in appendix table 1. The North West Hutton platform was installed in 1981, with oil production commenced in 1983 and continued until 2003 (Blacklaws & Johnston, 2013). Topsides of the platform were removed in 2008 and removal of the jacket structure was completed in 2009 (BP, 2005, 2011). Water depth at this platform is 144.3 m (BP, 2005) with prevailing currents in a NE/SW direction alongside weak residual currents (BP, 2005) with maximum current speeds being 0.73 m/sec at the surface and 0.47 m/sec at the seabed. The Miller platform was installed in 1991 and produced oil from June 1992 to

September 2007 (BP, 2011). Topsides were removed between 2017 and 2018; jacket structure removal was completed in 2018 (BP, 2011). Water depth at the Miller platform is 103 m, with the Fair Isle/Dooley current affecting the Miller platform which flows in a SE/NW direction with maximum current speeds being 0.84 m/sec at the surface and 0.43 m/sec at the seabed (BP, 2011). For both sites the jacket footings and drill cuttings piles remain *in-situ*. Jacket footings were cut at 45 m and 20 m above the seabed for the North West Hutton and Miller platforms, respectively. The drill cutting pile at North West Hutton lies directly beneath the footings, while at Miller, it is offset to the southeast footing. These sites were selected due to age (over 40 years since installation) and decommissioning status. Where possible, triplicate sediment cores were taken at various distances along northern and southern transects extending away from the decommissioned platforms (50, 100, 200, 400, 800, 1600 m). Due to safety features of the research vessel, samples could not be taken any closer than 50 m away from the platforms. Control sites of similar sediment composition were selected at 3200m away along each of the gradients. These control samples were known to not be near other oil rigs at any phase during their use (i.e., construction, operational or decommissioned). There were no visible signs of oil contamination on the sea surface during the survey.

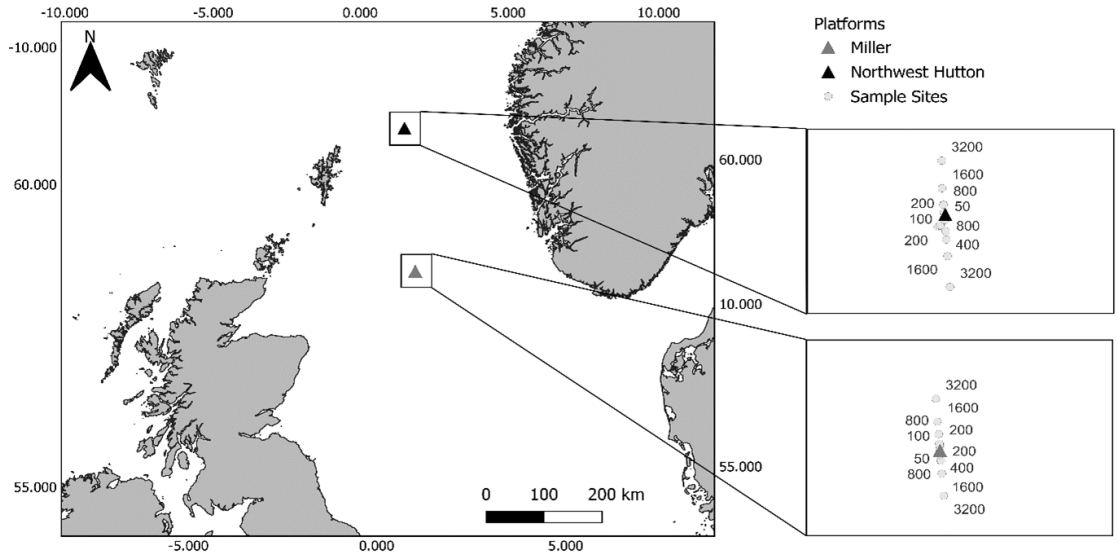

Figure 6: Location of North West Hutton and Miller decommissioned platforms in the North Sea with sampling sites at varying distances (50- 3200 m (Control)).

2.2.2. Sediment core sampling and processing

Samples were obtained using a multi-corer, when weather permitted, to extract three replicate sediment cores (inner Ø 9.8 cm) at each sampling distance. When weather was too severe for the multi-corer, cores were collected using a VanVeen grab, and cores taken from the grab only if the sediment surface was intact. Depths of each core collected were noted. Cores were extruded onboard and sliced into 1 cm depth increments and stored in plastic bags at -20°C until further analysis. Each sediment slice was measured for wet weight (g) and freeze dried to give dry weight to determine porosity and dry bulk density (DBD).

2.2.3. Biogeochemical analysis

Three homogenous powder subsamples of each 1 cm layer were analysed for organic and inorganic carbon using a Formacs^{HT} TOC Analyser with Primacs^{MCS} add-on module (SKALAR, The Netherlands). Between 50-100 mg of each sample was weighed into quartz crucibles, manually inserted into the analyser, and then heated to >1000 °C. For inorganic carbon, samples were acidified using 5 M phosphoric acid and resultant CO_2 was measured. For each sample, inorganic carbon was subtracted from total carbon to give a measurement of organic carbon, giving measures of total, organic and inorganic carbon for each core slice.

Particle size analysis (PSA) was conducted using the laser diffraction unit Bettersizer S3 Plus (China). PSA methodology was adapted from the National Marine Biological Analytical Quality control scheme (Mason, 2022). Freeze dried sediment samples were analysed using laser diffraction. Sediment samples were wetted before input into the laser diffraction unit. The quantity of sample entered was varied to ensure laser beam obscuration remained within 8 and 12%. Samples were sonicated for two minutes before laser readings were taken and dispersant was not used throughout. One replicate was analysed for each 1 cm depth of the core with the particle size analyser, taking another three replicate readings from each. Sediment characteristics statistics, mean and median grain size, skew, and kurtosis were calculated using GRADISTAT software version 9.1 (Blott & Pye, 2001). Characterisation of sediment was determined using Folk description, assigning sites to one of the fifteen major textural groups as defined by the relative percentage of gravel (>2 mm), sand (0.0625-2 mm), mud (<0.625 mm) (Folk, 1954).

Preliminary GC-MS analysis of hydrocarbon content in sediment showed an insignificant contribution to total carbon content (<2%) even at sampling points closest to both platforms (50 m) see appendix material 1. Total hydrocarbon content (mg/g of sediment) at varying distances from both North West Hutton and Miller decommissioned platforms is included in appendix figure 1 from the UK Benthos database v5.17 (Offshore Energies UK,

2015). As both measures indicate hydrocarbon content within sediment to be <8% of measured organic carbon content this was not considered in this paper.

2.2.4. Estimated mass accumulation and sedimentation rates

Mass accumulation and linear sedimentation rates (MAR/LSR) were determined using the Constant Flux – Constant Sedimentation (CF-CS) ^{210}Pb-based modelling approach (Krishnaswamy et al., 1972) from ten sediment cores collected at five distances (50, 100, 200, 400 and 3200 m) from each directional transect at North West Hutton. Approximately 27 g of each 1 cm slice were freeze dried, sieved down to 500 μm, compressed, and sealed into plastic containers. After a period of three weeks (to allow for secular equilibrium between ^{226}Ra and ^{214}Pb), samples were analysed by gamma spectrometry using Broad Energy Germanium detectors (ORTEC, GEM-FX 8530-S model, USA) to determine the total ^{210}Pb and ^{137}Cs activity concentrations with the emission peaks of 46.5 and 662 keV respectively. Activity concentrations of total ^{226}Ra were indirectly measured using the peak at 352keV from the presence of ^{214}Pb, one of its decay products. A certified reference material from International Atomic Energy Agency – IAEA-465 Baltic Sea Sediment was used as a reference for quantifying these radioelements in the studied samples (International Atomic Energy, 2021).

2.2.4.1 Lead-210 based modelling and validation

Lead-210-based modelling approaches have been widely used to estimate organic carbon accumulation rates (OCAR) in marine sediment cores (Arias-Ortiz et al., 2018; De Haas, 1997; Masque et al., 2002). These approaches rely on the depth distribution of unsupported fraction of ^{210}Pb, directly sourced from the decay of radon gas (^{222}Rn) present in the atmosphere and decaying at rate of 22.23 years. As the studied cores were relatively shallow (<15 cm) and many natural and anthropogenic disturbance were anticipated, including the presence of oil and gas produced water derived particles enriched in ^{226}Ra, ^{210}Pb and stable

elemental analogues, such as Ba and Pb (Ahmad et al., 2021; Haanes et al., 2023) the constant flux-constant sedimentation (CF-CS) modelling approach was favoured against other common modelling approaches and selected to estimate directly the mass accumulation rate (MAR) from each core. The CF-CS model was selected to enable the estimation of a mean MAR below a potential surface mixed layer and was assumed to be constant over time following equation 1:

$$^{210}Pb_x = {}^{210}Pb_0.e^{-\lambda mx/MAR} \quad [1]$$

with $^{210}Pb_x$: activity concentration of unsupported ^{210}Pb at mass depth x (in $Bq.kg^{-1}$); $^{210}Pb_0$: activity concentration of unsupported ^{210}Pb at water/sediment interface (in $Bq.kg^{-1}$); λ: decay constant of ^{210}Pb = 0.031 y^{-1}; m_x: accumulated mass stock (in $g.cm^{-2}$) at depth x; MAR: mass accumulation rate ($g.cm^{-2}.y^{-1}$).

Linear sedimentation rates (LSR) could then be estimated at each studied location by dividing with the average dry bulk density of the core segment selected in the CF-CS model. Organic carbon accumulation rates (OCARs) were determined using MAR multiplied by percentage of organic carbon derived from the average along the entire core depth at each site (%OC).

Fractions of anthropogenic ^{226}Ra were subtracted from the total ^{226}Ra activity concentrations prior to utilising the CF-CS model, by referring to barium (Ba) depth profiles, a chemical analogue of ^{226}Ra, and measured by ICP-MS following total microwave-assisted digestion, alongside other stable elements (Agilent, 7900ce model, USA).

Where possible, the 1978 Sellafield-derived ^{137}Cs signature (i.e., 1974-1975 peak discharge including a 4-year transient time from discharge point (Gray et al., 1995; Povinec et al., 2003) were also used to validate LSR results obtained from CF-CS modelling. For highly contaminated cores at 50 m, mid-core enrichment of ^{226}Ra was used as an estimate to validate

^{210}Pb excess based CF-CS modelling rather than to estimate MAR/LSR directly. This mid-core enrichment was determined as the mid-point of production from the platform. However, due to this contamination, MAR/LSR were not calculated at 50 m due to uncertainties without a clear fingerprinting tool.

2.2.5. Organic carbon stock calculations

Stock calculations of sedimentary carbon surrounding both platforms were calculated using methods and equations from (Diesing et al., 2017). Estimation of mass of particulate organic carbon (m_{POC}) was calculated by multiplying particulate organic carbon as a dimensionless fraction, dry bulk density (ρ_d), sediment depth (d) and area (A) using equation 2.

$$m_{POC} = POC \cdot \rho_d \cdot d \cdot A \quad (2)$$

2.2.5.1. Dry bulk density

Dry bulk density was calculated using equation 3. Where dry bulk density (p_d) was determined using porosity (φ) and grain density (ρ_s). Grain density was assumed to be 2650 kg m^{-3}.

$$p_d = (1 - \varphi)\rho_s \quad (3)$$

2.2.5.2. Porosity

Porosity was calculated using weight before ($Weight_{Wet}$) and after ($Weight_{Dry}$) freeze drying as well as the specific gravity of the sediment (SG_{Sed}) and density of water calculated based on salinity (ρ_{Water}) (Equation 4). For offshore sediments of this nature this was assumed to be composed of mostly quartz/feldspar so specific gravity was assumed to be

2.7. Salinity for the density of water was assumed to be that of offshore water (35) and a density of 1.035 kg/l.

$$\varphi = \frac{\left[SG_{Sed} - SG_{Sed}\left(Weight_{Wet}/Weight_{Dry}\right)\right]}{\left[SG_{Sed} - SG_{Sed}\left(Weight_{Wet}/Weight_{Dry}\right)\right] + \left[\rho_{Water} - \rho_{Water}\left(Weight_{Wet}/Weight_{Dry}\right)\right]} \quad (4)$$

2.2.6. Statistical analysis

All statistical analysis was conducted using R version 4.2.1. All figures were generated using the '*ggplot2*' (Wickham, 2010), '*corrplot' (Wei & Simko, 2021) a*nd '*cowplot*' (Wilk, 2020) packages. Data was initially tested for normality using Shapiro-Wilk tests (Shapiro & Wilk, 1965) and subsequent Bartlett tests (Bartlett, 1937) to determine homogeneity of variance between groups. Normally distributed data were tested for significance using ANOVAs, with p-values adjusted for multiple comparisons using the Benjamini-Hochberg procedure (Benjamini & Hochberg, 1995), followed by a Tukey's HSD (Tukey, 1953) post hoc test within the '*agricolae*' (De Mendiburu, 2020) package. Non-normally distributed data were tested for significance using a Kruskal-Wallis test, with *p*-values adjusted for multiple comparisons with Bonferroni corrections (Bonferroni, 1936), followed by Dunn's post hoc test (Dunn, 1964) within the '*FSA*' package (Ogle et al., 2020). Spearman correlation tests were applied to assess correlations between organic carbon content, inorganic carbon content, mud content, sand content sedimentation rates and distance from platform. To test for effect size of Kruskal-Wallis tests, Cohen's f (Cohen, 1988) was calculated using the *'rcompanion'* package (Mangiafico & Salvatore, 2023), followed by a power analysis using the *'pwr'* package (Champely, 2020). For pairwise comparisons Cliff's delta (Cliff, 1996) (with a large effect size being > 0.474) was calculated with the *'effsize'* package (Torchiano, 2020) and subsequent power analysis was

calculated for each comparison with an acceptable threshold of 0.8. Averages are reported as Mean ± standard deviation. Details of pairwise comparisons can be found in appendix table 2.

2.3 Results

2.3.1 Sediment composition

Sediment classifications varied from sand to sandy mud across both sites and distance gradients. Mud content across all sites ranged from 1.58% to 86.28%, although North West Hutton had higher average mud content across all distances compared to Miller (Figure 7). Highest average mud content was found at 50 m and 100 m away from North West Hutton, with average mud percentage being 59% and 38%, respectively. Average mud content at Miller was similarly high at the 50m distance with an average of 47%. Mud content remained lower with greater distance from Miller. Sediment composition at both sites was predominantly either sand or mud, with very few observed gravel particles, hence, mud and sand percentages inversely mirror each other. Sand content across all sites ranged from 13.72% to 96.96% (Figure 7). Miller consistently had higher sand content across all distances compared to North West Hutton.

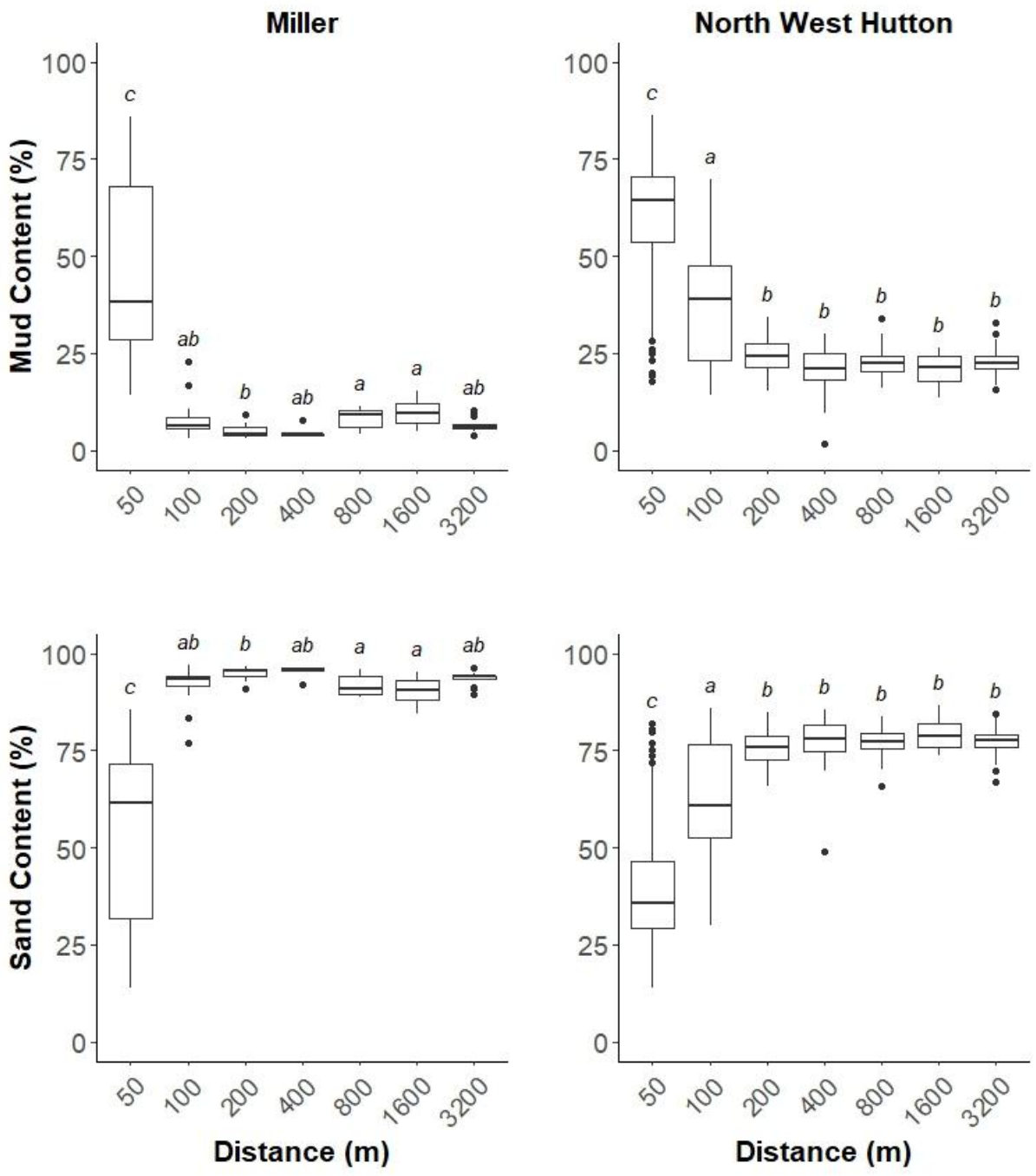

Figure 7: Mud and sand content (%) of 1 cm sediment core slices collected at increasing distances (50- 3200 m) away from two decommissioned oil and gas platforms, Miller and North West Hutton. Sediment was analysed to 10 cm at North West Hutton and 6 cm at Miller. Letters above boxes (a, b, c) indicate significant differences between distances ($P < 0.05$, Kruskal-Wallis test followed by Dunn's post hoc test); different letters indicate significant differences.

2.3.2. Organic carbon content

Organic carbon content ranged from 0.26 to 51.78 mg/g of sediment (Figure 8). Highest average organic carbon content (31.62 ± 1.09 mg/g of sediment; mean ± SD) was found 1600 m from North West Hutton, followed by the control site (3200 m) (27.78 ± 1.12 mg/g of sediment). Organic carbon content was significantly lower at 200 m (17.86 ± 1.22 mg/g of sediment) away from North West Hutton (Kruskal-Wallis, $\chi2 = 76.535$, $P = 1.854e^{-14}$, $1 - \beta = 1$) compared to all other sampling distances. Conversely, a different trend was seen at the Miller, with the highest average organic carbon content at the closest distance (50 m) (24.54 ± 2.49 mg/g of sediment), which was significantly higher (Kruskal-Wallis, $\chi2 = 66.084$, $P = 2.635e^{-12}$, $1 - \beta = 1$) than all other distances. On average, organic carbon content was higher at the North West Hutton compared to Miller, for example average organic carbon content at the control site of North West Hutton was up to 6.6-fold higher compared to sediment collected at the corresponding site at Miller. Organic carbon depth profiles are displayed in appendix figures 2 to 5.

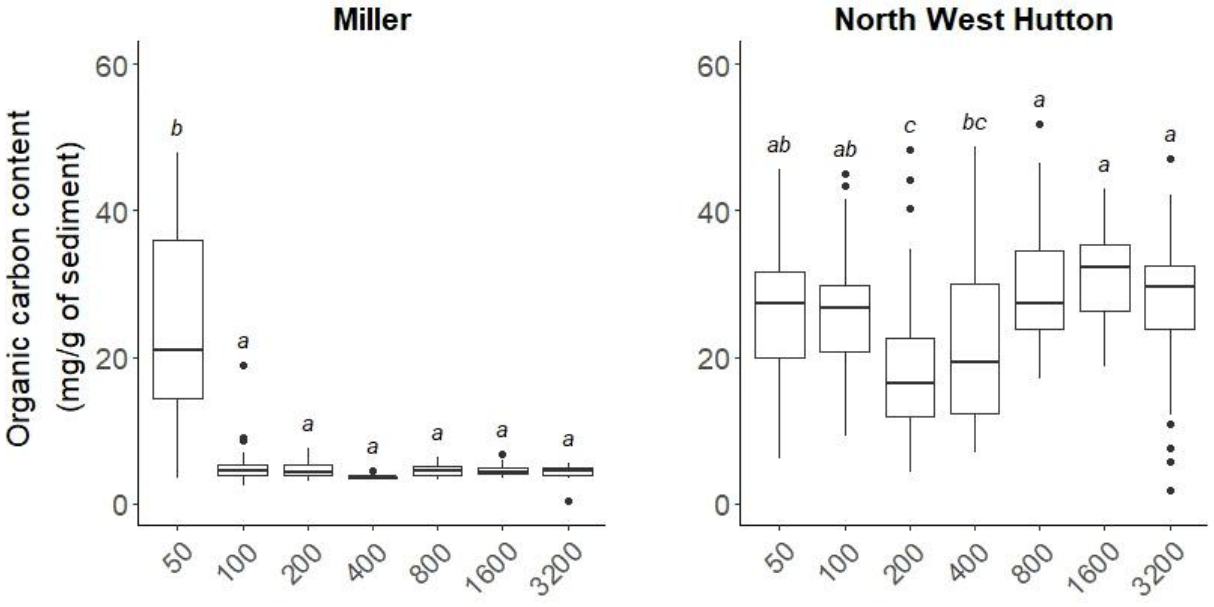

Figure 8: Organic carbon content (mg/g of sediment) of 1 cm sediment core slices collected at increasing distances (50 - 3200 m) from two decommissioned oil and gas platforms, Miller and North West Hutton. Sediment was analysed to 10 cm at North West Hutton and 6 cm at Miller. Letters above boxes (a,b,c) indicate significant difference between distances ($P < 0.05$ Kruskal-Wallis test followed by Dunn's post hoc test) with differing letters indicating significant differences.

2.3.3 Inorganic carbon content

Inorganic carbon content ranged from 0.14 to 45.14 mg/g of sediment across both decommissioned platforms (Appendix figure 6). A similar pattern was observed for inorganic carbon content, that was also seen for organic carbon content. A significantly higher average inorganic carbon content (Kruskal-Wallis, $\chi2 = 133.16$, $P = 2.2e^{-16}$) was found at the control site of North West Hutton (24.29 ± 0.62 mg/g of sediment), when compared to closer distances (e.g. 50, 100, 200, 400 and 800 m) away. The lowest average inorganic carbon content was found at the 50 m distance, closest to North West Hutton (6.04 ± 0.66 mg/g of sediment). Conversely, at Miller, average inorganic carbon content was significantly higher (Kruskal-Wallis, $\chi2 = 82.07$, $P = 1.334e^{-15}$) closer, at 50 m distance (7.27 ± 1.19 mg/g of sediment) than all other distances (100, 200, 400, 800, 1600 and 3200 m). On average, organic carbon content was higher at North West Hutton compared to Miller. For example, average inorganic carbon content at the control site of North West Hutton was up to 20.4-fold higher compared to sediment collected at the same site at Miller.

2.3.4 Sediment organic carbon stocks

Average sediment organic carbon stocks ranged from 0.59 to 5.01 kg m^{-2} across both sites and distances (Figure 9). Resolution of stocks ranged from 3 cm to 10 cm with consistently higher resolution at North West Hutton (ten sampling sites had 10 cm depths analysed). Miller resolution ranged from 3 to 10 cm, but had an average depth of 6 cm. Estimated carbon stocks were averaged and extrapolated to 10 cm (Fig. 4; represented by hashed portions of each bar). The largest average organic carbon stocks were found at 800 m on the southern transect from North West Hutton (5.01 ± 0.62 kg m^{-2}) and lowest was found at 400 m on the southern transect of Miller (0.59 kg m^{-2}), though this distance only had one replicate to 5 cm depth.

Miller had highest organic carbon stocks at 50 m on both the northern and southern transects with averages of 1.47 ± 0.53 kg m^{-2} and 3.74 ± 0.36 kg m^{-2}, respectively. At greater distances (100 to 3200 m) along the southern transect, organic carbon stocks remained consistently lower with an average of 0.88 ± 0.13 kg m^{-2} , at 100 m distance, to 0.72 ± 0.05 kg m^{-2}, at 1600 m, and 0.68 kg m^{-2} at 3200 m, however at 3200 m there was only one core available. A similar trend occurred on the northern transect with average organic carbon stocks of 0.65 ± 0.04 kg m^{-2}, at 100 m, and 0.65 ± 0.03 kg m^{-2} at 3200 m.

Comparatively, North West Hutton had consistently higher organic carbon stocks than those found at Miller, which generally remained constant with distance. Along the southern distance transect, average organic carbon stocks at 50 m were 2.44 ± 0.223 kg m^{-2} which gradually increased to 3.65 ± 0.35 kg m^{-2} at 400m. At 800 m, organic carbon stocks increased to 5.01 ± 0.63 kg m^2, but subsequently decreased to 3.27 ± 0.67 kg m^{-2} at 3200 m. Along the northern transect at North West Hutton, average organic carbon stocks increased from 2.75 ± 0.20 kg m^{-2} at 50m to 3.38 ± 0.32 kg m^{-2} at 100 m. However, average organic carbon stock decreased at 200 and 400m to 1.44 ± 0.24 kg $m^{-2}$and 1.63 ± 0.13 kg m^{-2} respectively. Organic carbon stocks then increased at 800 and 3200 m to 3.33 ± 0.16 kg m^{-2} and 3.95 ± 0.18 kg $m^{-2,}$ respectively.

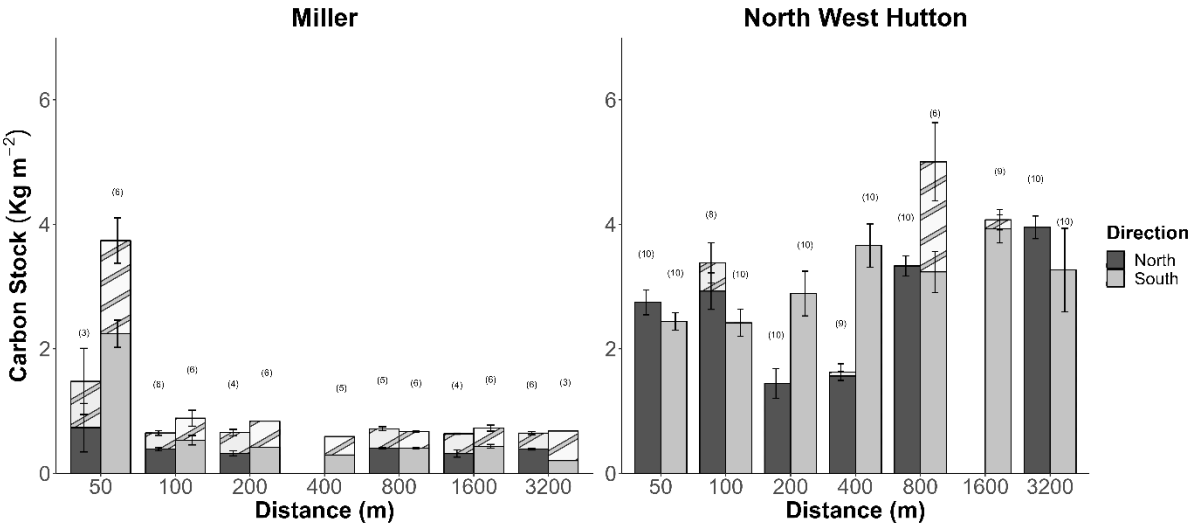

Figure 9: Mean ± SE of sediment organic carbon stocks (kg m^{-2}) f at increasing distances (50, - 3200 m) from two decommissioned oil and gas platforms, Miller and North West Hutton. Numbers in brackets indicate deepest sampling depth (cm). Where sampling depth was <10 cm, stocks were averaged and extrapolated to 10 cm (this is represented by hashed portion of each bar). Where bars are missing this indicates no samples taken at that distance.

2.3.5. Mass accumulation and sedimentation rates

Radiometric depth profiles of total ^{210}Pb, total ^{226}Ra, ^{137}Cs as well as stable Ba and Pb depth profiles at 50 m North/South and 3,200 m North/South (control) are displayed in Figs. 10 and 11, respectively.

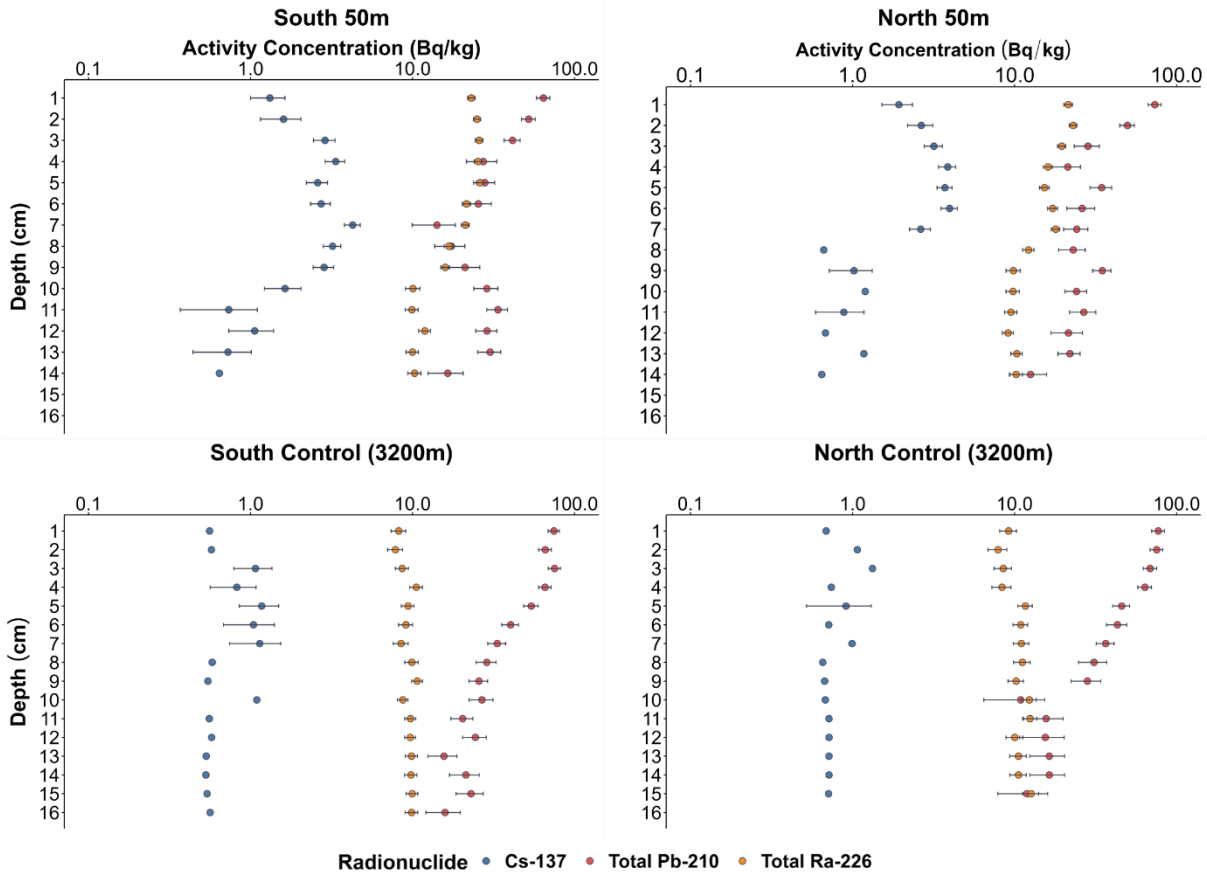

Figure 10: Depth (cm) profiles of activity concentration (Bq/kg) of three radionuclides (Cs-137, Total Pb-210, Total Ra-226) in four sediment cores taken at 50 and 3200 m away from North West Hutton decommissioned platform on both North and South transects. Error bars indicate unsupported fractions of each radionuclide. Absence of error bars indicates radionuclide levels were below the limit of detection.

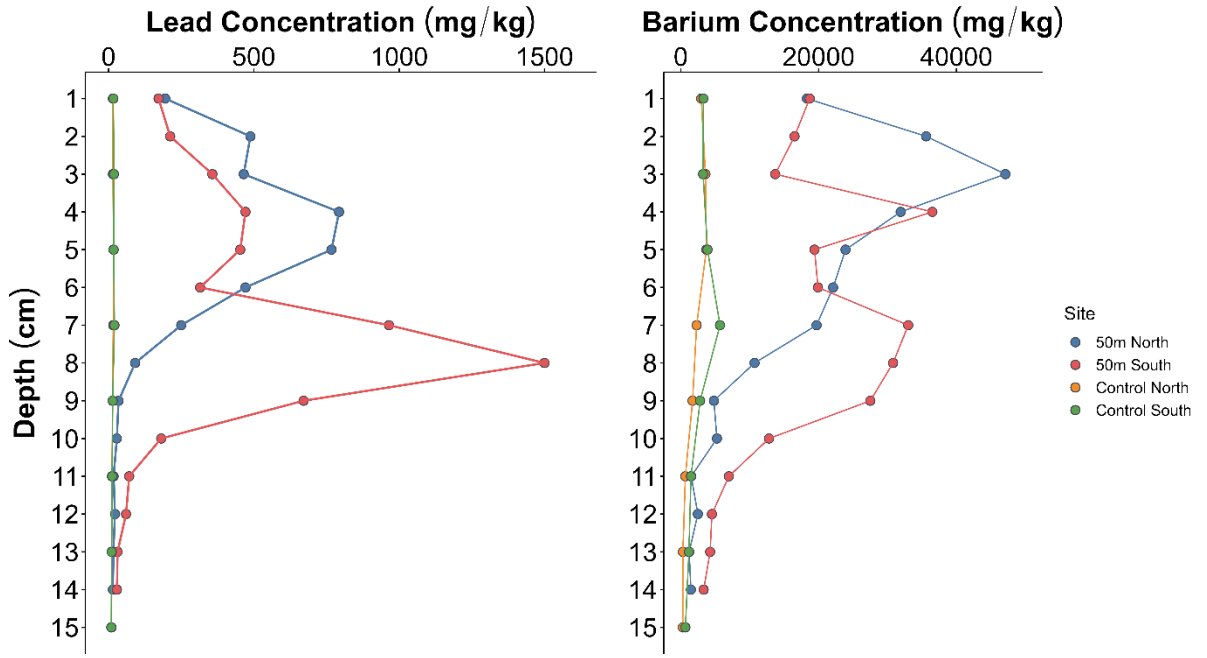

Figure 11: Depth (cm) profiles of stable lead and barium concentrations (mg/kg) of within four sediment cores taken at 50 and 3200m away from North West Hutton decommissioned platform on both North and South transects.

As shown in figure 10, the depth profiles at 50 m North and South of North West Hutton presented enhanced concentrations of ^{226}Ra in the top 10 cm, a clear signature from the legacy discharges of oil and gas produced water. This observation was confirmed when measuring its chemical analogue Ba (figure 11), showing a net increase of barium in the top 9 cm in the 50 m North core and 10 cm depth in the 50 m South core, suggesting the presence of radiostrontiobarite particles (Ahmad et al., 2021). These industrially derived signatures were subsequently used to estimate LSR at these two locations. As the fate of radium particles remains unclear (Ahmad et al., 2021) and operational discharge information was not available, the middle of the two contaminated core segments (i.e., 4.5 cm in the 50 m North and 5 cm in the 50 m South) were assumed to correspond to the middle of the operational life of North West Hutton (1993) and indicated the LSR to be ranging between 0.16 and 0.18 cm.y^{-1} .

Due to the presence of low activity concentrations of ^{137}Cs observed near North West Hutton, unconfirmed at control distances, as well as the potential presence of other ^{137}Cs sources (i.e., from major nuclear fallout events such as Chernobyl), the use of this nuclear-derived fingerprint was not further considered in this study.

Also, as shown in figure 11, the Pb depth profiles did not follow the same pattern as Ba profiles, implying the ratio of anthropogenic ^{226}Ra/anthropogenic ^{210}Pb to be variable over time. Therefore, it was not possible to estimate the fraction of anthropogenic ^{210}Pb accurately close to the platform (50 m). It is worth noting that the direct measurement of ^{210}Pb by gamma spectrometry in sediment materials highly contaminated in Pb and other heavy metals such as Zn, Ba, Sr, would have also suffered from high matrix self-attenuation (Dal Molin et al., 2018) limiting event further the application of ^{210}Pb based modelling approaches for these contaminated sediment cores above 10 cm. In addition, the levels of unsupported natural ^{210}Pb

observed below 10 cm were found to be very low and associated with high uncertainties from gamma counting. Consequently, the CF-CS ^{210}Pb modelling approach could not be applied in cores collected within 200 m N/S from North West Hutton. Nevertheless, a negligible influence was observed at 400 m and 3,200 m N/S (control), enabling the use of the full core ^{210}Pb excess profiles for CF-CS modelling at these four sampling locations.

Averaged MARs were found to be approximately 0.27 and 0.19 g cm^{-2} y^{-1} within the North and South transects, respectively (Table 1). Organic carbon accumulation rates (OCARs) ranged from 0.003 to 0.009 g cm^{-2} y^{-1} across both transects (Table 1). The subsequent LSRs were estimated to be averaging at 0.21 cm y^{-1} within the North transect and found to be slightly lower within the South transect, ranging between 0.14 and 0.15 cm y^{-1} and agreeing with the estimations from ^{226}Ra fingerprinting.

Table 1: Linear sedimentation rates from traditional ^{210}Pb radiometric dating techniques and novel ^{226}Ra oil and gas attributed fingerprint, average dry bulk densities (DBD), ^{210}Pb mass accumulation rates (MAR) and ^{210}Pb organic carbon accumulation rate (OCAR) of six cores collected at increasing distances (50 – 3200 m) along two directional gradients (North and South) from North West Hutton decommissioned platform.

Distance (m)	**Direction (N/S)**	**^{210}Pb LSR (cm/y)**	**Mean Dry Bulk Density (DBD)**	**^{210}Pb MAR (g/cm^2/y)**	**Average carbon content (%)**	**Pb OCAR (g/m^2/y)**	**^{226}Ra LSR O&G fingerprint (cm/y)**
50	North	*	1.102	*	2.83	*	0.161
400	North	0.211	1.211	0.258	1.26	30	N/A
3200	North	0.216	1.330	0.286	3.24	90	N/A
50	South	*	1.056	*	2.78	*	0.179
400	South	0.141	1.252	0.176	2.45	40	N/A
3200	South	0.154	1.292	0.199	3.16	60	N/A

*not estimated

2.3.2 Correlation analysis

Spearman's correlation analysis between the measured variables was separated by site (Figure 12). Where Spearman's ρ values are positive this shows a positive correlation and where they are negative this shows a negative correlation. For Miller, organic carbon was

significantly positively correlated to mud content (Spearman's $\rho = 0.65$, $P = 2.2e^{-16}$), porosity (Spearman's $\rho = 0.59$, $P = 1.19e^{-15}$), inorganic carbon (Spearman's $\rho = 0.39$, $P = 8.07e^{-7}$) and gravel content (Spearman's $\rho = 0.18$, $P = 0.03$) and significantly negatively correlated with distance (Spearman's $\rho = -0.49$, $P = 9.37e^{-11}$), dry bulk density (Spearman's $\rho = -0.59$, $P = 1.19e^{-15}$), mean grain size (Spearman's $\rho = -0.52$, $P = 2.2e^{-16}$) and sand content (Spearman's $\rho = -0.65$, $P = 2.2e^{-16}$). Conversely, organic carbon content at North West Hutton was weakly positively correlated with distance (Spearman's $\rho = 0.18$, $P = 0.001$), dry bulk density (Spearman's $\rho = 0.25$, $P = 1e^{-6}$), sand content (Spearman's $\rho = 0.13$, $P = 0.01$) and weakly negatively correlated with mud content (Spearman's $\rho = -0.11$, $P = 0.04$), porosity (Spearman's $\rho = -0.25$, $P = 1e^{-6}$).

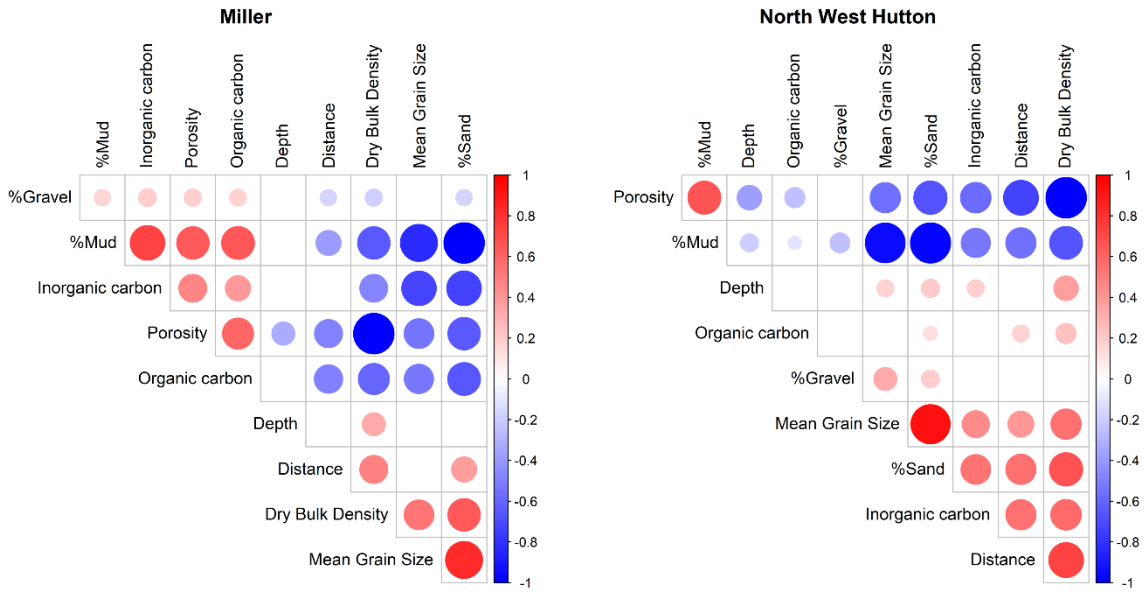

Figure 12: Correlogram of spearman's correlation (ρ) ($P < 0.05$) between measured variables, organic carbon, inorganic carbon, porosity, dry bulk density, distance from site, mean grain size, percentage sand, percentage mud and percentage gravel from sediment cores at Miller and North West Hutton. Size of circles represent level of significant with larger circles indicating higher significance. Colour of circles indicates direction (blue = positive, red = negative). Relationships without significance are left blank.

2.4. Discussion

2.4.1. *Organic carbon content/stock variability between sites*

Organic carbon content of sediments varied spatially around both study sites with distinct trends observed at each. North West Hutton showed consistently higher average organic content across all sampling distances compared to Miller. Additionally, the relationship between organic and distance varied between sites, with North West Hutton carbon content increasing slightly with distance, whereas Miller displayed elevated levels closer to the structure (50 m), with consistently lower levels at increasing distance. Overall, organic carbon content in this region of the North Sea was higher than modelled studies such as Diesing et al (2017, 2021) and Wilson et al (2018). In these estimations, carbon percent ranges from 0.39% at North West Hutton and 0.68% at Miller (Wilson et al., 2018). However, these predictive models do not account for the presence of MMS which likely explains their inability to capture the site-specific trends observed in this study.

In this study, Miller exhibited an enrichment of organic carbon within close proximity (50 m) to the structure, displaying a ‘halo’ effect, likely linked to activity from the O&G platform during its active production stage. The combination of a large effect size and statistical power indicates that this is a reliable and reproducible result. This enrichment could be caused by the presence of attached epifauna on the remaining jacket footings, potentially increasing organic carbon content through deposition of faecal matter (Schutter et al., 2019). Artificial structures can support significantly higher biomass (up to 500 times more) than soft sediments, due to the availability of hard substrate for epifauna attachment (Maar et al., 2009). Organisms that colonise artificial structures tend to be fouling attached epifauna dominated by filter feeders (Schutter et al., 2019). These organisms may act as a large-scale biofilter, depleting organic matter from the water column while enriching nearby sediment with faeces, larvae,

dissolved organics, and nutrients (Coates et al., 2014; Maar et al., 2009). For example, in Maar et al's model, sedimentation rate around an offshore wind structure in the North Sea significantly increased up to 40 m from the foundation due to the excretion of faecal pellets. Similar patterns are observed at southern North Sea windfarms, where colonizing organisms accumulate carbon during operation and only a small proportion (0.50 ± 0.06%) of the area is disturbed by decommissioning activities (Heinatz & Scheffold, 2023). In this study, measurements of attached epifauna were not taken, however, other offshore platforms in the North Sea have been shown to be fully covered with marine fouling organisms (Van Der Stap et al., 2016), particularly at the depth of the Miller footings. Despite O&G platforms having less structures in each area compared to wind farms, the principle of localised carbon enrichment through biodeposition could explain the higher carbon content close to the Miller platform. Without epifauna or associated carbon flux values, future work determining organic carbon composition could further qualify this conclusion. This also highlights a significant knowledge gap to fill in pre-decommissioning assessments.

The 'halo' trend seen at Miller is consistent with environmental impact assessments of other decommissioned North Sea platforms. At the Ninian Northern decommissioned platform, sediment organic matter was higher near the structure (4.9 - 5.5% at 0 m) compared to more distant sites (0.9 – 3.8 % at 100 – 10,000 m) (CNR International, 2017) mirroring the elevated carbon content near Miller. Similarly, sediment near the Murchison decommissioned platform showed elevated organic carbon at 250 m and 500 m (3 and 4% respectively) when compared to sites up to 8000 m, where values remained below 1% (CNR International, 2013). This pattern was attributed to drilling activity at the site, which elevated the proportion of fine-grained sediment and organic matter content (CNR International, 2017), with some of this likely being hydrocarbons. This aligns with Miller sediment composition results, where higher fines were observed at 50 m compared to the rest of the distances, indicating a localised halo area of mud

content (fines) and organic carbon. However, having data pre and post decommissioning of other platforms would allow for comparison and ability to determine relative effects of decommissioning on carbon stocks.

While elevated mud content was also observed at North West Hutton, its weak negative correlation with organic carbon suggests that this factor alone does not fully explain the observed variance with distance. The higher sediment carbon content near the platform could be due to elevated epifauna based faeces, increased fine-grained sediments, increased hydrocarbons, or a combination of these factors. Regardless, this halo effect at Miller has implications for decommissioning practice of specific platforms to protect the seabed integrity, and the carbon stored within them. MMS (active or decommissioned) will likely have distinct signatures and impacts on the seabed, linked to environmental context such as water depth, distance from MMS, and time and activity since decommissioning (change in trawling activity on seabed since decommissioning and removal of exclusion zone). As current OSPAR regulations require complete removal of these structures, except for a few derogations (such as those presented in this study), this practice of removing embedded structures causes a significant disturbance to the seabed carbon (Heinatz & Scheffold, 2023).

In contrast to Miller, sediments at North West Hutton, exhibited the lowest organic carbon content at 200 and 400 m with similar levels at all other distances. Comparisons between 200 m and distances other than 400 m showed large effect size and high statistical power which indicates that this is a reliable result avoiding type I/II errors. This lower carbon content may reflect increased carbon mineralisation from microbes or bioturbation from macrofauna (Burdige, 2007) present from a lack of sediment disturbance. During the operation of the platform, the 500 m exclusion zone limits disturbance from activities, such as trawling (De Borger, Tiano, et al., 2021; Sciberras et al., 2016; van der Molin et al., 2013) which would alter macrofauna assemblages within sediment (Eigaard et al., 2017). Carbon mineralisation

rates are strongly impacted by physical organic carbon removal through trawling-induced resuspension of sediment, which is further exacerbated by removal of bioturbating macrofauna (De Borger, Tiano, et al., 2021). Bioturbation is the movement of sediment particles by organisms, such as bivalves, and burrowing polychaetes, which create burrows and move sediment (and carbon) within the surface layers (Kristensen & Blackburn, 1987; Michaud et al., 2006). This movement oxygenates sediment which enhances mineralisation through oxidation (Soetaert et al., 1996; Talin et al., 2002) causing a reduction in organic carbon content in the surface layers (Glud et al., 2016). The lack of trawling activity within the exclusion zone would increase the presence and abundance of these bioturbators (De Borger, Tiano, et al., 2021), increasing the oxic status of the sediments and reducing the amount of carbon sequestered in the surface sediments. The observed dip in carbon content at 200 and 400 m may therefore have resulted from long term exclusion of trawling and distance from localised contaminants. Trawling is known to cause mortality of benthic organisms (Eigaard et al., 2017; Epstein et al., 2022; Hiddink et al., 2017; Sciberras et al., 2016), which may explain why the amount of carbon increases again outside of the set exclusion zone distance, and at 800 m (the next distance increment) the carbon content is similar to what is seen at the control site (3200 m), where reduced bioturbation enhances carbon content in surface sediments.

This trend in decreasing carbon with distance, as seen in the carbon stock values, from the MMS was also in a study around the L7A decommissioned platform (in the Southern North Sea), where decreasing carbon content at greater distances away from the structure was observed in 3 out of 4 directional transects (Klunder et al., 2018). The L7A platform is located much further south, but this suggests that decommissioned platforms may affect organic carbon differently depending on a variety of factors such as sediment composition and subsequent natural background particular organic carbon, decommissioning practices, sedimentation rates, current regimes, drill cutting composition and time of production (Klunder et al., 2018). The

L7A platform, in a different location, combined with the carbon dynamics seen around North West Hutton and Miller in this study, implies patterns of carbon storage around different decommissioned platforms are site specific and cannot be generalized for all MMS; each needs to be assessed on a case-by-case basis considering the different environmental variables and age of structures.

Interestingly, organic carbon results correlated differently with mud percentage between sites with a positive correlation at Miller and a weak negative correlation at North West Hutton. A positive relationship between organic carbon and mud/fines content is typical of shelf sediment (De Falco et al., 2004; Diesing et al., 2017; Leipe et al., 2011; Smeaton, Hunt, et al., 2021). However, this study observed a weak reverse correlation, indicating that there are some underlying and unknown variables, perhaps the presence of North West Hutton, may alter this relationship, as despite highest mud content occurring at 50 and 100 m, these were sites with the lowest recorded organic carbon content.

This study presents both organic carbon content (mg/g of sediment) and organic carbon stocks (kg m^2) in sediments surrounding these decommissioned platforms. By calculating organic carbon stocks (which include porosity and dry bulk density) (Graves et al., 2022) this provides a more comprehensive understanding of carbon dynamics than content alone. Carbon stock values are a useful indicator of how sediment composition affects carbon content. Uniquely, unlike other carbon stock assessments this study provides mass accumulation rates for the North West Hutton site, allowing quantification of the rate that carbon accumulates over time (g cm^{-2} yr^{-1}) which is rarely directly measured in offshore shelf sediment, with the exception of de Haas (1997) and Lerida-Toro (2022). Comparing carbon stocks between the two sites was limited by poor resolution of sediment core depths at the Miller decommissioned platform, necessitating the extrapolation of stock measurements from shallow core depths. Despite this, a clear trend was still seen at this site with significantly higher carbon content at

the 50 m distance. Furthermore, due to limitations in sampling opportunities, this study was unable to fully disentangle the effects of decommissioning on sedimentary carbon stocks without pre-decommissioning sample collection.

2.4.2. *Naturally occurring radioactivity from legacy oil and gas produced water discharges and impact on sedimentation rate estimations*

Elevated levels of ^{226}Ra were observed in the top 10 cm fraction of the cores collected within 200 m from North West Hutton likely reflecting the legacy discharge of produced water during the platform's operational phase (Ahmad et al., 2021; Olsgard & Gray, 1995). While the radiological and chemical impacts of these industrial contaminants on benthic communities remain unclear, these site-specific signatures offer a powerful tool for assessing the spatial and temporal extent of the impact of wastewater contamination to nearby sediment and help estimate sedimentation rates near oil and gas platforms.

The combination of ^{226}Ra and Ba concentrations provides a novel tool in environmental forensic science to determine the impact of offshore oil and gas platforms on local sedimentary processes in the North Sea. This method may overcome limitations associated with traditional nuclear tracers like ^{137}Cs (from Chernobyl and Sellafield), which are less effective offshore due to multiple sources and low concentrations (Arias-Ortiz et al., 2018). Determining offshore carbon accumulation rates remains a constraint on UK shelf sea carbon budgets (Luisetti et al., 2019). Currently, there are few novel forensic approaches including less conventional nuclear derived isotopes such as ^{129}I, but these approaches are generally limited to specific UK marine regions (Lérida Toro et al., 2022). As demonstrated in this study, using known operational timelines of offshore platforms allows the tracking of sedimentation and carbon accumulation rate in recent timescales. While current carbon stock measurements offer valuable insight into carbon dynamics, accurate accumulation rates are essential for understanding temporal changes

and improving carbon budget estimates for the UK shelf (Graves et al., 2022; Luisetti et al., 2019). In turn, we can disentangle the long-term impacts of man-made structures from other anthropogenic activities and determine how carbon stock dynamics vary across the shelf in an area of ocean which has historically had a poor resolution of mass accumulation of sediment.

Mass accumulation rates could not be determined accurately for sediment cores taken within 400 m of North West Hutton through traditional lead-210 measurement by gamma spectrometry, as these sediments showed elevated levels of heavy metals, including Pb and Ba causing high levels of matrix self-attenuation during gamma counting (Dal Molin, et al, 2018). In this context, the use of the alternative alpha spectrometric method for measuring polonium-210, ^{210}Po, a direct decay product of ^{210}Pb, would offer a more suitable analytical alternative.

2.4.3. *Influence of drill cuttings pile*

Both sites sampled in this study exhibit extensive drill cutting piles near the decommissioned structures, resulting from drilling operations that return hydrocarbon-rich rock to the seafloor (Ball et al., 2012). Drill cuttings often consist of drilling fluids (oil-based fluids, synthetic fluids, and water-based fluids) depending on the age of the structure and the drilling practice at the time of construction (Breuer et al., 2004). The higher mud content close to each site, and the subsequent change in sediment composition to finer, carbon rich particles, could be due to drill cuttings, which remain close to the drilling well (Breuer et al., 2004). At North West Hutton, wells were drilled with two types of drilling fluid, water-based fluids, for shallower (1000 m) sections of the well, and oil-based fluids for deeper drilling (BP, 2005). Similarly, at Miller, oil-based fluids were used throughout production as drilling fluids (Aquatera, 2007). Despite the presence of oil-based drilling fluid within drill cuttings piles at North West Hutton, organic carbon content at 50 m to 100 m was similar to 800 m to 3200 m, indicating that the pile had little effect on carbon content likely due to the final trawling

operations during decommissioning (BP, 2005) that would resuspend and disperse carbon enriched sediment. Conversely, Miller showed elevated organic carbon at 50 m suggesting possible enrichment from the cutting's pile. However, the influence of elevated hydrocarbons on sediment carbon storage from drill cutting piles was determined as an insignificant proportion of total organic carbon from initial results from Gregson et al., (under review) and measurements from the UK Benthos Database (Offshore Energies UK, 2015) (Appendix figure 1). Determining the contaminant composition and hydrocarbon influence on carbon stored around oil and gas decommissioned platforms would help identify the effect of drill cuttings piles on local microbes and fauna involved in carbon cycling.

2.4.4. *Local current regime*

Organic carbon stocks vary between direction of transects, particularly at North West Hutton. One potential influence is the local hydrodynamics. A study by Klunder et al (2018) observed a 'shadow' effect at the L7A decommissioned platform in the southern North Sea where the predominant current direction dictated a depleted gradient of total organic carbon with increasing distance; explained by a biofilter effect of epifauna and acceleration of flow due to the physical structure causing a deposition of particles at greater distance. However, North West Hutton is located on the edge of the North East Atlantic Current and only experiences small residual currents below 0.1 m/sec (De Dominicis et al., 2018; Winther & Johannessen, 2006) with a maximum current speed of 0.43 m/sec at the seabed (BP, 2005). Therefore, it is unlikely that hydrodynamics was the driver in different benthic measurements. Despite being affected by the Fair Isle/Dooley current, very little difference in organic carbon was seen between the North and South transects at Miller. However, hydrodynamics would likely play a larger role in more dispersive environments, such as the Southern North Sea, where the 'shadow' effect has previously been recorded (Klunder et al., 2018), and where drill cuttings piles do not persist due to dispersive hydrodynamics.

2. 5. Conclusion

In conclusion, this study finds that carbon dynamics around decommissioned platforms are site specific and therefore extrapolating carbon dynamics from one or two decommissioned sites across the North Sea is not recommended. Decommissioning practice and activity may have an impact on organic carbon stocks and dynamics within surface sediments; however, this requires sampling pre and post decommissioning to disentangle the effects. Future work could include carbon stock, sediment composition, and carbon accumulation assessments during all phases of oil and gas activity to determine the overall effect of these structures on sedimentary blue carbon throughout their operational and then decommissioning lifespan. By sampling pre-construction, during operational phase and pre- and post-decommissioning could provide greater insight into the effect of oil and gas activity on sedimentary blue carbon. This would also give an insight into OSPAR mandatory decommissioning; partial removal may reduce the impact on sedimentary blue carbon and maintenance of a small-scale exclusion zone at specific sites could provide protection for this elevated carbon.

Chapter 3: Correcting organic carbon accumulation rates in contaminated shelf sediments

3.1 Introduction

Continental shelf sediments are natural carbon stores (Diesing et al., 2017; Graves et al., 2022) and can accumulate vast amounts of organic carbon, particularly in depositional environments such as glacial troughs (Diesing et al., 2024). Due to their large spatial extent, shelf sea sediments are one of the largest carbon stores worldwide and globally marine sediments are estimated to store around 2,322 Pg of carbon in the top metre of sediment (Atwood et al., 2020). The North Sea and Skagerrak accumulates between 0.02 and 66.18 gC m^{-2} yr^{-1} (Diesing et al., 2021). This significant amount of sedimentary carbon has led to increasing study into the use of these natural ecosystems to mitigate climate change (Epstein & Roberts, 2022; Legge et al., 2020; Luisetti et al., 2019). Despite this, these environments are subject to various physical pressures including sediment dredging (Robinson et al., 2005), bottom trawling (Eigaard et al., 2017) and the introduction of man-made structures such as oil and gas platforms (Fowler et al., 2020; Techera & Chandler, 2015).

Determining the standing stock of carbon provides a useful snapshot of how much carbon is within a given area (Diesing et al., 2017; Krause et al., 2022; Smeaton, Hunt, et al., 2021), but assessing how this stock will vary temporarily by assessing organic carbon accumulation rates (OCARs) provides key evidence to establish the rate at which these stocks will increase over short term (accumulation) and long term (burial) timescales (Wilkinson et al., 2018). Despite their importance, observational measures of shelf sediment OCARs are rare and remain a significant research gap.

Organic carbon accumulation rates are calculated by either: measuring the concentration of organic carbon within sediment layers and ascribing dates to specific deposits; or by

determining sediment accumulation rates (SAR) via lead-210 (^{210}Pb) dating (Arias-Ortiz et al., 2018). Traditionally, ^{210}Pb, a naturally occurring radioisotope of lead (Pb) has been used as a tracer for dating aquatic sediments as its half-life of 22.2 years and its ubiquity in natural sediments offer a detailed geochronological framework for reconstructing sediment deposition within the last 100 years (Koide et al., 1972). Lead-210 is derived from uranium-238 through its decay series (Appleby & Oldfield, 1978). Its presence in marine sediments is primarily a result of in situ decay of radium-226 (^{226}Ra) (also known as supported ^{210}Pb) and atmospheric deposition following radon gas emission (also known as unsupported or excess ^{210}Pb). Various ^{210}Pb dating models can be applied to determine SARs and each modelling approach is associated with different assumptions (Arias-Ortiz et al., 2018). These ^{210}Pb derived estimations of SARs can then be multiplied by the organic carbon content to provide OCARs.

Nevertheless, despite the relatively straightforward preparative, analytical and modelling processes involved, the application of this geochronological tool is not without challenges (Barsanti et al., 2020). Quantification of ^{210}Pb via direct gamma spectrometric measurement can be affected by the presence of elevated levels of heavy elements that interfere with the low energy gamma-rays it emits (Dal Molin et al., 2018; Denny et al., 2022).. More worryingly, many non-nuclear industries, also known as Naturally Occurring Radioactive Material (NORM) industries, discharge waste containing elevated levels of heavy metals and naturally occurring radioelements, often including ^{210}Pb, ^{226}Ra (SEPA, 2014) into the marine environment, ending up in sediments. For example, phosphogypsum waste, produced during phosphate ore processing and fertilizer production, is known to contain enhanced levels of ^{226}Ra and ^{210}Pb along with many heavy metals and stable elemental analogues (Rutherford et al., 1994). This presents an additional challenge when using this ^{210}Pb dating technique to estimate SARs in marine regions directly affected by this type of industrial activity. The oil and gas industry is also a NORM emitting industry with oil extraction creating significant

discharges of waste water, also known as produced water, containing insoluble barium and strontium sulphate particles enriched in radium-226 (^{226}Ra), and to a lesser extent, ^{210}Pb (Ahmad et al., 2021). Recent work has shown changes in sedimentary carbon stocks around decommissioned oil and gas platforms, with clear elevation of ^{226}Ra in sediments linked to the operating lifetime of the structures themselves (Woodward-Rowe et al., 2025). Therefore, when assessing OCARs in sediments potentially contaminated by any NORM industry, such as legacy oil and gas extraction activity, it is important to consider the potential attenuation effect during gamma counting and subsequent impact on these OCAR estimations.

This study aims to refine OCAR estimations in sediments affected by legacy oil derived NORM and heavy metal contamination. By building on previous estimations of OCAR calculations around a decommissioned oil and gas platform (Woodward-Rowe et al., 2025), this study accounts for enhanced levels of heavy metals and naturally occurring radionuclides-present in the sediment to improve accuracy of OCAR estimations. Additionally, it presents an opportunity to develop a refined approach for correcting total ^{210}Pb via gamma spectrometry and validate it by comparing with an alternative radioanalytical method used for measuring ^{210}Po via alpha spectrometry, assuming and ensuring secular equilibrium with ^{210}Pb (Sanchez-Cabeza & Ruiz-Fernández, 2012). Corrected and uncorrected ^{210}Pb results along with ^{210}Po results are used to determine OCAR averages using CF-CS modelling. Finally, this study provides a framework for future organic carbon accumulation assessments in other offshore and coastal areas suspected of being affected by similar industrially contaminated sediment and derived NORM interferences.

3.2. Methods

3.2.1. Sample site, preparation and elemental characterisation

Sediment cores were collected at 50, 100, 200, 400 and 3,200 m (control) North and South of the decommissioned North West Hutton oil and gas platform (Figure 13). Each sediment core was sliced every 1 cm. After freeze-drying and sieving down to 500 µm, approximately 200 mg of each slice was digested using 15 mL of a mixture of ultra-pure HNO_3/HCl/HF (8/4/3) in a microwave system (CEM Mars 6, USA) for 60 minutes. The resulting acid digests were then further diluted prior to ICP-MS analysis (Agilent 7900ce, USA). Quantification of the six most abundant and interfering heavy elements (Al, Ba, Fe, Mn, Pb, Sr and Zn) was performed by external calibration using standard solutions ranging between 0 and 500 $\mu g.L^{-1}$. Levels were also determined in the certified reference material (CRM) IAEA-465 Baltic Sea sediment (International Atomic Energy Agency (IAEA)) used as a reference in the presented corrective approach (see section 2.2) (Pham et al., 2024).

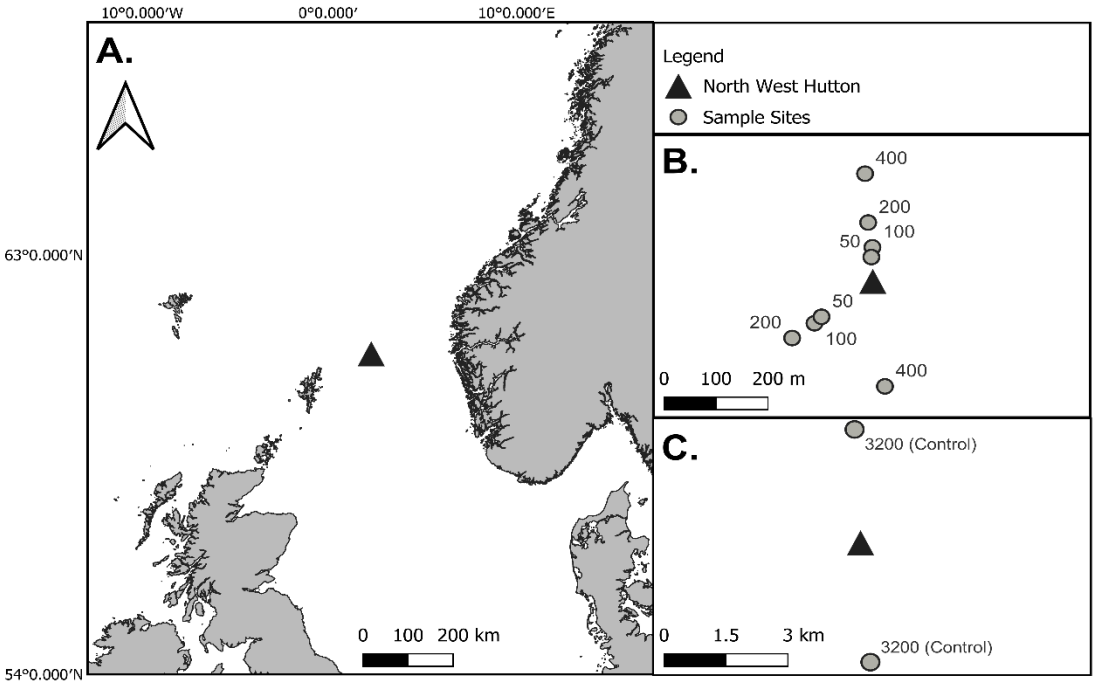

Figure 13: Location of the former North West Hutton oil and gas platform in the North Sea (A). Sampling sites closer (50 – 400 m) to the platform (B) and control sites (C). Note the difference in scale between B and C.

Between 50 and 100 mg of each slice was also analysed for total organic carbon (TOC) using a FormacsHT TOC Analyser with PrimacsMCS add-on module (SKALAR, The Netherlands). The amount of silicon (i.e., assumed in the form of pure silicate was also estimated from the relative percentage of sand (i.e., between 63 μm and 2 mm) obtained from particle size analysis using the laser diffraction unit Bettersizer S3 Plus (Bettersize Instruments Ltd, China) and sediment textural characterisation (Folk, 1954).

Additionally, approximately 30 g of each sample was mechanically compressed in a uniform plastic container that was then radon gas sealed and kept for at least for 21 days prior to high resolution gamma spectrometry analysis (ORTEC Broad Energy Germanium detector (BEGe), USA) to determine the activity concentration levels of total ^{210}Pb, ^{226}Ra (via lead-214) and ^{137}Cs, at 46.5, 352 and 662 keV, respectively (Barsanti et al., 2020). Each sample was counted for a minimum of 24 h to minimise the limit of detection and reduce counting

uncertainty as low as practically possible. A mixed radioelement standard solution in 4M HCl (National Physical Laboratory (NPL), UK) and the CRM IAEA-465, presented in the same geometry as other sediment samples, were used to perform the energy and efficiency calibrations of each BEGe detector used in this study, respectively.

To validate the presented matrix self-attenuation corrective approach (see section 2.2), total ^{210}Pb was also determined indirectly via alpha spectrometry by measuring ^{210}Po in several sediment slices. Approximately 0.3 g of freeze-dried material was spiked with a known amount of polonium-209 (^{209}Po) radiotracer (NPL, UK) and digested using 12 mL of a mixture of HNO_3/HF (3/1) in a microwave system (CEM Mars 6, USA). Saturated H_3BO_3 was then added to neutralise any remaining free fluoride ions. Thereafter, each sample was transferred to a glass beaker with 1M HCl solution and evaporated to dryness. 10mls of 6M HCl solution was then added and reduced to low volume. The sample was taken up in 25mls of 0.5M HCl solution to allow spontaneous deposition of ^{209}Po & ^{210}Po on a silver disc for 5 hours at 90°C. Each silver disc was finally counted via alpha spectrometry for up to 5 days (ORTEC Octête Plus, USA). Secular equilibrium was verified in selected slices collected at 50 m South of the former NWH platform. The sample solutions from the first silver plating were sealed and stored for approximately three months to allow for the ingrowth of ^{210}Po from ^{210}Pb decay. A second and similar plating operation was then performed, and discs were counted for up to 10 days via alpha spectrometry. Ingrowths of ^{210}Po then enabled to indirectly determine the initial amount of ^{210}Pb in each selected sediment core slice.

3.2.2. Matrix self-attenuation correction

The low energy 46.5 keV gamma rays emitted by ^{210}Pb can be severely attenuated by the presence of heavy elements as well as the bulk density of the material it is present in. As described in a study conducted by Dal Molin et al. (2018), the relative degree of attenuation

for a specific sample matrix can be determined using measurements of bulk density (ρ) and elemental composition and by comparing with a certified reference material containing a known amount of ^{210}Pb

As shown in Table 2, each element considered in this study presented a different mass attenuation coefficient (μ_i/ρ), expressed in cm^2/g. These coefficients were estimated by interpolating linearly between theoretical values presented in the literature at 40 and 50 keV. (NIST, 2004).

Table 2: Theoretical elemental mass attenuation coefficients estimated at 46.5 keV via linear interpolation between 40 and 50 keV. Attenuation coefficients for all values were sourced from the National Institute of Standards and Technology (NIST, 2004) Standard Reference Database 126.

Element	***Attenuation coefficient*** μ_i/ρ **(cm^2/g)**
C	0.194
O	0.229
Al	0.438
Si	0.530
Mn	2.223
Fe	2.543
Zn	3.764
Sr	6.885
Pb	10.250
Ba	17.560

The total mass attenuation coefficients μ_i/ρ for all selected sediment samples and the reference material (CRM IAEA-465) could then be calculated as follows (1):

$$\mu/\rho = (\Sigma\ (\mu_i/\rho))\ f_i \quad (1)$$

where f_i is the elemental weighing fraction (%) (Dal Molin et al., 2018).

A relative correction factor was determined using the certified ^{210}Pb activity concentration in the reference material (CRM IAEA-465 of 163 +/- 17 Bq/kg), combined with its mass attenuation coefficient and the mass attenuation coefficient calculated for each sediment sample from partial bulk chemical composition, particle size analysis and TOC. analysis Corrections were applied to characterised slices (where both ^{210}Po/^{210}Pb were measured) from cores collected within 200 m North and South from North West Hutton and, as NORM derived elemental signatures could not be observed beyond that distance.

3.2.3 CF-CS Modelling

See chapter 2 section 2.3.5 for detailed methods of radionuclide CF-CS modelling.

Both uncorrected and corrected ^{210}Pb activity concentrations obtained for each core slice from gamma spectrometric analysis and alpha spectromic were used as total ^{210}Pb inputs into the CF-CS models to assess the effects of the presented self-attenuation corrective approach on the estimations of SAR and age-depth relationship.

3.2.4. Estimation of Organic Carbon Accumulation Rates

Average MARs were determined from CF-CS of ten sediment cores collected at five distances (50, 100, 200, 400 and 3200 m) from each directional transect at North West Hutton (North and South). For each core, an OCAR (expressed in gC/cm^2/yr) was then calculated by multiplying the corresponding average MAR with the average OC concentration (%) information as follows (2):

$$OCAR = MAR \times \%OC \quad (2)$$

3.2.5. Statistical analysis

All statistical analysis was completed using R version 4.2.2. All figures were generated using '*ggplot2' (Wickham, 2010)* and '*cowplot*' (Wilk, 2020) packages. Data was initially tested for normality with Shapiro wilk tests (Shapiro & Wilk, 1965). Normally distributed activity concentrations from each method were compared with ANOVAs. For testing specific relationships between ^{210}Po ingrowths and ^{210}Pb linear models were used to test for significant relationships. Averages are reported as Mean ± standard deviation.

3.3. Results

3.3.1. Heavy metal distribution

Depth profiles of total barium, lead, and strontium which represented the three highest attenuation factors (Table 2) are displayed in Figure 14. The highest concentrations of all three elements were highest in the top 5 cm at 50 m on the northern transect. Specifically, highest concentrations of barium were predominantly observed within the top 5 cm of the cores obtained 50 m North and South from the former North West Hutton platform, with the highest concentration of 76,600 mg/kg observed in the top (surface) slice (0 – 1 cm) at 50 m on the northern transect. The highest concentration of lead was 950 mg/kg and was observed between 3 and 4 cm depth in the same core collected 50 m North. The highest concentration of strontium was also found at the top slice (0 – 1 cm) at 50 m on the northern transect with a value of 3300 mg/kg. These oil-derived heavy metal signatures were generally not detected beyond 200 m North but were marginally visible beyond 400 m South.

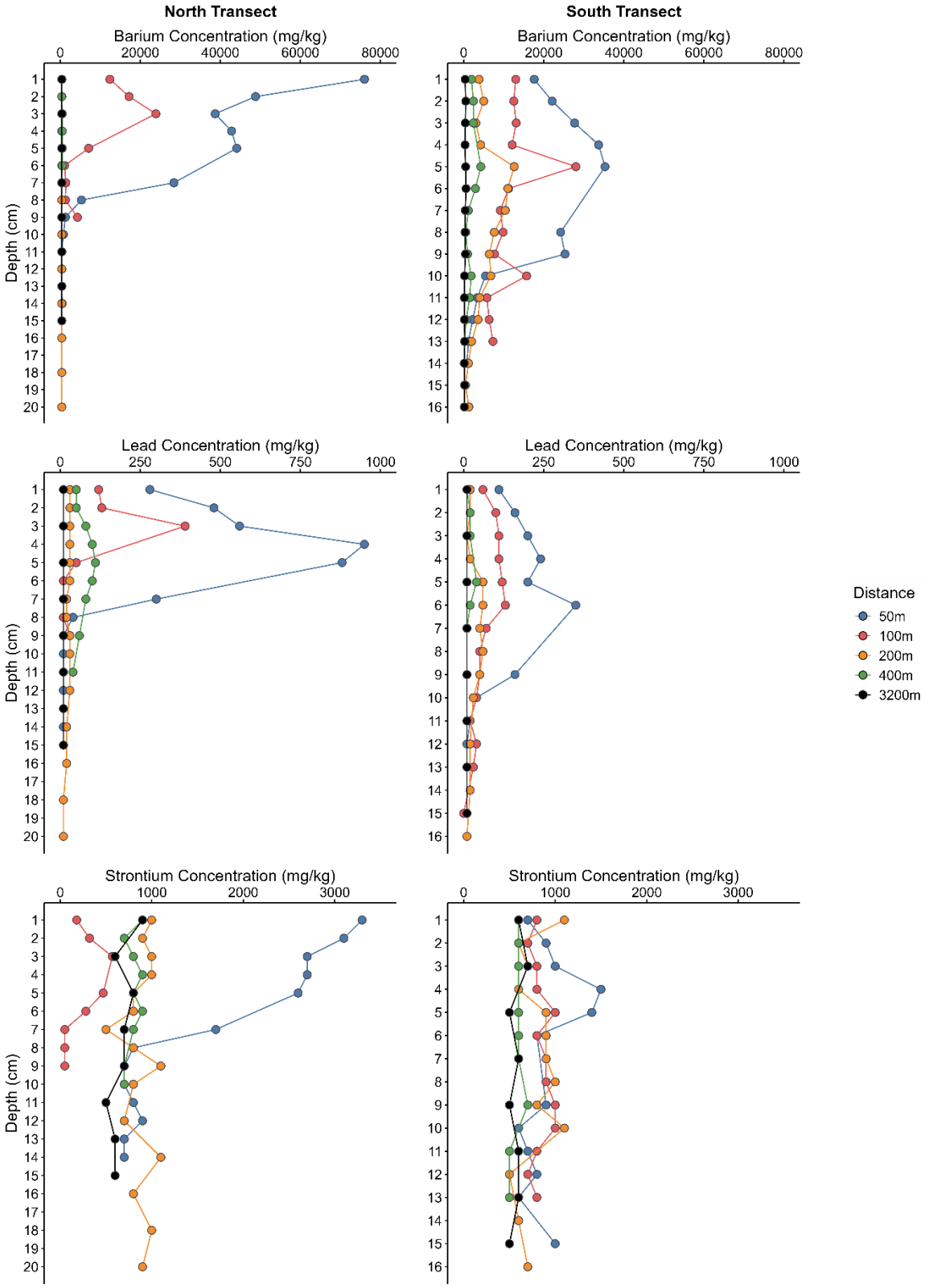

Figure 14: Barium, lead and strontium concentrations (mg/kg) of eight sediment cores from two distance transects (N/S) from the former North West Hutton with ranging distanced away (50, 100, 200, 400, 3200 m). Distance is indicated by colour.

3.3.2. Comparison of radioanalytical methods

Three different radioanalytical methods were used to determine activity concentrations of ^{210}Pb: i) via alpha spectrometry (i.e., ^{210}Po), ii) direct and uncorrected gamma spectrometry and iii) corrected gamma spectrometry (using relative attenuation coefficients) (Table 2). As illustrated in Figure 15, the corrected ^{210}Pb results obtained from initial gamma spectrometric analysis of the top 5 cm sediment slices collected at 50 m, 100 m and 200 m to 3200 m North and South of the North West Hutton were in relatively good agreement with the ^{210}Po results acquired from alpha spectrometric analysis. Activity concentrations derived from uncorrected gamma spectrometry showed significantly lower activity concentrations of ^{210}Pb compared to both alpha spectrometry (^{210}Po) and corrected gamma spectrometry (ANOVA, P = 0.00786). For example, at 50 m on the northern transect within the top 4 cm, the maximum activity concentration obtained from direct gamma spectrometric analysis was 73.48 Bq/kg, lower than maximum of 135.92 Bq/kg from alpha spectrometry analysis and 137.56 Bq/kg after attenuation correction. Similarly, both alpha spectrometry and corrected gamma spectrometry at these sites are within standard error bars and not significantly different. At greater distances on the southern transect (100 and 200 m), all three methods displayed similar activity concentrations (ANOVA, P = >0.05). Similarly, for the northern transect, activity concentrations were consistent and generally decreased with depth. At control sites, there is a good agreement between corrected ^{210}Pb and ^{210}Po results with elevated uncorrected ^{210}Pb likely from the uncharacterized fraction of the chemical composition used in the correction.

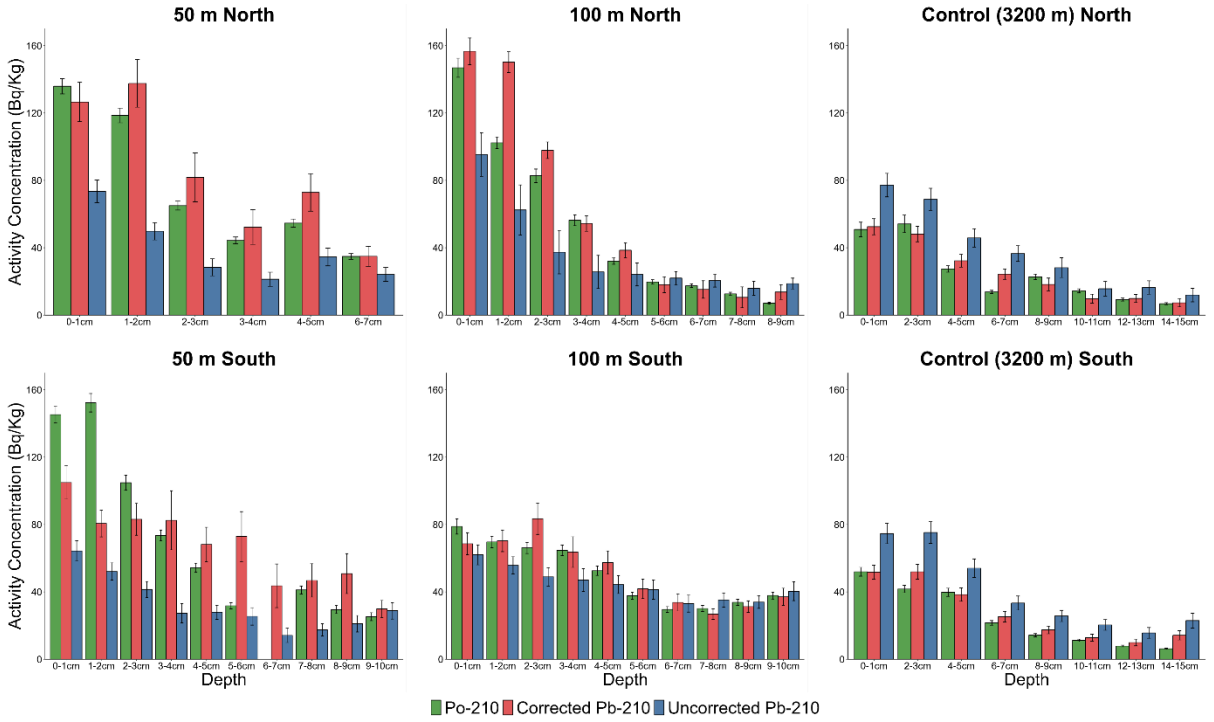

Figure 15: Determination of ^{210}Pb activity concentrations (Bq/kg) via three different radioanalytical techniques: alpha spectrometry (green), corrected gamma spectrometry (red) and uncorrected gamma spectrometry (blue) in six sediment cores collected at 50, 100 and 3200 m (Control) away from North West Hutton

Minor discrepancies were also observed between ^{210}Po and ^{210}Pb results obtained via ^{210}Po ingrowth, especially in top 5 cm slices collected close to North West Hutton (Figure 16), implying the presence of a small disequilibrium between ^{210}Po and ^{210}Pb. Nevertheless, the agreement remained acceptable ($R^2 = 0.86$) and a significant positive relationship was observed between ^{210}Po and ^{210}Pb results (ANOVA, $P < 0.001$).

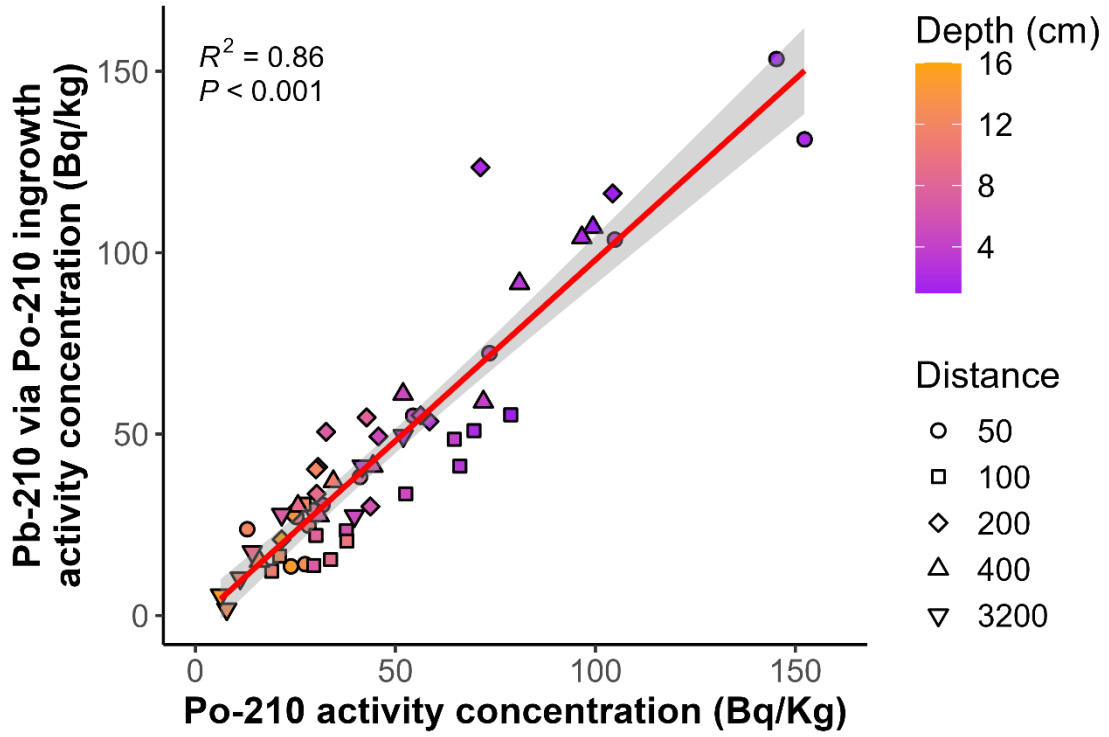

Figure 16: Correlation between ^{210}Po and ^{210}Pb determined via alpha spectrometry (i.e., ^{210}Po ingrowth after a period of 3 months) from sediment cores taken at the south transect from North West Hutton. Slice depth is represented using a colour gradient (purple = shallow depths, orange = greater depths). The solid red line represents the linear regression model which represents the overall trend between the two variables. The grey shaded area surrounding the regression line depicts the 95% confidence interval.

3.3.3. Organic carbon accumulation rates

Overall, OCARs determined using uncorrected ^{210}Pb activity concentrations from gamma spectrometric measurements were consistently higher than both other methods, especially at distances 50 m and 100 m from North West Hutton, more impacted by legacy NORM discharges. Estimations of OCAR using corrected ^{210}Pb values and ^{210}Po via alpha spectrometry generally showed little difference between values at each site with an average difference of 2.86 ± 12.88 gC/m^2/yr.

OCAR results from all three methods (uncorrected gamma spectrometry, corrected gamma spectrometry and alpha spectrometry) varied from 25.47 to 121.27 gC/m^2/yr around North West Hutton. However, OCARs calculated from indirectly estimated ^{210}Pb activity

concentrations via alpha spectrometry and attenuation correction values varied from initial gamma spectrometry values across all distances (Table 3). OCARs calculated using corrected gamma spectrometry and alpha spectrometry decreased at distances 50 m and 100 m on the northern transects and at 100 m on the southern transect. The mean OCARs estimated from corrected ^{210}Pb results at distances of 50, 100, and 200 m North and South appeared consistent with the mean OCAR estimations observed at 400 m with slight variation at 3,200 m. Furthermore, the mean OCARs derived from initial uncorrected ^{210}Pb data were overestimated by approximately 25.47% and 99.99% at 50 m and 100 m on the North respectively when compared to corrected values. On the southern transect, initial uncorrected ^{210}Pb data were overestimated at 100 m and 200 m (149.99 % and 9.10 % greater respectively). However, at 50 m initial OCARs by uncorrected ^{210}Pb underestimated slightly compared to corrected values (9.52%). These overestimations decreased to an average of 10.36 ± 7.55 % at from 400 to 3200 m on both transects.

Table 3: Comparison of carbon accumulation rates (gC/cm^2/yr), dry bulk density (DBD), average carbon content (%) from different distances (50, 100, 200, 400, 3200 m) on two transects (North/South) from North West Hutton decommissioned platform.

Distance (m)	**Direction (N/S)**	**Dry bulk density (DBD)**	**Average carbon content (%)**	**Uncorrected ^{210}Pb derived MAR (g/m^2/yr)**	**Corrected ^{210}Pb derived MAR (g/m^2/yr)**	**^{210}Po derived MAR (g/m^2/yr)**	**Uncorrected ^{210}Pb derived OCAR (gC/m^2/yr)**	**Corrected ^{210}Pb derived OCAR (gC/m^2/yr)**	**^{210}Po derived OCAR (gC/m^2/yr)**	**Increase/ Decrease**
50	N	1.42	2.83	2100	1700	1600	59.47	48.15	45.31	Decrease
100	N	1.55	2.28	1400	700	900	50.94	25.47	32.75	Decrease
200	N	1.42	1.31	2800	2800	3100	57.89	57.89	64.10	Same/Increase
50	S	1.40	2.78	1900	2100	1700	52.83	58.39	47.27	Slight Increase/Slight Decrease
100	S	1.12	2.17	3500	1400	1200	121.27	48.51	41.58	Decrease
200	S	1.44	2.02	1700	2200	1400	98.59	90.37	115.02	Slight decrease/Increase

3.4. Discussion

3.4.1.Correction of organic carbon accumulation rate estimations

This study demonstrated that OCARs determined using uncorrected ^{210}Pb values from direct gamma spectrometry can be significantly influenced, in this case, overestimated by up to 149.99 %, in chemically and anthropogenically impacted marine environments. The miscalculations observed in this study could be mainly attributed to matrix attenuation caused by the presence of enhanced levels of heavy metals (Dal Molin et al., 2018). While gamma spectrometry is a widely adopted, cost-effective analytical tool used in blue carbon assessment studies (Arias-Ortiz et al., 2018; Masque et al., 2002), its accuracy can be compromised in areas affected by NORM industrial effluent discharges. Two alternative radioanalytical approaches were used to overcome this limitation: (1) using relative factors based on the bulk chemical composition to correct initial gamma spectrometric measurements of ^{210}Pb, and (2) using ^{210}Po measured via alpha spectrometry after verifying secular equilibrium with ^{210}Pb (Figure 16). Although these approaches require more labour-intensive analytical work, they were essential for obtaining more accurate OCARs in marine environments impacted by industrially derived contamination.

Our findings revealed a clear spatial correlation between heavy metal contamination and the overestimation of OCARs. At distances close to North West Hutton (50 – 100 m), which were highly contaminated by heavy metals (Figure 14), OCARs generally decreased from initial estimations determined by ^{210}Pb derived from uncorrected gamma spectrometry (Table 3). Specifically on the southern transect at 100 m, OCARs decreased from 121.27 gC/cm^2/yr to 48.51 gC/cm^2/yr following correction. This represented an approximate 149.99 % initial overestimation. This discrepancy in OCARs diminished at greater distances from the platform, where heavy metal concentrations were lower.

Activity concentrations of ^{210}Pb and ^{210}Po were used to compare the accuracy between methods (Figure 16). Variance in OCARs was corroborated by readings of activity concentration from each technique as these provide the basis for ^{210}Pb derived sediment and OCARs (Arias-Ortiz et al., 2018). At sampling locations close to North West Hutton (50 – 100 m), both alpha spectrometry and corrected gamma spectrometry outputted significantly higher activity concentrations than uncorrected gamma spectrometry. Whereas at greater distances (200 – 3,200 m), there was no significant difference between activity concentrations from each method, likely linked to minimal presence of anthropogenically derived heavy metals.

3.4.2 Benefits and drawbacks of corrective methods

The development of site-specific attenuation correction factors enables the refinement of existing gamma spectrometry data without the need to repeat radionuclide measurements via other techniques. Correction values were calculated by determining the levels of most abundant heavy metals (Fe assumed as Fe_2O_3, Al assumed as Al_2O_3, Ba, Mn assumed as MnO, Sr, Zn, Pb), organic carbon and sand (assumed as pure SiO_2) concentrations within samples and multiplying the percentage mass of element/compound by a corresponding attenuation factor (Table 2). While this approach requires additional sample preparative and analytical work, this may be circumvented if relevant data, such as heavy metals concentration, are available from existing environmental impact assessments. Furthermore, collecting this supplementary data contributes to a more comprehensive understanding of the environmental context, as the determination of heavy metals is pertinent to a variety of environmental descriptors in polluted marine settings.

Determination of ^{210}Pb via gamma spectrometry is particularly susceptible to matrix attenuation caused by heavy metals, leading to an underestimation of activity concentrations (Dal Molin et al., 2018). Using alpha spectrometry removes the risk of heavy metal matrix

attenuation as sample preparation involves the destruction of the matrix through acid digestion (Jia & Jia, 2012). However, this method is labour intensive and requires additional health and safety considerations (e.g., use of hydrofluoric acid (HF)) to ensure full digestion of marine sediments.

3.4.3. Spatial distribution of NORM derived heavy metals

The highest concentrations of heavy metals, particularly Ba, Sr and Pb, were detected in the shallow sediments (0−10cm depth) at distances of 50−200m from the former North West Hutton platform (Figure 14). These heavy metals, particularly Ba, are likely to be present due to contaminated drills cuttings piles (Bakke et al., 2013; Breuer et al., 2004; Haanes et al., 2023) and produced water discharge (Ahmad et al., 2021; Dal Molin et al., 2023). Drilling cutting piles are a waste product of oil extraction where cuttings and residual drilling fluids (often oil based muds) are discharged directly into the water column and accumulate in sediments surrounding the operational oil and gas platform (Breuer et al., 2004). These often persist in the benthic environment long after decommissioning (Fortune & Paterson, 2020). These piles are known to contain higher concentrations of heavy metals such as Ba, Cr, Cu, Ni, Pb and Zn than those found in background sediments (Haanes et al., 2023; Olsgard & Gray, 1995). At distances greater than 400 m from North West Hutton, heavy metal concentrations were comparable to those of the control sites (i.e., 3,200 m), indicating that the contamination was localised to the immediate vicinity of the cuttings piles with some potential transport from the predominant NE/SW local current. This spatial pattern of heavy metal contamination directly corresponds to the sediment depths and distances where the largest discrepancies were observed between uncorrected gamma spectrometry, corrected gamma spectrometry, and alpha spectrometry measurements.

3.4.4 Study considerations and limitations

Despite accounting for heavy metal attenuation to correct radionuclide measurements, a remaining confounding factor is the input of anthropogenic radionuclides, specifically ^{210}Pb and ^{226}Ra to nearby sediments from oil and gas produced water. Produced water discharges include micro-sized radiostrontiobarite particles which elevate the activity concentration of ^{226}Ra and levels of Ba and Sr above the background level (Ahmad et al., 2021). This artificial enrichment can also compromise the accuracy of OCAR calculations, as ^{226}Ra activity is typically used to determine the supported fraction of ^{210}Pb (Appleby & Oldfield, 1978). Nevertheless, this can be overcome by averaging the ^{226}Ra activity concentration from deeper sediment slices (>10 cm), which are below the depth of this impact, and are similar to levels observed at 400 and 3,200 m which were outside the zone of contamination throughout sediment cores (Woodward-Rowe et al., 2025).

Furthermore, discrepancies were observed between the ^{210}Po and corrected ^{210}Pb results (Figure 16), which can be attributed to several factors. First, the high levels of silicates (>80%) in some sediment materials may have led to incomplete digestion processes despite the use of hydrofluoric acid (HF), which is essential for accurate ^{210}Po estimations via alpha counting. Additionally, both stable elemental and ^{210}Po analyses were performed on small aliquots, which may not be fully representative of the potentially heterogeneous sediment core materials. This could be overcome by analysing a higher number of replicates, however, this would be far more labour intensive. Secondly, minor discrepancies were also noted between the ^{210}Po and ^{210}Pb results from ingrowth analysis in selected top 5cm slices at 50m South of North West Hutton. This suggests a minor disequilibrium between ^{210}Po and ^{210}Pb, likely indicating the presence of anthropogenically derived ^{210}Po and ^{210}Pb. Similarly to ^{226}Ra, this can also cause inaccuracy in OCAR calculations. This highlighted the need for a non-impacted control site (such as the 3200m distance described in this study) which allows for the determination of background

^{226}Ra and ^{210}Pb. The presence of anthropogenic ^{210}Pb also provided a challenging limitation as decerning the fraction of anthropogenic ^{210}Pb to unsupported/supported ^{210}Pb can only be achieved through stable isotopic fractionation (Dinsley et al., 2019). Therefore, future work could include determining the anthropogenic fraction of ^{210}Pb to further refine the presented estimations of OCARs or using dating tools other than ^{210}Pb such as ^{228}Th (Tamborski et al., 2022).

3.4.5 Recommendations for future blue carbon assessments

Including these considerations into future blue carbon assessments would provide greater confidence and resolution of OCARs in sediments impacted by anthropogenically derived contamination particularly from NORM industries. While continental shelf sediments generally exhibit lower sedimentation and carbon accumulation rates compared to vegetated coastal habitats (Duarte et al., 2013; Macreadie et al., 2019; Macreadie et al., 2017; Ouyang & Lee, 2014), the UK coastline is host to numerous NORM industries, including iron, steel, aluminum, thorium, uranium, titanium dioxide production and China clay extraction sites (SEPA, 2014). For example, in Maryport Harbour, UK, anthropogenic inputs of ^{210}Pb and ^{226}Ra from a legacy phosphate production site presented challenges for ^{210}Pb dating and required further forensic investigation and complex modelling considerations (Abril-Hernández, 2025; McCartney et al., 1990). Similarly, the approach provided can be applied further, and globally, to specific blue carbon stock accumulation assessments. For example, recent work describing Tunisian blue carbon accumulation rates in coastal sediments included some sites influenced by phosphogypsum (Oueslati et al., 2025). This type of industry is likely to emit anthropogenic ^{226}Ra and ^{210}Pb and alter subsequent calculations (Abril-Hernández, 2025). Therefore, without corrective or alternative measures, SAR estimations using uncorrected ^{210}Pb values from gamma spectrometric analysis in these coastal areas would likely be biased. Our findings highlighted the critical need for a more comprehensive approach to blue carbon assessments in

these coastal environments to ensure the accuracy and reliability of carbon budget estimations, and identification of areas of potential contamination could highlight where this approach may be better suited for alternative OCAR measurements.

While alpha spectrometry and attenuation factors to correct original gamma spectrometry reading have been shown to improve estimations of OCARs, these techniques require significant additional analytical work. Therefore, we recommend focusing these more intensive techniques only on areas known to be affected by heavy metal and/or NORM contamination rather more generically. Although this study focused on offshore sediments, where OCARs are typically low unless in specific depositional environments such as trenches and glacial troughs (Diesing et al., 2024), it still clearly demonstrated how not accounting for localised metal contamination can lead to the over estimation, albeit small in this case, of OCAR estimations. These findings are particularly significant when applied to coastal environments, where both SARs and organic carbon concentrations are typically higher (Ouyang & Lee, 2014; Wilkinson et al., 2018). Coastal environments are also subject to a wider range of anthropogenic pressures, including industrial effluent discharges, which can lead to widespread sediment contamination (Li et al., 2022). Consequently, future blue carbon research initiatives requiring OCAR estimations in these environments should incorporate these analytical considerations and challenges to ensure the accuracy of carbon inventory and budget estimations.

3.5 Conclusion

This study highlighted a critical issue in calculating OCARs in marine sediments affected by human activities, specifically heavy metal contamination and NORM, which in this case originated from legacy oil extraction activities in the North Sea (North West Hutton). This work demonstrated that the use of ^{210}Pb data from direct gamma spectrometry can lead to significant

overestimations of OCARs in these impacted environments due to the presence of elevated concentrations of heavy metals affecting the weak 46.5 keV gamma ray emitted by ^{210}Pb.

Our findings showed that sediments collected near the former North West Hutton platform (50 − 100 m) contained elevated levels of heavy metals, in particular, Ba, Sr and Pb which directly inhibited the accuracy of activity concentration measurements through traditional gamma spectrometry. To overcome this limitation, we validated two alternative approaches: the use of either heavy metal attenuation correction factors, or alpha spectrometry to quantify ^{210}Po. Both methods yielded more accurate activity concentrations, leading to more reliable and robust OCAR estimations.

However, these improved methods require additional analytical work such as determining heavy metal concentrations through ICP-MS and more intensive sample preparative steps prior to alpha spectrometry analysis. Therefore, these techniques should be targeted to marine areas known to be contaminated by heavy metals. Although our study focused on shelf sediments, which typically exhibit low OCARs, the implications of this work are particularly relevant to coastal environments with increased contaminant loadings. These zones often have higher organic carbon accumulation potential but are also subject to greater levels of contaminants. Therefore, integrating these rigorous methods into blue carbon assessments is crucial to ensure accuracy and reliability of OCAR estimations in industrially impacted coastal zones.

Chapter 4: Source Identification of Sedimentary Organic Carbon at Decommissioned North Sea Platforms

4.1. Introduction

Despite only accounting for 10-20% of the global seafloor, shelf sediments play a key role in the global carbon cycle (Ausín et al., 2021) and act as significant stores of organic carbon (Hedges & Keil, 1995; Legge et al., 2020). This source of this organic carbon is varied (Middelburg, 2018), with a large proportion being supplied by marine phytoplankton (De Haas, 1997). These organisms convert CO_2 into organic carbon via photosynthesis (De La Rocha & Passow, 2007) and a small proportion of this settles on seabed sediments after travelling though the water column (Soetaert et al., 2000). Typically shelf sediment also experience organic carbon input from terrestrial sources (Smeaton & Austin, 2022b) from coastal zones and rivers outflows with dominant inputs often dictated by proximity to land, oceanographic conditions and currents (Diesing et al., 2017).

Determining provenance of organic matter within shelf sediment provides valuable insight into carbon flows from various sources (Alt-Epping et al., 2007; Tesi et al., 2007). This distinction is often determined using stable isotopes specifically $\delta^{13}C_{org}$ and $\delta^{15}N$ (Craig, 1953) as well as C/N ratio (Middelburg & Nieuwenhuize, 1998). Terrestrial organic carbon typically has a $\delta^{13}C_{org}$ range of between 26 and 28% and a $\delta^{15}N$ of around 3.5% (Middelburg & Nieuwenhuize, 1998), whereas marine derived organic carbon typically has a $\delta^{13}C_{org}$ of around 22% and a $\delta^{15}N$ of 9% (Fontugne & Duplessy, 1981). Methods using stable isotopes to determine carbon origin rely on assigning these end member values to terrestrial and marine organic carbon sources (Thornton & Mcmanus, 1994). When combined with simple binary mixing models, these values can determine the fractional contribution of each source to the total organic carbon.

Carbon sources within shelf sediments can also include non-natural inputs, particularly hydrocarbon pollution from oil and gas infrastructure. Offshore O&G platforms represent point sources of hydrocarbon-derived organic carbon to marine shelf environments (Ball et al., 2012). These sites are often the source of hydrocarbon rich cutting muds (Bakke et al., 2013; Breuer et al., 2004) that accumulate on the seabed surrounding the structure into drills cuttings piles (Olsgard & Gray, 1995). These piles often persist near the platform even after decommissioning, providing a unique anthropogenic organic carbon source in addition to established marine and terrestrial sources. Attributing this anthropogenic carbon source as ‘blue’ or marine without proper provenance determination may incorrectly assume its climate mitigation potential. Therefore, distinguishing the proportion of anthropogenic carbon from natural carbon in sediments provides insight into the climate change mitigation potential of anthropogenically modified shelf sea carbon storage, thereby preventing an overestimation of sedimentary 'blue' carbon.

The source and composition of organic carbon is intrinsically linked to its reactivity, which is defined as how easily organic carbon is degraded or remineralised into CO_2 (Bianchi et al., 2018; Smeaton & Austin, 2022a). The organic carbon that settles in shelf sediments consists of a variety of molecules ranging from highly reactive (labile) to lower reactivity (recalcitrant) (Capel et al., 2006). In these systems, labile organic carbon is fresh, marine material from phytoplankton or faeces that will be quickly mineralised by microbes using oxygen pathways in the oxic layer of sediments (Middelburg, 2018). Terrestrially sourced organic carbon usually has a lower reactivity in marine systems (Hedges & Keil, 1995). Anthropogenic hydrocarbon-derived organic carbon is characterized by its unique molecular signatures such as polycyclic hydrocarbons (PAHs), alkanes, and alkenes (Abbasian et al., 2015). The lability of this complex mix of compounds can vary depending on their specific composition (e.g., long-chain vs. short-chain PAHs) and environmental conditions like

temperature (Potts et al., 2019). Therefore, determining the fraction of sedimentary carbon that is either labile or recalcitrant can indicate how physical disturbance and resuspension might alter organic carbon storage over time (Hiddink et al., 2023; Sciberras et al., 2016).

The aim of this study is to identify the source contribution and lability of organic carbon found within sediment at varying distances from two decommissioned O&G platforms in the North Sea by using stable isotope, thermogravimetric and hydrocarbon analysis. By combining analytical approaches, this study aims to robustly demonstrate how O&G infrastructures can alter sedimentary carbon pools in shelf sediment.

4.2. Methods

4.2.1 Study site

For a detailed summary of study area, see chapter 2 section 2.1.

4.2.2 Stable isotope analysis

Each 1 cm slice was freeze dried to ensure majority of water loss. To determine stable isotope ($\delta^{13}C_{org}$ and $\delta^{15}N$) composition of samples, approximately 15 mg of sediment was placed into tin capsules and sealed, and a further 15 mg of sediment was placed into silver capsules. Samples within silver capsules were treated with 15 µl of 10% HCL and left to dry for 48h at 40 ºC . Pipetting of HCL was repeated until no visual effervescing was seen to indicate all carbonate ($CaCO_3$) was removed. Following this step, samples in silver and tin capsules were sealed.

Stable isotope analysis was conducted using an isotope ratio mass spectrometer (IR-MS)(Agilent 7500, USA). Samples treated with acid within silver capsules were analysed for $\delta^{13}C_{org}$ and samples within tin capsules were analysed for $\delta^{15}N$.

4.2.2.1.1 *Fraction of terrestrial/marine/hydrocarbon organic carbon*

End members of marine and terrestrial sources with stable isotope ($\delta^{13}C_{org}$ and $\delta^{15}N$) and bulk (C/N) values from coastal, nearshore and offshore sediment associated samples were taken from a dataset by Smeaton et al. 2022. Marine source values were taken from macroalgae, microalgae zooplankton, finfish aquaculture waste; intertidal source values were from saltmarsh vegetation and roots, seagrass; and terrestrial source values were from soil, peat and living and dead biomass. For determining a marine/hydrocarbon ratio, a mixing model was run with average $\delta^{13}C$ values from crude oil from North West Hutton oil field (Sofer, 1984).

4.23 Thermogravimetric analysis (TGA)

Approximately 40mg of freeze-dried sample was weighed into 70ml aluminium oxide crucibles and places into a Mettler Toledo TGA2. The sample was heated from 40ºC to 1000ºC under ramp heating at a rate of 10ºC min^{-1} while under a constant stream of N_2. Thermograms were clipped to remove 40ºC - 200ºC and 650ºC – 1000ºC to eliminate interference from inorganic sources and absorbed water.

4.2.3.1 Carbon reactivity Index (CRI)

Methods for calculating CRI were acquired from Smeaton and Austin, 2022. TGA thermal output was characterized into reactivity fractions (Capel et al., 2006) to indicate liability. These fractions were defined as labile (200°C–400°C), recalcitrant (400°C–550°C) and refractory (550°C–650°C). CRI was determined using equation 1 (Smeaton & Austin, 2022). Where OM_R is organic matter recalcitrant.

$$CRI = \frac{\%OM_R}{\%TotalOM} \quad (1)$$

Results of CRI range from 0, indicating organic matter within the sample is fully biodegradable and reactive, to 1 where organic matter is entirely non-biodegradable/recalcitrant/refractory.

4.2.4 Fluorescence Spectrometry

A subset of cores from North West Hutton (50 and 3200 m North transect and 50 and 3200 m South transect) were analysed for total hydrocarbon content (THC) by ultra-violet fluorescence spectrometry (UVF) (Kelly et al., 2000). Freeze dried samples of sediment core slices (using the same samples as in Chapter 2) were analysed using established analytical methods described in detail in Kelly et al., 2000.

Briefly, sediment samples were treated by spiking with an analytical surrogate consisting of a suite of deuterated PAHs (naphthalene-d8, acenaphthylene-d8, anthracene-d10, dibenzothiophene-d8, pyrene-d10, benzo[a]anthracene-d12, benzo[a]pyrene-d12 and dibenz[a,h]anthracene-d14) and extracted by alkaline saponification in methanolic potassium hydroxide followed by liquid/liquid solvent extraction using glass-distilled grade pentane and drying of the extracts with sodium sulphate. The total hydrocarbon concentration in the extracts was determined by means of ultra-violet fluorescence spectrometry as a screen of the level of hydrocarbon contamination in the sample.

It should be noted that there is no absolute measure of fluorescence emission, and the spectrofluorometer is first calibrated with an appropriate reference standard solution of North Sea Forties crude oil, appropriate for the geographic context of this current study. Thus, THC by UVF is a semiquantitative estimate of the level of hydrocarbon contamination on a dry weight basis.

4.2.5 Statistical analysis

All statistical analysis was conducted using R version 4.2.1. All figures were generated using the '*ggplot2*' (Wickham, 2010), and '*cowplot*' (Wilk, 2020) packages. Data was initially tested for normality using Shapiro-Wilks tests (Shapiro & Wilk, 1965) and subsequent Bartlett tests (Bartlett, 1937) to determine homogeneity of variance between groups. Normally distributed data were tested for significance using ANOVAs, with p-values adjusted for multiple comparisons using the Benjamini-Hochberg procedure (Benjamini & Hochberg, 1995), followed by a Tukey's HSD (Tukey, 1953) post hoc test within the 'agricolae' (De Mendiburu, 2020) package. Non-normally distributed data were tested for significance using a Kruskal-Wallis test, with p-values adjusted for multiple comparisons with Bonferroni corrections (Bonferroni, 1936), followed by Dunn's post hoc test (Dunn, 1964) within the 'FSA' package (Ogle et al., 2020). To test the relationship between THC and F_{anthro} a linear model was fitted. Spearman correlation tests were applied to assess all other correlations between variables from each platform. Averages are reported as Mean ± standard deviation.

4.2.5.1 Binary mixing model

Two binary mixing models (2,3), based on Thornton and McManus (1994) was used to determine the fraction of terrestrial organic carbon and anthropogenic organic carbon using $\delta^{13}C_{org}$ from each sediment slice samples and end members of from marine, terrestrial and hydrocarbon averages. These binary mixing models were chosen over Bayesian techniques to allow for a comparison between other studies (Smeaton & Austin, 2022b). The average F_{anthro} value from all sediment at the control sites from both Miller and North West Hutton was averaged and subtracted from all other F_{anthro} values as no contamination was seen in control cores.

$$Fterr = \frac{(\delta^{13}C_{sample} - \delta^{13}C_{marine})}{(\delta^{13}C_{terrestrial} - \delta^{13}C_{marine})} \quad (2)$$

$$F_{terr} + F_{marine} = 1$$

$$\%OC_{terr} = F_{terr} \times \%OC$$

$$Fanthro = \frac{(\delta^{13}C_{sample} - \delta^{13}C_{marine})}{(\delta^{13}C_{anthropogenic} - \delta^{13}C_{marine})} \quad (3)$$

$$F_{anthro} + F_{marine} = 1$$

$$\%OC_{anthro} = F_{anthro} \times \%OC$$

4.3. Results

4.3.1. Bulk elemental and stable isotope analysis

Bulk elemental and stable isotope concentrations are displayed in table 4. Mean organic carbon content of sediments across all distances from Miller was 1.15% with significantly higher values closer to the platform at 50 m compared to all other distances (Kruskal-Wallis, $\chi2 = 33.85$, df = 3, $P < 0.001$). For North West Hutton, organic carbon content of sediments across all distances were consistently higher with a mean of 3.19%, the only difference at 200 m being significantly lower than sediment at 100 m, 400 m and 3200 m, but otherwise staying constant (Kruskal-Wallis, $\chi2 = 31.59$, df = 4, $p < 0.001$) (Figure 18). At Miller the carbon reactivity index (CRI) of sediments had a mean value of 0.77. CRI at Miller did very significantly with distance, with sediments at 200 m having a significantly lower CRI than those at 50 m (Anova, F = 6.08, df = 2, $P < 0.05$). Conversely at North West Hutton CRI did not vary with distance with a mean CRI of 0.78. Additionally, the mean $\delta^{13}C_{org}$ at Miller was -22.27. This significantly varied with distance (Anova, F = 39.37, df = 3, $p < 0.001$), with $\delta^{13}C_{org}$ significantly increasing from 50 m to 200 m (Tukey, $P < 0.05$) where it remined consistent with the control site ($P = 0.92$). For North West Hutton, mean $\delta^{13}C_{org}$ was -21.94 with significant differences between all distance groups with higher $\delta^{13}C_{org}$ with distance (Anova, F = 71.61, df = 4, $p < 0.001$) expect for 200 with 400 m and 3200 m which did not vary. Comparison of $\delta^{13}C_{org}$ and organic carbon content (%) are displayed in appendix figure 7. Mean $\delta^{15}N$ values at Miller was 5.91 and at North West Hutton the mean value was 6.05 and did not vary with

distance. At Miller, the mean N/C value was 0.11, with significantly higher values at 200 m and 3200m compared to 50 m and 100 m (Kruskal-Wallis, $\chi 2 = 31.82$, df = 3 $P < 0.001$). At North West Hutton the mean N/C value was 0.12 but did not vary with distance.

Table 4: Mean ± standard deviation for bulk chemical and stable isotope characteristics for sediment cores at varying distances (50 – 3200) from Miller and North West Hutton.

Site	OC (%)	$\delta^{13}C_{org}$	$\delta^{15}N$	CRI	N/C
Miller	1.15 ± 1.00	-22.27 ± 0.06	5.91 ± 0.47	0.76 ± 0.05	0.11 ± 0.04
North West Hutton	3.19 ± 1.37	-21.93 ± 0.54	6.05 ± 0.41	0.79 ± 0.02	0.11 ± 0.02

4.3.2. Source distribution of organic matter

Organic carbon derived from marine, terrestrial and anthropogenic average end members were assigned $\delta^{13}C_{org}$ and N/C values (Table 5) to determine the relative contribution of each source (Figure 18). For sediment samples located near Miller and North West Hutton $\delta^{13}C_{org}$ and N/C values were closer to the marine end member than either anthropogenic or terrestrial end members. For this study, results are primarily focused on the marine/anthropogenic source contribution however, results from the terrestrial mixing model for comparison can be found in appendix figure 8. Sediments at greater depths were closer to a marine source of carbon (Figure 18). The mean fraction of anthropogenic carbon (F_{anthro}) at Miller was 0.06 (range 0 to 0.21) with significantly higher values found close to the site at 50 m and 100 m (0.09 ± 0.05) at shallow depths compared to 200 m and 3200 m (0.01 ± 0.01) (Anova, F = 39.37, df = 3, p <0.001) (Figure 18). The same pattern was seen at North West Hutton, mean F_{anthro} was 0.05 (range of 0 to 0.20) with significantly higher values at 50 m and 100 m (0.11 ± 0.04) compared to all other distances (200 m, 400 m and 3200 m) (0.02 ± 0.02) (ANOVA, F = 71.61,, df = 3, $p < 0.001$) (Figure 18).

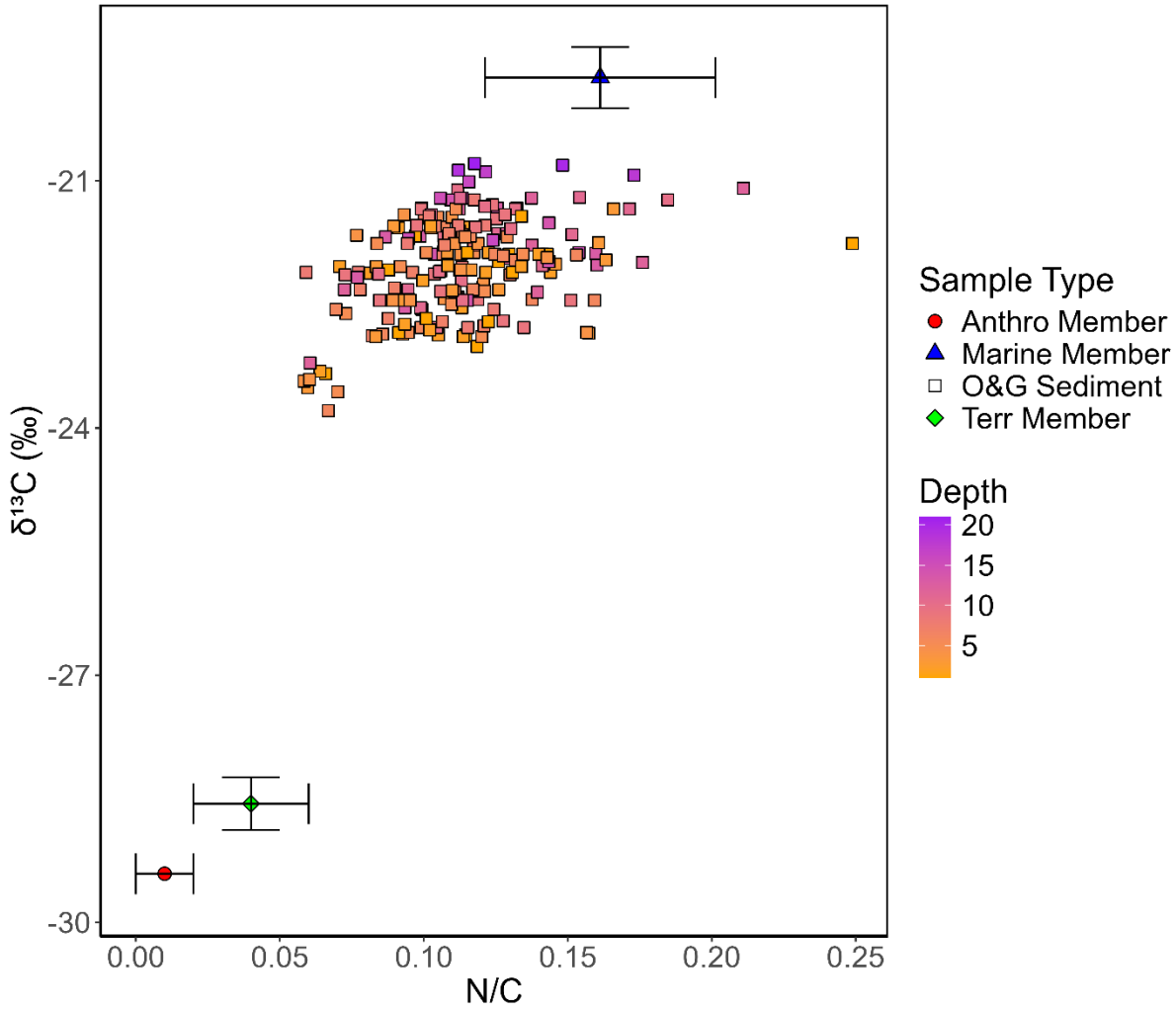

Figure 17: Comparison of nitrogen/carbon ratio and stable isotope values for sediments from two decommissioned oil and gas platforms with corresponding values from marine, terrestrial and anthropogenic end members used in binary mixing models The bars around the end member values represent standard deviation.

Table 5: Organic carbon sources and their end members using in binary mixing models and data visualisation Full data set for marine and terrestrial values are detailed in Smeaton et al. 2022. Anthropogenic end member was determined from Sofer (1984) and Nagham and Nuha (2021).

Source	**$\delta^{13}C_{org}$**	**N/C**
Marine	-19.74 ± 0.37	0.16 ± 0.04
Terrestrial	-28.56 ± 0.32	0.05 ± 0.02
Anthropogenic	- 29.41	0.01 ± 0.01

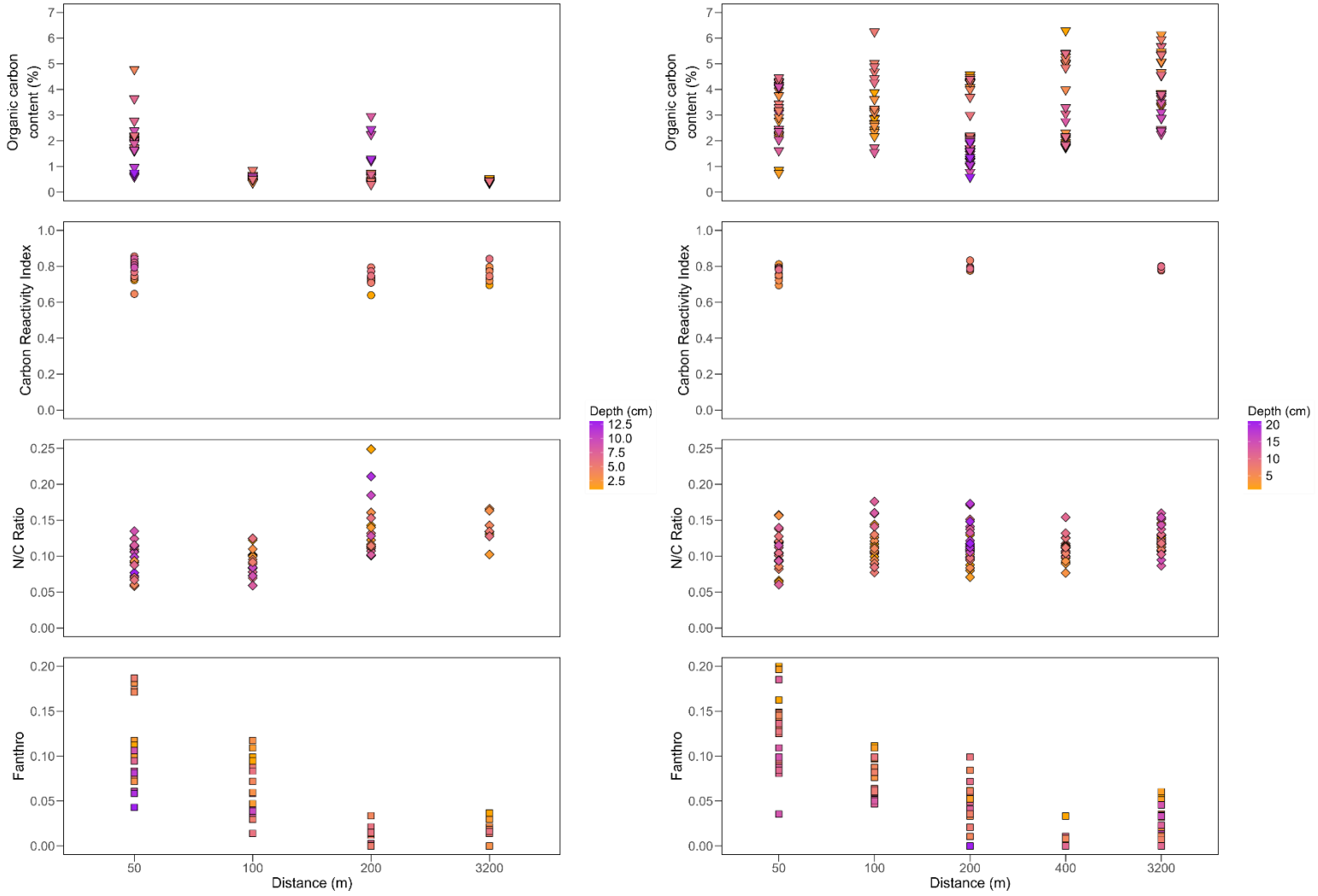

Figure 18: In order from the top: organic carbon content (%), carbon reactivity index , N/C ratio (atomic) and the calculated fraction of organic carbon content from anthropogenic sources (F_{anthro}) from sediment cores from varying distances (m) from two decommissioned O&G platforms, Miller (left plots) and North West Hutton (right plots). F_{anthro} at control sites was averaged and removed from other results .

4.3.3. Hydrocarbon contribution to total carbon

The mean source contribution to total organic carbon (%) from hydrocarbons across 50 m and control sites was 4.60 % and ranged from 0.02 to 42.99% (Figure 19). Highest contribution was found in shallower sediment depths (> 10 cm) at both 50 m North and South with a range between 0.32 to 42.99%. Of the total organic carbon content in the top 10 cm of sediment cores at 50 m hydrocarbons made up 10.67% on the south transect and 15.90% on the north transect. At both control sites, the contribution of hydrocarbons to total organic carbon was minimal with a range between 0.0008% to 0.001%.

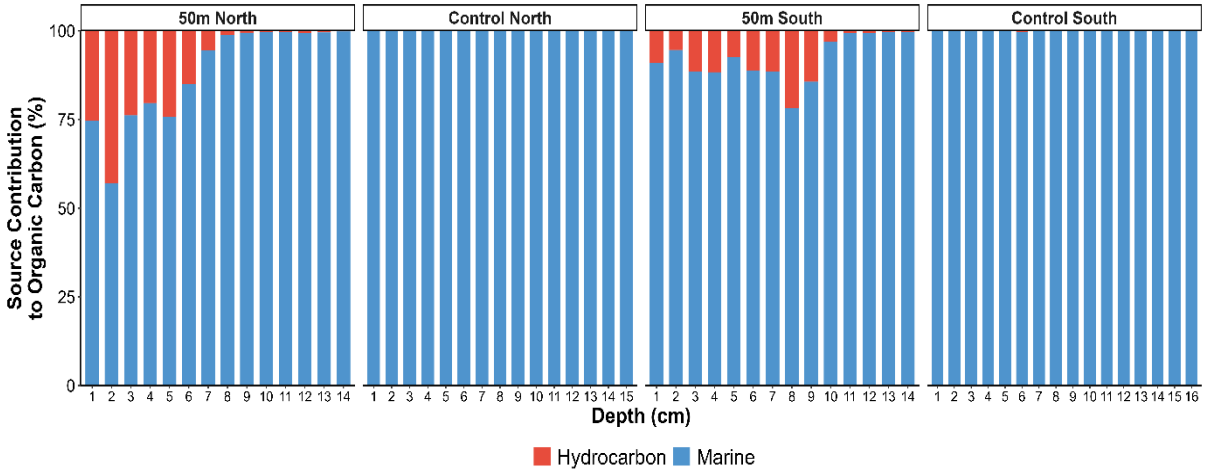

Figure 19: Source contribution of total hydrocarbon content and to total organic carbon content (%) within four sediment cores taken at 50 m and 3200 m (Control) from North West Hutton. Hydrocarbon contribution is indicated by red bars and marine contribution is indicated by blue bars.

4.3.4. Relationship between total hydrocarbons and F_{anthro}

To validate F_{anthro} output from binary mixing models for North West Hutton, this was compared to the source contribution of hydrocarbons to organic carbon (Figure 20). The F_{anthro} produced from the binary mixing model has a significant strong positive correlation ($P < 0.001$) with hydrocarbon percent of organic carbon ($R^2 = 0.47$).

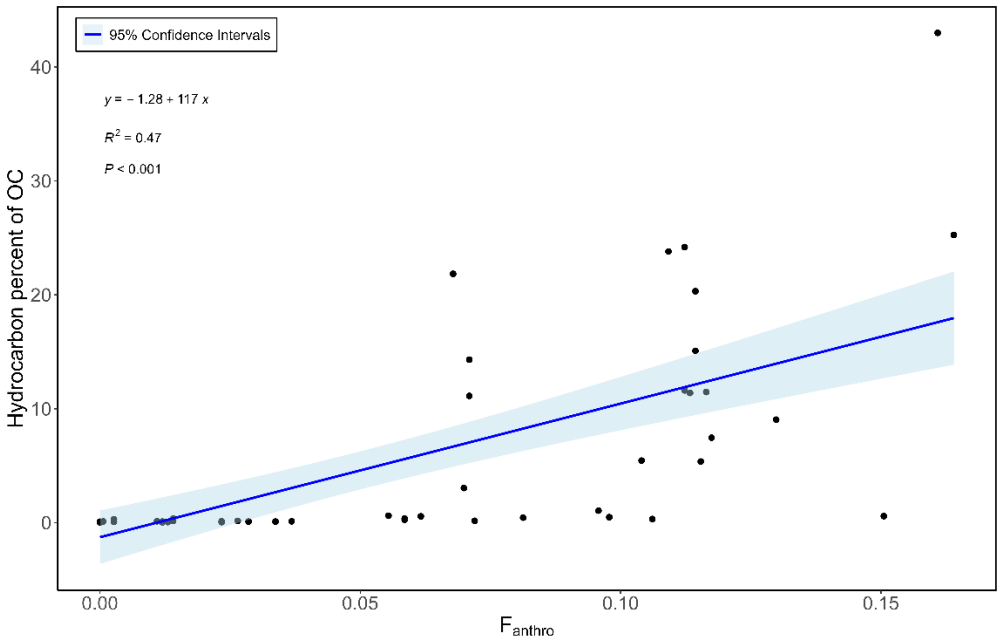

Figure 20: Comparison of F_{anthro} values from the binary mixing model to log-transformed hydrocarbon percent of organic carbon. The solid blue line represents the regression line (y = -9.95 + 35.9x) and the shaded blue area indicates 95% confidence intervals. R^2 is 0.47 a p-value ($P < 0.001$) suggests a statistically significant correlation.

4.3.5. Correlation analysis

Spearman's correlation analysis between measured variables was separated by site (Figure 21). Where Spearman's ρ values are positive this shows a positive correlation and where they are negative this shows a negative correlation. For Miller, F_{anthro} was significantly negatively correlated to distance (Spearman's ρ = -0.81, P > 0.001), percentage sand (Spearman's ρ = -0.63, P > 0.001), N/C (Spearman's ρ = -0.59, P > 0.001), dry bulk density (Spearman's ρ = -0.70, P > 0.001) and significantly positively correlated to organic carbon (Spearman's ρ = 0.42, P > 0.001), percentage mud (Spearman's ρ = 0.63, P > 0.001). At North West Hutton, F_{anthro} was significantly negatively correlated to distance (Spearman's ρ = -0.66, P > 0.001), depth (Spearman's ρ = -0.39, P > 0.001), percentage sand (Spearman's ρ = -0.32, P > 0.001), N/C (Spearman's ρ = -0.17, P > 0.05), dry bulk density (Spearman's ρ = -0.49, P > 0.001) and significantly positively correlated to total hydrocarbons (Spearman's ρ = 0.83, P >

0.001), organic carbon (Spearman's ρ = 0.17, P > 0.05), percentage mud (Spearman's ρ = 0.32, P > 0.001). At Miller CRI was significantly negatively correlated to distance (Spearman's ρ = -0.37, P > 0.05), percentage sand (Spearman's ρ = -0.71, P > 0.001), dry bulk density (Spearman's ρ = -0.48, P > 0.05), and significantly positively correlated to depth (Spearman's ρ = 0.53, P > 0.001), organic carbon (Spearman's ρ = 0.49, P > 0.05), percentage mud (Spearman's ρ = 0.71, P > 0.001). At North West Hutton, CRI was not significantly correlated to any variable. Finally, at North West Hutton, total hydrocarbon content was significantly negatively correlated with distance (Spearman's ρ = -0.85, P > 0.001), depth (Spearman's ρ = -0.80, P > 0.001), percentage sand (Spearman's ρ = -0.52, P > 0.001), dry bulk density (Spearman's ρ = -0.80, P > 0.001), $\delta^{13}C_{org}$ (Spearman's ρ = -0.84, P > 0.001), N/C (Spearman's ρ = -0.40, P > 0.05) and significantly positively correlated to percentage mud (Spearman's ρ = 0.52, P > 0.001).

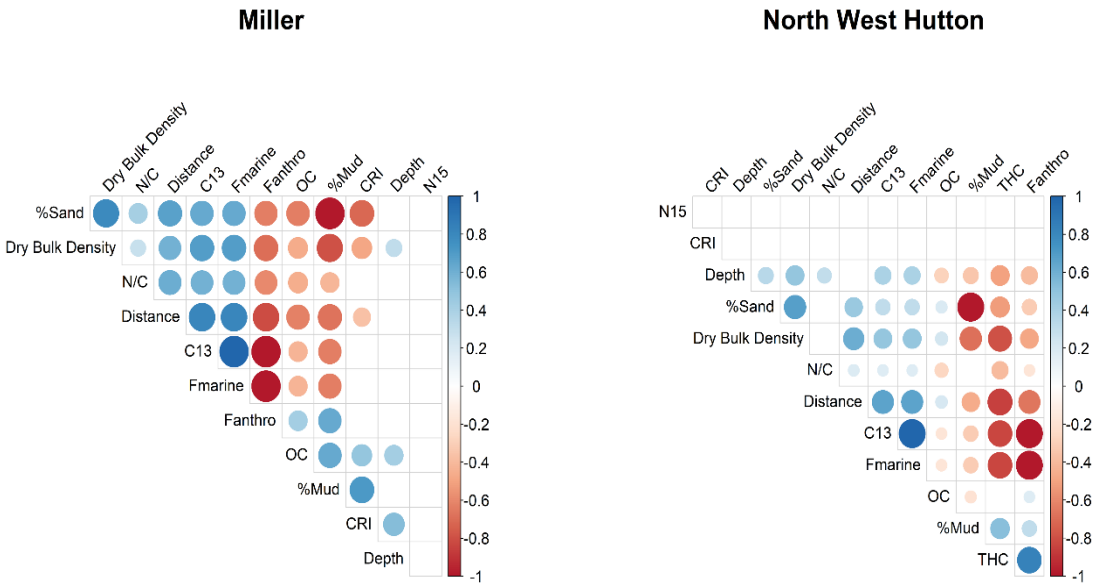

Figure 21: Correlogram of Spearman's correlation (ρ) (P < 0.05) between measured variables, organic carbon (OC), distance, depth, total hydrocarbons (THC), percentage sand, percentage mud, $\delta^{13}C_{org}$, $\delta^{15}N$, N/C, fraction marine and fraction anthropogenic for both Miller and North West Hutton. Size of circles represent level of significant with larger circles indicating higher significance. Colour of circles indicates direction (blue = positive, red = negative). Relationships without significance are left blank.

4.4. Discussion

Shelf sediments are a globally important ecosystem which contain vast amounts of organic carbon due to their large spatial extent (Bianchi et al., 2018; Diesing et al., 2017; Diesing et al., 2021; Legge et al., 2020). However, these systems have been historically impacted by the construction of energy infrastructures, particularly O&G platforms which can emit contaminants that affect the environment and the organisms therein (Bakke et al., 2013; Breuer et al., 2004; Chen et al., 2024) and can potentially alter the existing organic carbon stock and its vulnerability. The contribution of anthropogenic carbon from these structures to the total carbon stock of shelf sediment is a significant research gap. This study determines the contribution of anthropogenic carbon to the total carbon pool from two, now decommissioned, O&G platforms in the North Sea; Miller and North West Hutton. Sediments surrounding both Miller and North West Hutton showed elevated fractions of organic carbon from anthropogenic sources (F_{anthro}) (0.09 to 0.11) close to each site (50 to 100 m) which decreased with distance to 200 m where it remined constant to the control site. The fraction of anthropogenic carbon had a strong positive correlation to measured total hydrocarbon at North West Hutton, which validates the results from the anthropogenic binary mixing model. Hydrocarbon percent of total organic carbon in the top 10 cm of sediment was significantly higher at 50 m (10.69 to 15.90%) from North West Hutton compared to the control site (0.0008% to 0.001%). Finally, the reactivity of sediments (from CRI) was consistently low and showed little variation with increasing distance from both sites, suggesting that the presence of these structures and input of HCs does not alter vulnerability of shelf sediment organic carbon.

4.4.1. Fraction of anthropogenic carbon

The highest fraction of anthropogenic carbon (F_{anthro}) was found predominantly in sediments closer to the Miller and North West Hutton platforms (50 m) and at shallower

sediment depths, with average values of 0.09 ± 0.05 and 0.11 ± 0.04 respectively. This finding was validated at the North West Hutton site by using ultra-violet fluorescence spectrometry (UVF) to measure total hydrocarbon content (THC) as a specific marker of the anthropogenic source. While organic carbon sources in shelf sediments are often defined on a spectrum from terrestrial to marine (Bianchi et al., 2002; de Haas et al., 2002), this study proposes a combined marine/anthropogenic model, given that these environments receive specific inputs of anthropogenic organic carbon. The high hydrocarbons concentrations near each site are likely due to drills cuttings piles that accumulate around the platform feet (Breuer et al., 2004). Drill cuttings piles are the accumulation of drilling solids, fluids, muds, sediments and chemicals as waste products from offshore drilling operations which are rich in various hydrocarbons (Lytle & Lytle, 1979; Olsgard & Gray, 1995). These piles often persist even following the decommissioning process (Martins et al., 2023; Sommer et al., 2019), which was seen at both Miller and North West Hutton (BP, 2005, 2011). F_{anthro} contribution to total carbon at both sites level out at 200 m and remain constant to the control sites. Elevated F_{anthro} was present in shallower sediment, due to hydrocarbon deposition being limited to the surface layers. This indicates that hydrocarbon contamination ends at a distance between 100 m and 200 m, supporting previous work showing contamination from North West Hutton has significantly reduced by 200 m (Chapter 2, and Woodward-Rowe et al, 2005).

While total hydrocarbons were only measured for sediment cores from North West Hutton, the strong correlation between total hydrocarbon content and F_{anthro} could be driving the fraction of anthropogenic contribution to organic carbon at Miller, which also saw highest F_{anthro} close to the site. Previous THC contributions to OC stock determined from the UK Benthos Database (Offshore Energies UK, 2015), which used GC-MS rather than florescence spectrometry, indicate that the Miller platform similarly shows higher THC closer than at greater distances (Woodward-Rowe et al., 2025). However, this can be further corroborated

with a strong correlation with THC and mud content, with only sediments close (50 m) to Miller having significantly higher percentage of fine particles (Woodward-Rowe et al., 2025), likely due to accumulated drilling muds (CNR International, 2013). However, this fails to explain the different relationships between organic carbon and distance from each site. Miller shows highest organic carbon content close to the site, whereas sediments at North West Hutton had lowest organic carbon content at 50 m which did not vary greatly at greater distances. Therefore, at North West Hutton, another variable such as lateral transport (Klunder et al., 2018), or protection from disturbance could be influencing how marine derived organic carbon content within sediment varies with distance (Woodward-Rowe et al., 2025). To better determine the site-specific contribution of hydrocarbons to total carbon, future work should include GC-MS or UVF analysis at multiple sites with a greater coverage of distance.

N/C ratio was also used to validate binary mixing models used to determine the source contribution to total organic carbon content. The N/C ratio was significantly negatively correlated to F_{anthro} at both sites. At Miller highest N/C values were present at 200 m and control site at Miller which mirror lower values of F_{anthro} with distance. However, at North West Hutton highest N/C values were found at 100 and 200 m with only a weak negative correlation (-0.17) to F_{anthro}. In this study, validating F_{anthro} results with the traditionally used N/C ratio was not as reliable or robust as THC. If the source causing the change in F_{anthro} is hydrocarbons, the N/C ratio, which is typically used for determining terrestrial/marine source contribution (Alt-Epping et al., 2007; Thornton & Mcmanus, 1994), is a poor indicator of source contribution. Therefore, combining multiple techniques and measurements is vital to maintain accuracy of results.

4.4.2. Hydrocarbons

Total hydrocarbons present in sediments, particularly close to North West Hutton, represent a broad spectrum of compounds including alkanes, alkenes, PAH's (Bakke et al., 2013; Olsgard & Gray, 1995; Peng et al., 2008). In the marine environment, various microbes use these hydrocarbons as an energy source or electron donors (Abbasian et al., 2015) through aerobic or anaerobic degradation (Leahy & Colwell, 1990). Microbial degradation rates will vary depending on the presence of oxygen (Leahy & Colwell, 1990) and the molecular structures of specific hydrocarbons within drill cuttings piles (Wang et al., 2018). Specifically low-molecular weight PAH's (those with two or three aromatic rings) are more labile than high-molecular weight PAH's (those with four or more aromatic rings) which leads to altered rates of microbial degradation (Wang et al., 2018). The final outputs of these interactions is H_2O and CO_2 which is released into the water column (Atlas, 1981). This represents an, albeit small, source of CO_2 to the water column as microbial degradation acts upon the hydrocarbons within the drills cutting piles. Therefore, this source of organic carbon not only fails to contribute to climate mitigation but also generates CO_2 that would have otherwise been sequestered for geological timescales. Future work to accurately constrain the amount of CO_2 produced from entire drills cuttings piles could determine how these sites might be sources of carbon to the water column.

Depending on the time since operation, the respective drills cutting piles at both sites will be degrading at different rates. North West Hutton commenced oil production in 1983 and produced for 20 years until 2003 (BP, 2005). Miller produced oil from 1992 for 18 years till 2003 (BP, 2011). With North West Hutton having an older drills cuttings piles, the degradation will have altered the composition of the piles to be more recalcitrant and contain PAH's with higher molecular weight as the lower-weight molecules will have be degraded preferentially (Wang et al., 2018). This represents a less reactive source of organic carbon at North West Hutton compared to Miller. This implies that at North West Hutton, since decommissioning

concluded 2009, higher amounts of CO_2 have been released from the cuttings piles through natural degradation (as with any OC source).

4.4.3. Carbon reactivity

Carbon reactivity at all distances from both sites was low, which is typical of shelf sediment (Smeaton & Austin, 2022a). Continental shelfs often have less reactive organic carbon, as there are high levels of labile matter degradation due to well oxygenated bottom waters (Hartnett et al., 1998); high rates of organic matter consumption through the water column and during diagenesis (Bianchi et al., 2021; Middelburg, 2019); and enhanced resuspension of sediment through natural mobility (Coughlan et al., 2021) and trawling (De Borger, Tiano, et al., 2021; Eigaard et al., 2017). The only variance with CRI was at 200 m from Miller which showed significantly higher reactivity compared to 50 m and the control site. However, the effect size was small therefore this result is unreliable. The addition of anthropogenic carbon, in this case hydrocarbons, is not likely alter the CRI measured from shelf sediment samples as these are also highly recalcitrant (Abbasian et al., 2015). The reactivity of organic carbon within sediment would likely change due to temperature changes, particularly with increasing bottom water temperatures (Malinverno & Martinez, 2015). With climate change increasing sea water temperatures the carbon stored within these sediments could be at greater risk to mineralisation (Bianchi et al., 2018; Legge et al., 2020).

Determining reactivity through TGA comes with limitations. TGA heats uses ramped heating of sediment samples to ~1000 ºC and measures the weight of the sample through this process to produce thermograms (Smeaton & Austin, 2022a). However, degradation of organic matter is facilitated by microbes using various pathways and electron doners to convert organic carbon to CO_2 (Soetaert et al., 2000). Therefore, how easily the organic fraction of sediment is converted to CO_2 by temperature increase might not directly relate to a biological lability, i.e.

how easily a microbe may be able to mineralise organic matter. Determining the activity concentrations of organisms actively mineralising the organic matter within in-situ sediment would give greater insight into the specific reactivity (and vulnerability) of the carbon stored within.

4.4.4. Implications for blue carbon science

These results have implications for the 'blue carbon' stocks of shelf sediments and their ability to contribute to climate change mitigation. This study shows that local near-site contamination can alter the typical organic carbon pool, specifically in shallower sediments where these deposits are made. As typical stock estimates are constrained to 10 cm (Graves et al., 2022), our results indicate that the organic carbon stocks in shelf seas are not all marine/terrestrially derived in localised areas of contamination and therefore vary in their ability to contribute to climate mitigation. It should be noted however, that this area of effect (within 50 m of an oil and gas platform) represents a small amount of the entire shelf. Both Miller and North West Hutton had up to 0.11 F_{anthro} (11%) close to the sites indicating a significant source contribution. Specifically at North West Hutton hydrocarbons made up between 10.67% and 15.90% of total carbon content in the top 10 cm at 50 m from the site with a similar potential result found at Miller. This increases initial estimates from previous estimations of 8% (Woodward-Rowe et al., 2025) using the UK benthos data set V5.17 (Offshore Energies UK, 2015). This highlights that carbon assessments should be more rigorous to not mislabel carbon as natural without identifying the carbon source.

With the North Sea containing over 1250 O&G installations (Fortune & Paterson, 2020), these results represents a localised source of organic carbon which is not typical of shelf sediments. However, THC did not correlate with organic carbon content, which suggests that elevated levels of hydrocarbons are not drivers of an increase in organic carbon at 50 m or at

greater distances. Furthermore, despite having high levels of THC at 50 m from North West Hutton, carbon content increases with distance from the platform site, with highest levels found at the control site. This suggests that hydrocarbon content does not drive organic carbon content in these sediments as it only explains up to 15.90% of total stock.

4.5. Conclusion

Anthropogenically derived organic carbon, particularly that which emit from O&G platforms in the form of drills cuttings piles, will account for a small percentage (between 10.67% and 15.90%) of the total organic carbon pool in the top 10 cm of shelf sediment near associated structures.

Due to site specific carbon source assumptions, this study used a binary mixing model to determine the fraction of anthropogenic carbon rather than traditional marine/terrestrial model. The fraction of anthropogenic carbon followed a similar trend as THC with significantly elevated levels close (50 and 100 m) to both sites at shallow depths. These hydrocarbons found in drills cuttings piles represent a local contamination which is deleterious to the marine environment but also are degraded over time which represents a minor potential source CO_2 from these sites. Furthermore, carbon reactivity, measured by TGA, was not affected by the presence of either site and was composed of unreactive recalcitrant organic carbon despite the addition of anthropogenic carbon in the source of hydrocarbons.

These findings highlight that various sources of organic carbon are present in the marine environment, and shelf sediments with energy infrastructure may contain anthropogenic carbon which needs to be accounted for in blue carbon assessments to ensure reliable carbon budgets.

Chapter 5: Organic carbon mineralisation of temperature controlled disturbed subtidal sediments

5.1. Introduction

Subtidal marine sediment has the potential to mitigate climate change by capturing and sequestering organic carbon over long term geological timescales (Lovelock & Duarte, 2019; Macreadie et al., 2019). These sediments contain the oceans largest organic carbon stores, estimated to up to ~ 87 Gt of OC globally (Atwood et al., 2020). Despite this, these sediment are subject to intense disturbance due to anthropogenic activity, including fisheries activity such as bottom trawling (De Borger, Tiano, et al., 2021; Eigaard et al., 2017; Epstein et al., 2022), and lifecycle activity and decommissioning of energy infrastructure (Birchenough & Degraer, 2020; Fowler et al., 2020; Heinatz & Scheffold, 2023; Sommer et al., 2019). This disturbance reworks and resuspends seabed sediments, mobilising stored organic carbon (Epstein et al., 2022; Heinatz & Scheffold, 2023). For offshore infrastructure, the construction phase is likely to cause significant sediment upheaval from a range activities including dredging for foundations (Guo et al., 2022; Schneider & Senders, 2010) and pile driving for steel jacket or monopiles (Wu et al., 2019). Disturbance is also caused during the removal or decommissioning of the structure, particularly under OSPAR in the North Atlantic regions, which requires complete removal of the whole structure as far as is feasibly possible (Fortune & Paterson, 2020). This process also involves significant sediment disturbance through removing of foundations and jackets (Fortune & Paterson, 2020), and a final trawl around the area to capture any snagging points (Woodward-Rowe et al., 2025).

These sediment disturbance events lead to the resuspension of sediment particles and organic carbon into the water column, where the carbon will be exposed to oxygenated seawater, particularly if it has come from below the oxic layer in the sediment (De Borger,

Tiano, et al., 2021; Epstein et al., 2022). This oxygenation could potentially increase the amount of organic carbon that is mineralised to dissolved organic carbon (DIC, or CO_2) (Black et al., 2022; Dauwe et al., 2001). This surface sediment disturbance leads to particle resuspension in the water column, with heavier particles falling back to the seabed quicker than the finer particles, which remain suspended for longer (Breimann et al., 2022). Recent studies have shown how the disturbance of surface sediment layers can increase mineralisation levels (Dounas et al., 2007; Justin Tiano et al., 2024). Some modelling studies, focusing on trawling as a disturbance, have implied that induced disturbance can release 55 – 60% of sediment organic carbon to atmospheric CO_2 within 7 – 9 years (Atwood et al., 2024; Sala et al., 2021). However, with the current lack of empirical evidence, the fate of disturbed sedimentary organic carbon remains and significant research gap (Hiddink et al., 2023), as organic carbon remineralisation is dependent on a complex series of biogeochemical factors including bottom water temperature, sediment type, carbon composition and benthic community composition.

The likelihood of remineralisation of marine organic carbon is directly linked to its vulnerability and lability (Arndt et al., 2013; Black et al., 2022; Howard et al., 2020). The reactivity of carbon is often measured as its likelihood of remineralisation (Epstein et al., 2022). This ranges from labile carbon, which is readily remineralised, to refractory carbon, which is not easily degraded (Smeaton & Austin, 2022a). For instance, in areas where deposition and accumulation is low, and organic carbon is more reactive , resuspension is more likely to cause higher rates of mineralisation. However, lability of marine organic carbon is not well understood or easily measured, and to date, the only way to characterise its liability is through using the carbon reactivity index (CRI) as described by Smeaton and Austin (2022) (and measured in Chapter 4). This index is derived from Thermogravimetric Analysis (TGA), where sediment samples are heated to above 1000 ºC under an inert gas (N_2), at increasing ramped temperature ‘steps’. The resulting mass loss across specific temperature ranges (Capel et al.,

2006) allows for the delineation of organic carbon lability fractions (labile, recalcitrant and refractory). The CRI itself is calculated as the proportion of refractory OC relative to total OC, where values approaching zero indicate higher lability (scale of 0 – 1). However, this method of ramped heating alone might not entirely capture how easily organic carbon within sediments is remineralised when it is microbes which are facilitating this degradation *in situ* (Hunter et al., 2006). Therefore, a more comprehensive understanding of marine organic carbon vulnerability requires bridging the gap between thermochemical lability and the actual *in situ* microbially mediated degradation rates, and has not yet been achieved.

Finally, subtidal sediments experience changes to the input of organic carbon as climate change warms both the water column and bottom water (Quante & Colijn, 2016), which alters the processes resulting in carbon deposition on the seabed (Burdige, 2007). This thermal forcing enhances organic recycling processes in the water column, consequently reducing the input of fresh organic carbon available for burial as proportionally less carbon reaches the seabed (Legendre et al., 2015). Critically warmer bottom temperatures will also increase the rate of mineralisation of stored organic carbon in the seabed (Middelburg, 2019), and the rate at which mineralisation may occur when carbon hits the seabed in warmer temperature conditions. Mineralisation rates generally increase with temperature until a thermal optimum is reach, as this process is driven by microbes, and increasing temperature elevates the metabolic rate of microbes (Malinverno & Martinez, 2015). Furthermore, these processes can become acute due to short-term marine heatwaves where water temperatures rise rapidly, leading to faster organic carbon mineralisation. Therefore, understanding the risk of disturbed organic carbon via multiple modes of action (trawling, infrastructure construction and other extractive uses) in a warming environment remains a key research gap.

This pilot study is primarily a methodological exploration to quantify how organic carbon remineralisation rates, measured via sediment oxygen consumption, are influenced by sediment

type, sediment depth within the core (representing trawling gear penetration depths), and temperature (ambient, elevated). This experimental design would provide insight to the potential mineralisation caused by acute disturbance of subtidal sediments from activities such as the construction, lifecycle and decommissioning of offshore infrastructure under changing temperature conditions, as well as the impacts of trawling.

5.2. Methods

5.2.1. Study area

Sediment cores were collected from subtidal coastal sediment near East Mersea, United Kingdom from 24/03/25 to 30/06/25 (Figure 22). Per sampling trip, five push cores (*⌀ 6cm)* of a length of 10 cm depth of sediment, and capturing bottom water to ensure an intact sediment water interface, were taken from the sample sites (one muddy site and one mixed sediment site). These were transported to the University of Essex and kept in a temperature controlled (8 ºC) dark room with aquarium aerators in each core's overlying water, and in situ water collected separately, until use (no longer than 5 days). One core from each sampling trip at each site was sliced into 1 cm increments and kept frozen at – 40 ºC for biogeochemical analysis (see section 2.4).

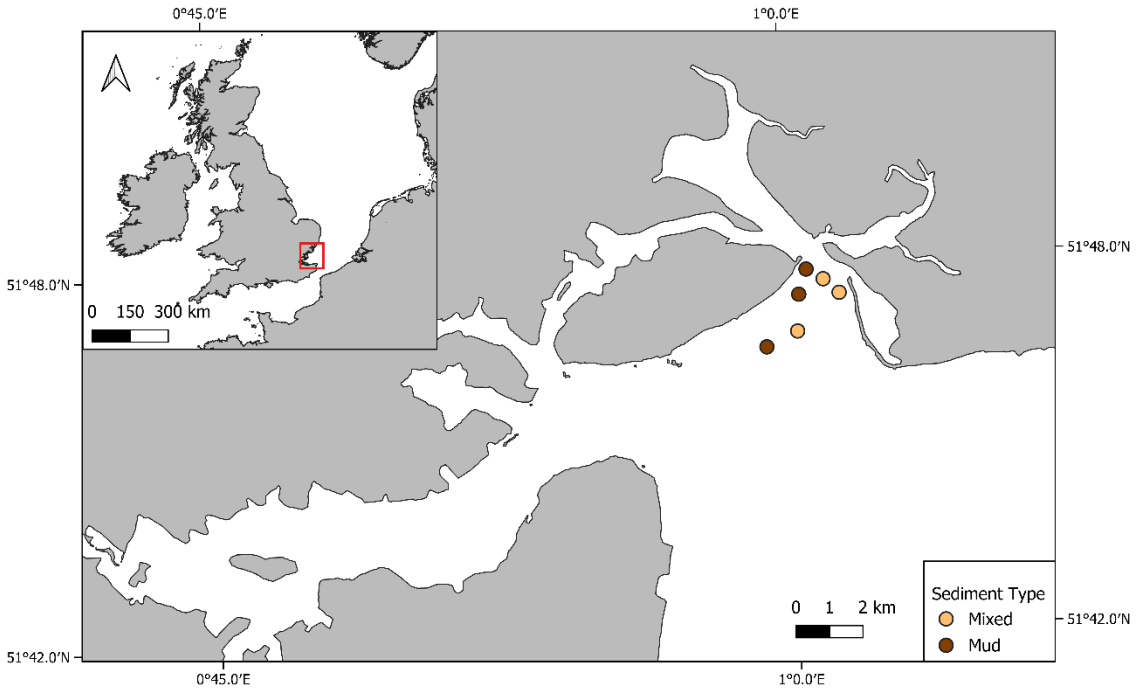

Figure 22: Map of sampling site, near Mersea Island (UK). Targeted sediment type sampling are displayed by colour (Mud = dark brown, Mixed = beige).

To test two varying sediment types specifically, sampling was targeted to collect either muddy (finer particles) or mixed sediment (generally higher sand/gravel content). Therefore, experiments would use both types of sediment per temperature treatment for comparison.

5.2.2. Experimental setup

Oxygen consumption experiments for individual cores were conducted directly after each sampling trip and each day henceforth. Sediment cores were extruded and sliced to 0 – 2 cm, 2 – 5 cm and 5 – 10 cm. These depths were chosen to mimic resuspension depths from disturbance events linked to trawling (Hale et al., 2017). Sediment was cut from each extrusion using modified syringes to ensure the entire length was included with similar volumes (~ 40 cm^3) for each depth. These were extruded into individual chambers (1.2 L volume) with a magnetic stirrer filled with *in situ* collected seawater, to maintain salinity conditions. An additional chamber was only filled with *in situ* seawater and stirred to provide a control measurement with no sediment. These were sealed with plastic lids with O-rings to ensure they

were gas tight. Oxygen sensors were attached to the chamber lids on microscope glass slides. Sensors were calibrated using a two point calibration with one measurement at 100 % oxygen by aerating a chamber and a 0% using ascorbic acid both using seawater from the study site for salinity consistency. All chambers were placed in a water bath to maintain constant temperature during the experiment with an internal temperature senor placed inside. Fiber optic cables were placed within holes in chamber lids with the attached oxygen sensors affixed to glued microscope slides on the inside of the lid. Cables were attached to Pyroscience O_2 firesting pro, and oxygen concentration was measured every second from each core over a 24 h period (Figure 23). The experimental setup was kept in complete darkness to prevent any photosynthesis from altering oxygen concentrations. This process was repeated for all treatments with varying temperatures and sediment type.

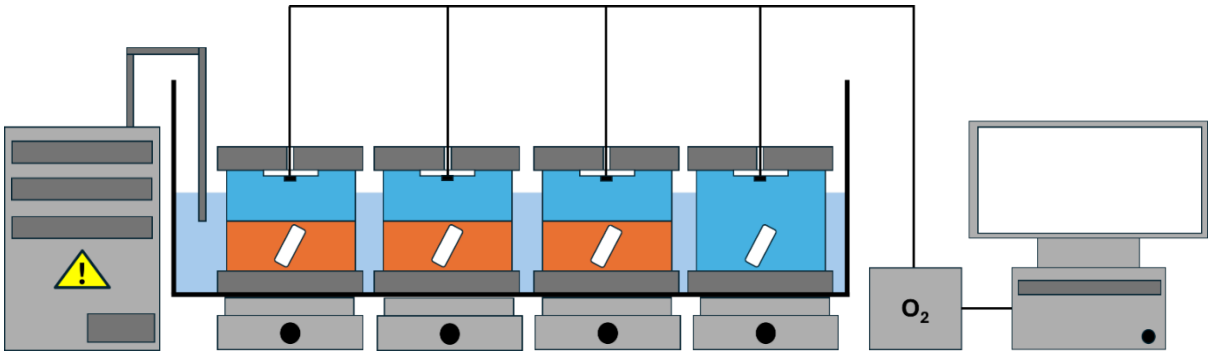

Figure 23: Experimental set up of four airtight incubation chamber atop magnetic stirrers in a temperature water bath. Infrared cables connect oxygen sensor dots to the oxygen sensor

Treatments consisted of two sediment types (mixed and muddy) and three temperatures (8, 12, 16 ºC) (Figure 24). For each treatment of sediment and temperature, three replicates were run. Following each experimental run, chambers were filtered, dried and weighed to

determine the exact amount of sediment used per treatment. This weight was used later to normalise oxygen consumption rate by amount of sediment.

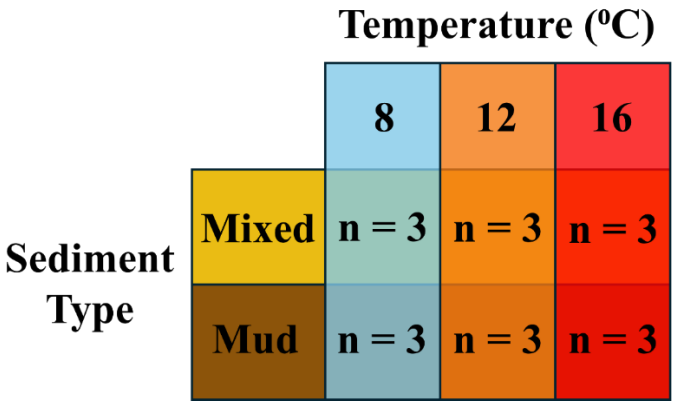

Figure 24: Schematic of experimental design. Temperature treatments were 8ºC, 12ºC and 16 ºC, with two types of sediment (mixed and mud). Three sediment depths were tested in each run, 0 – 2 cm, 2 – 5 cm and 5 – 10 cm. Three replicate cores were run for each treatment. For each experimental run, an additional incubation chamber was run with *in situ* water only as a control.

5.2.3. Sediment oxygen profiles

To obtain representative oxygen penetration depths for each sediment type, five vertical oxygen profiles of each sediment type were acquired using an oxygen microelectrode (Unisense, Denmark). The microelectrode was mounted on a profiler frame and slowly lowered into each sediment core, in increments of 100 microns, using a micromanipulator motor (Hicks et al., 2017). Linear calibration of the microelectrode was achieved by taking measurements in 100 % oxygenated water (aerated water) and 0 % water treated with ascorbic acid. This calibration was used to calculate oxygen saturation (%) of the overlying seawater and then at increasing depth in the sediment. The position of the sediment water interface was determined from the oxygen profiles by assigning the interface position to a break in the oxygen profile, where the oxygen concentration starts to decline as the microelectrode enters the sediment.

Sediment oxygen penetration depth (OPD) was determined using the depth on the vertical profile at which oxygen concentration reached zero.

5.2.4. Biogeochemical analysis and sediment characterisation

Biogeochemical analysis was conducted on the frozen, sliced core from each sampling trip to characterise sediment type and organic carbon content. Each 1 cm sediment slice was weighed before and after freeze drying to allow for the calculation of dry bulk density (DBD). To determine the bulk elemental OC and N approximately 5 mg of freeze-dried sediment was acidified using 10 % hydrochloric acid (HCL) until effervescence ceased. These were subsequently kept at 60 ºC until fully dry. Next an aliquot of each acidified sediment slice was transferred into tin capsules and then into the CHNS analyser (Elementar, Germany).

For particle size analysis (PSA), freeze dried samples were dry sieved at 0.5 φ intervals and each fraction was weighed. The > 1mm fraction was sized by laser diffraction by inserting a small aliquot of sample into the Bettersizer S3 Plus (Bettersizer Instruments Ltd, China). These results were combined to give the particle size distribution across the entire sample. Sediment characteristics statistics, mean and median grain size, skew, and kurtosis were calculated using GRADISTAT software version 9.1 (Blott & Pye, 2001).

5.2.5. Statistical analysis

All statistical analysis was conducted using R version 4.2.1. Following each experimental treatment, oxygen consumption rates were specifically determined by analysing the oxygen consumption data from 20,000 to 40,000 seconds only, ensuring the processes captured were organic carbon degradation and not initial chemical oxidation. From these, in R, linear models were fitted to the lines from each sediment depth to obtain oxygen consumption rates. Where oxygen concentration had decreased to zero before the end of this time period, these consumption rates were removed completely (n = 17 out of 72*)*. Oxygen consumption rates

were normalised by the amount of sediment introduced to the chamber and this was multiplied by OC% per sediment type at that temperature to give %/hr/g of organic carbon.

To test which predictor variable from depth (in sediment), temperature, and sediment type, best explained the change in O_2 consumption %/hr/kg of sediment, a 3-way ANOVA was used. Organic carbon content was determined as either high (>0.5 %) or low (< 0.5 %). Sediment type was determined as either Mud or Mixed based on average grain size, with less than 63 microns classified as Mud (based on Folk classification). Model simplification was used to exclude non-significant variables and predictor variables to obtain the simplest model explaining the most amount of variance, removing non-significant interactions in turn. All figures were generated using the '*ggplot2*' (Wickham, 2010), and '*cowplot*' (Wilk, 2020) packages. Averages are reported as Mean ± standard deviation.

5.3.Results

5.3.1. Sediment composition

As sediment collection was targeted for two different types, each temperature treatment was run with two distinct sediment classes, mud (fine grained) or mixed (coarse grained) (Figure 25). Highest average grain size in the mixed sediments was used for the 16 ºC incubation (2621.9 um) with similar coarseness (1388.1 and 1308.8) at 8 and 12 ºC. Mixed cores did show some mud content throughout with an average mud content of 8.48 ± 8.19 %, average sand content of 49.70 ± 19.31 % and average gravel content of 41.82 ± 16.17 %. Of note, the mixed core with the most mud content (16.08 ± 6.92 %) was used in the 8 ºC temperature incubation. Muddy targeted incubations showed consistently low mean grain sizes with average grain size ranging from 26.3 µm to 17.86 µm. Mud targeted cores were predominately muddy with and mud average content of 80.37 ± 11.30 %, average sand content of 18.17 ± 8.59 % and average gravel content of 1.5 ± 3.96 %.

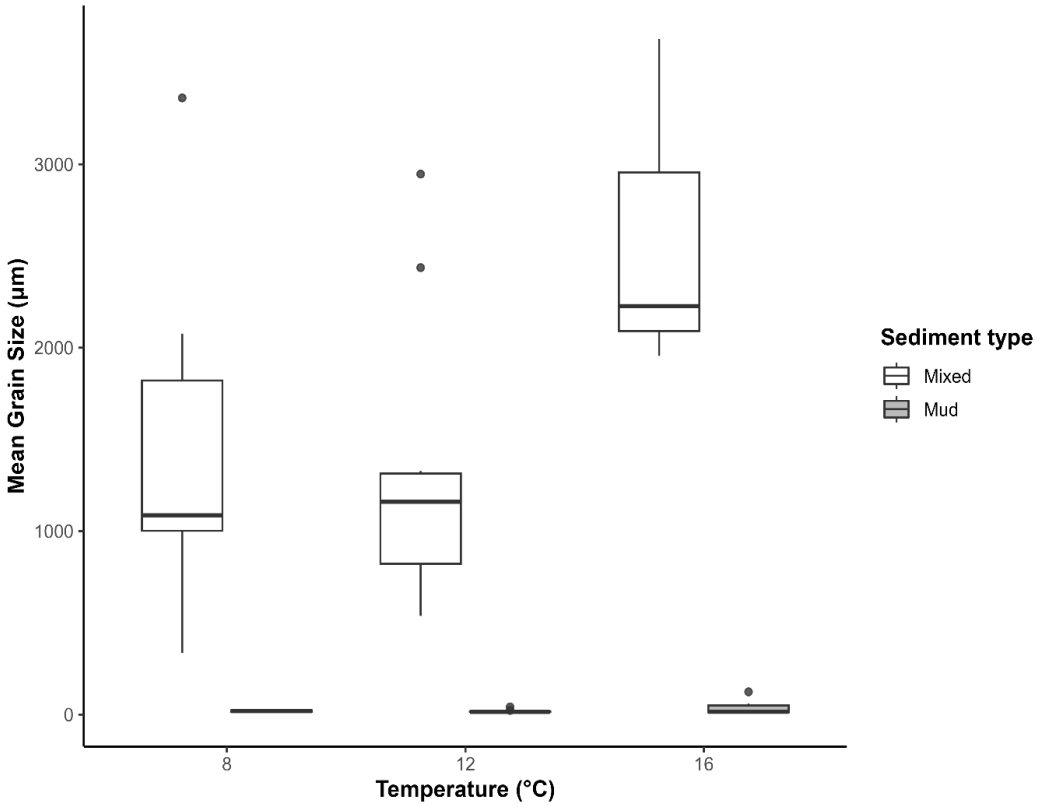

Figure 25: Sediment composition of representative sliced cores (10 cm) used for geochemical analysis from each site. Sediment type was determined as either mud (grain size less than 63 µm) or mixed (mean grain size more than 63 µm).

5.3.2. Oxygen penetration depth

Five cores from each sediment type were profiled to determine average oxygen penetration depth (OPD) (Figure 26). Oxygen penetration depth showed a clear difference between sediment types. All five muddy sediment cores OPD was below 1 cm with less variability between each. Mixed cores had a mean OPD of 1.04 ± 0.34 cm compared to the muddy cores which has a shallower mean OPD of 0.6 ± 0.16 cm.

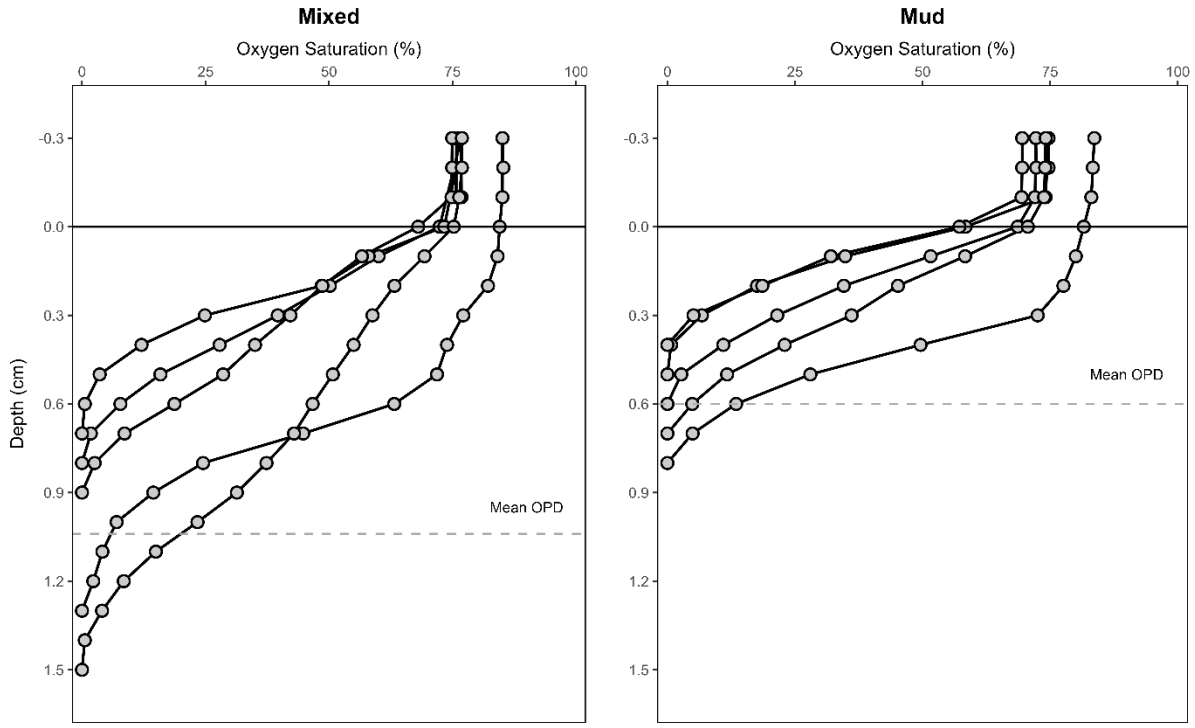

Figure 26: Oxygen sediment depth profiles of five sediment cores collected of mixed and muddy sediment. Solid line indicates the sediment surface. The dashed line displays the mean oxygen penetration depth from the five cores of each sediment type. This was determined as the depth at which oxygen saturation reached 0 %.

5.3.3. Organic carbon content

Organic carbon content from representative treatment cores varied from 0.11 to 1.02 % (Figure 27). Mean organic carbon content of muddy treatment cores was 0.55 ± 0.32 % with generally higher OC in surface sediments (between 0.12 and 1.02 %). The two incubations which had the highest organic carbon content input were muddy cores used for 12 ºC and 16 ºC with average OC being 0.76 % and 0.79 % respectively. The temperature treatments which had the lowest OC input was 12 ºC mixed sediment and 8 ºC muddy sediment core, which both had an average OC of 0.15 %. respectively. Organic carbon content in mixed sediment cores was lower than muddy cores with a mean of 0.31 ± 0.18 %. Largely, in mixed sediment cores organic carbon did not vary with depth.

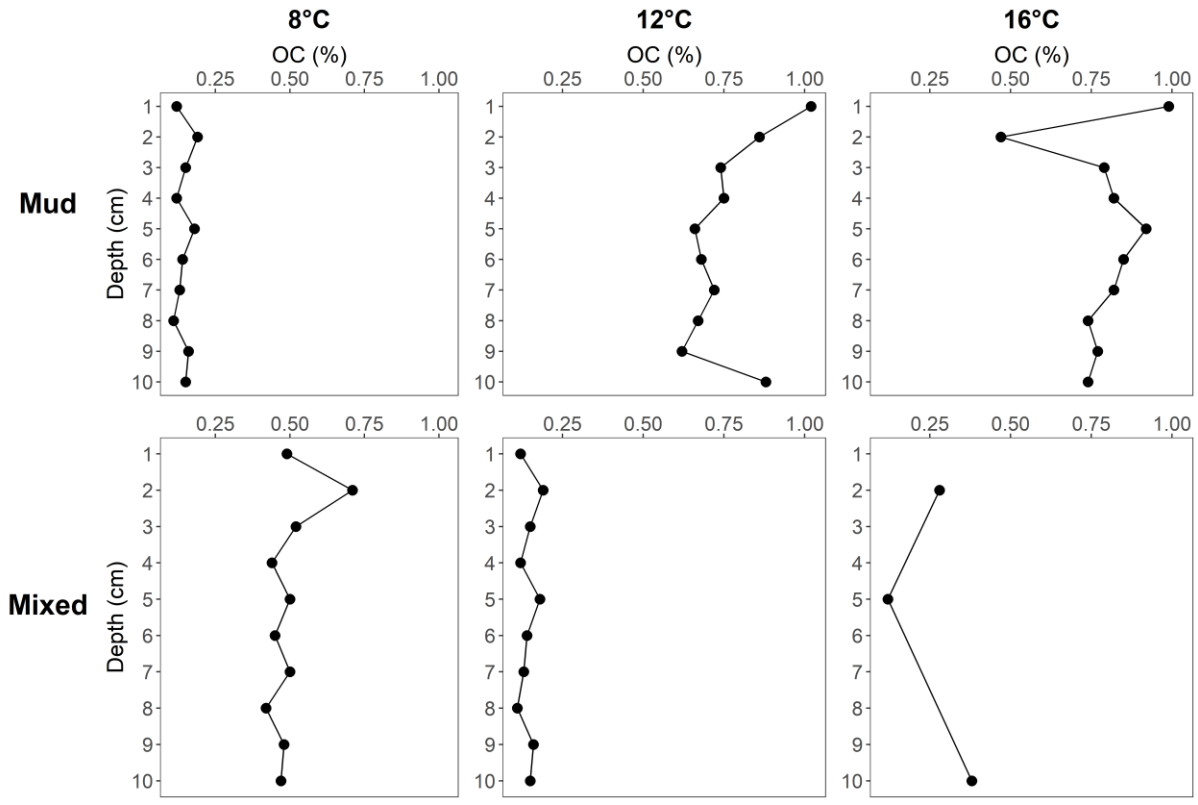

Figure 27: Organic carbon (%) depth profiles of six cores as representative samples taken during each sampling trip, with muddy sediments on the top, and mixed sediments on the bottom row. The plots on the left show the 8 ºC temperature, with 12 ºC in the middle and 16 ºC on the right. OC was measured at each 1 cm increment except for sediment the mixed 16 ºC where measurement were taken for 0 – 2 cm, 2 – 5 cm and 5 – 10 cm due to sampling constraints.

5.3.4. Oxygen consumption rates

Oxygen consumption between treatments varied between sediment type, temperature and depth (Figure 28). However, model results show that none of the main predictor variables has a significant effect on oxygen consumption (ANOVA, $F = 15.63$ $df = 45$, $P > 0.05$). There were two, two-way interactions which were significant predictor variables when together, these were sediment type/temperature and sediment type/depth ($p < 0.01$). Post-hoc analysis showed that oxygen consumption in the mixed sediment treatment was significantly higher at 12 ºC compared to 8 ºC, and at 12 ºC oxygen consumption was significantly lower in the mud sediment compared to the mixed sediment. At 8 ºC, shallow (0 – 2 cm) mixed sediment showed

the lowest oxygen consumption (-1.35 ± 0.86 %/hr/gOC) compared to a higher average rate in shallow (0 – 2 cm) muddy sediment (-12.04 ± 0.83 %/hr/gOC). However, in muds at 8 ºC all deeper sediment depths (other than mixed 2 – 5 cm) dropped to zero before 20,000 seconds so therefore was omitted from results. At 12 ºC average oxygen consumption rate varied from -2.77 ± 0.21 %/hr/gOC in deeper (5 – 10 cm) muddy sediment to -11.03 ± 6.99 %/hr/gOC to 2 – 5 cm mixed sediment. In the 16 ºC treatment, highest average oxygen consumption occurred in mixed sediment at 2 – 5 cm (-10.25 ± 5.92 %/hr/gOC) and lowest occurred in shallow (0 – 2 cm) mixed sediment (- 1.62 ± 0.83 %/hr/gOC)

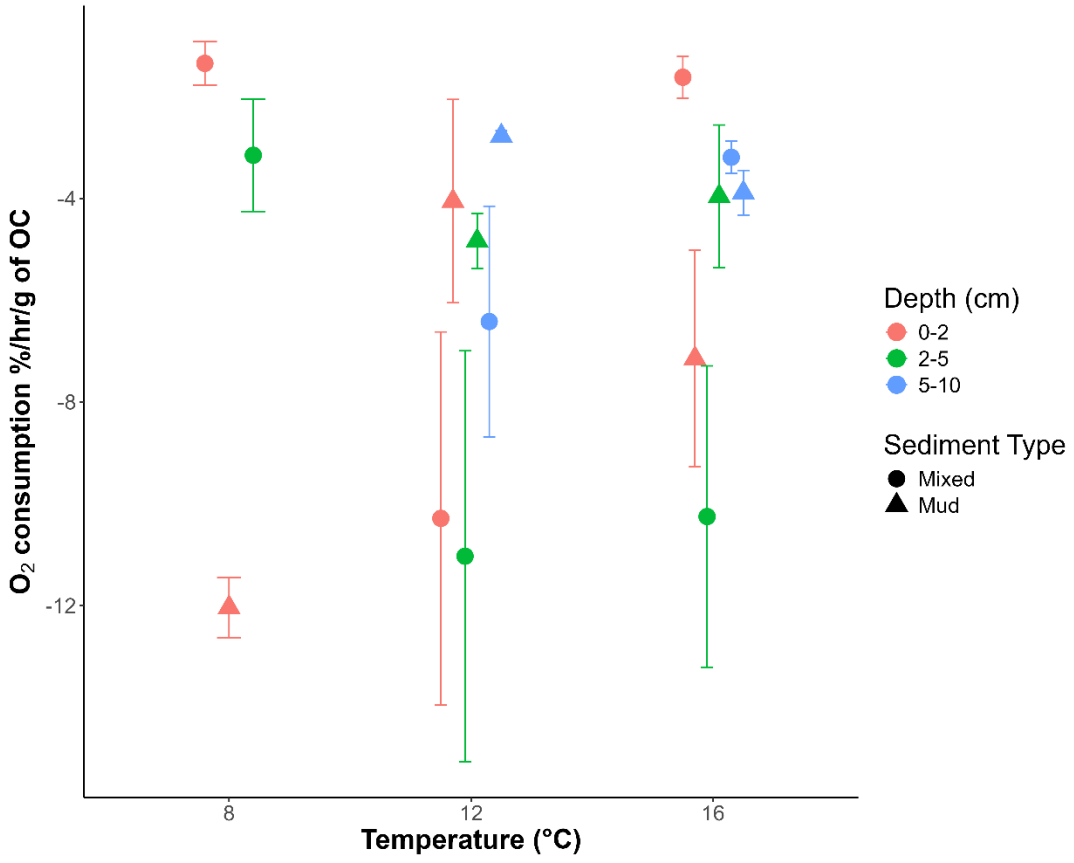

Figure 28: Oxygen consumption (%/hr/g of organic carbon) within each sediment incubation under varying temperatures on the x axis (8, 12, 16 ºC). Sediment (mixed is circle, mud is triangle) depths for each incubation were 0 – 2 cm, 2 – 5 cm and 5 – 10 cm and are indicated by colour (red, green and blue respectively). Error bars show standard error.

5.4.Discussion

5.4.1. Predictors of oxygen consumption rates

This pilot study investigated the effect of disturbance on carbon reactivity (measured through oxygen consumption rates) within different subtidal sediments at three temperature regimes. By using oxygen consumption (normalised with amount of OC (in grams) per treatment) as a proxy for organic carbon mineralisation, in this case, temperature and depth together showed significant differences in oxygen consumption rate. Firstly, mixed sediments at 12 ºC had a significantly greater oxygen consumption compared to mixed sediments at 8 ºC and when comparing between sediment types, the only significant difference was observed at 12 ºC, where mixed sediment showed significantly greater oxygen consumption than all muddy sediments. There was a significant overall interaction between sediment type and depth however no specific difference was observed between incubations. These findings corroborate similar studies and show that muddier sediments generally contain generally higher organic carbon content (Diesing et al., 2017; Middelburg, 2019; Smeaton, Hunt, et al., 2021; Woulds et al., 2007). Despite this, these results showed the muddier sediments had less OC mineralisation, particularly at 12 ºC compared to mixed, coarse-grained sediment. Muddy sediments often contain greater fractions of labile organic due to higher sedimentation and carbon burial and shallow OPD (Figure 26) (Hedges & Keil, 1995; Mayer, 1994), which protects the labile organic carbon fraction from prolonged degradation at the sediment water interface in more aerobic conditions (Middelburg, 2018). When these highly reactive sediments are re-exposed to oxygen through disturbance (typically below 2cm depth and deeper), it is likely that this labile carbon causes higher rates of organic carbon mineralisation. However, this trend was not observed in this experiment even in muddy sediment with high levels of organic carbon. This may be due to adsorption of carbon to clay minerals forming protected aggregates (Hedges et al., 1997; Mayer, 1994), which upon resuspension were not exposed to

oxygen for mineralisation and therefore not available for microbial remineralisation. These results show wide variability, partly due to the limitation on replicates (n=3) per treatment, and if this work was repeated, a higher number of replicates run with the same sediment types would provide more data to reduce this variability.

Results indicated that in mixed sediment, oxygen consumption was greater at 12ºC compared to 8ºC. This is in line with expectations of increased microbial activity at these greater temperatures, as microbial processes drive organic carbon mineralisation and degradation in sediments (Arnosti et al., 1998; De La Rocha & Passow, 2007; Le Moigne, 2019). This also provides insight into how mineralisation may change due to climate change driven warming of bottom temperature (Arnosti et al., 1998; Hunter et al., 2006). For example, temperature in coastal sediments significantly change the species composition of benthic bacterial communities which can alter the efficiency of biogeochemical cycles (Hicks et al., 2017; Jørgensen et al., 2022). Specifically, Arnosti et al, (1998) demonstrate that optimum temperatures for microbial activities which break down OC (hydrolysis, O_2 consumption and SO_4^{2-}) were significantly higher (up to 20 ºC) than ambient environmental temperatures in temperate and arctic marine sediments, suggesting that warmer seabed temperatures may increase OC breakdown in these processes. Therefore, this increase oxygen consumption (and therefore OC mineralisation) from 8 ºC to 12 ºC is likely driven by more optimum conditions for carbon degrading microbial communities, and is representative of changes in the North Sea bottom water temperature. However, in this case sediment oxygen consumption rates did not show a significant increase in oxygen consumption at 16 ºC. It may be that 12 ºC is optimum for OC degradation in these sediments, but future work could test a range of temperatures to ascertain if this is representative of North Sea sediments.

Depth in sediment, in combination with sediment type, also significantly described the changes observed oxygen consumption rate. While not significantly different, deeper

sediments (5 – 10 cm) generally had lower oxygen consumption rates. Organic carbon content in subtidal sediments typically varies with depth, with highest concentrations at the sediment surface, and then decreasing to a constant further down the core depth (Figure 1, Chapter 1). Furthermore, the composition of organic carbon typically varies as the material that has escaped degradation through initial diagenetic processes (Soetaert et al., 1996) is often more recalcitrant (Arndt et al., 2013; Burdige, 2007) and therefore remains stable at greater depths (Arndt et al., 2013). The remaining organic matter at depth is being continually depleted by microbes which leaves a residue of refractory organic carbon (Arndt et al., 2013). The high surface concentrations of organic carbon content in cores (particularly muds) in the higher temperature treatments (Figure 25) may explain the greater oxygen consumption rate. There is higher carbon in the 8 ºC mixed sediment treatment than the muddy one at the same temperature, possibly linked to the higher percentage of fines in this mixed sediment run than the other two mixed sediment temperatures. The higher surface organic carbon is likely freshly deposited labile organic matter which is easily degraded upon being resuspended in the water column (Porz et al., 2024), particularly as these sediments were sampled around the spring time, which may have seen an increase in carbon to the seabed through increased water primary productivity. Similarly, deeper muds showed lower oxygen consumption, likely due to recalcitrant organic carbon being suspended but not mineralised (Arndt et al., 2013). These factors highlighted the need to measure organic carbon content throughout the cores as this is a key driver for mineralisation rates, and account for changes in fines percentage across different sediment types, particularly in coarse sediments. It is also important to interpret the oxygen consumption rates in the context of the amount of organic carbon within the sample, as not doing so can produce inaccurate results (Appendix Figure 9).

5.4.2. Experimental design limitations

As a pilot study, this work represents a first attempt to constrain carbon mineralisation associated with sediment disturbance and resuspension , using oxygen consumption as a proxy, and it carries inherent limitations that can inform further recommendations. Primarily our results do not directly measure the transformation of particulate organic carbon to dissolved inorganic carbon (CO_2). To accurately determine if the process being observed is organic carbon mineralisation this would require directly measuring dissolved inorganic carbon throughout the incubation period. This could be achieved by periodically sampling water from the chamber throughout the incubation period and then using a DIC analyser for precise results.

Furthermore, to constrain specifically mineralisation rather than chemical oxygen demand we only determined consumption rate from 20,000 to 40, 000 seconds. This was assumed to be after the window of chemical oxygen demand which is typically faster (seconds to hours) (Findlay et al., 2020; Richard et al., 2013) whereas organic carbon mineralisation can be hours to days (Aller et al., 2004; Mori et al., 2021). Rather than making this assumption, this chemical oxygen demand could be estimated through pH sensors alongside oxygen sensors, as a proportion of these reactions (e.g. sulfide oxidation) produce H^+ thereby accurately isolating the period dominated solely by microbially driven OC mineralisation.

There is high variability in these results, likely due to natural variability across cores and sample collection across different seasons. Sample collection occurred between March and June, spanning a period likely to capture the onset of seasonal productivity and the subsequent deposition of fresh, highly labile organic carbon from the spring/summer phytoplankton bloom, as well as an increasing temperature with seasonal change. This was evidenced by incubations run later in the year, whereby oxygen concentrations in chambers dropped so rapidly that they could be no rate observed between 20,000 and 40,000 seconds (Example in Appendix 10). As

this rate was so fast that all the oxygen in the chamber was consumed, it was impossible to differentiate this reaction between chemical oxygen demand and organic carbon mineralisation, and assume that the initial mineralisation was missed in the time between adding the sediment to the chamber, and the commencement of measurements. This also highlighted that during the incubation set up stage, the oxygen consumption process was happening prior to the start of measurements. Although much of the disturbance from trawling or infrastructure occurs offshore, the sediments used in this study were close to shore, and may not be representative of offshore sediments, which are typically less reactive (Smeaton & Austin, 2022a). By sampling these less reactive shelf sediments in future work, organic carbon mineralisation through the long-term degradation of organic material can be targeted for more realistic measurements. Additional measurements, such as the use of TGA (Smeaton and Austin, 2022) or ramped pyrolysis would provide additional information on carbon reactivity.

5.4.3. Applications to infrastructure interactions

The subtidal sediments used in this study were collected from a coastal setting to facilitate low-effort sampling during the development of the experimental methodology, and test the proof of concept for the methodology. Consequently, extrapolations of these results to the impact of offshore infrastructure should be approached with caution. As previously mentioned, coastal sediment is typically much more reactive than shelf sediment (Smeaton & Austin, 2022a) as they receive a higher flux of terrestrial input and fresh labile organic material, particularly in summer months due to phytoplankton blooms (Huppert et al., 2002) that is more easily remineralised (Epstein et al., 2022). Applying the rapid mineralisation rates observed here directly to deeper-water infrastructure, or even trawling, may therefore be inappropriate. However, these initial results tentatively highlight the risk that mechanical disturbance events such as the construction, operation, or decommissioning of offshore infrastructure could have a disproportionate effect on carbon cycling at sites, with increasing temperatures and in site

specific context such as different sediment types. This suggests a critical need to factor sedimentology, as a key controller of carbon levels and reactivity, into environmental impact assessments for offshore development.

Moving forward, the approach provided in this study could be used as a basis for determining the effect of disturbance on organic carbon caused by the installation, maintenance or decommissioning of offshore infrastructure. To effectively tailor these experiments to specific projects, sediment samples should ideally be collected directly from sites of interest. In addition, mesocosm incubations can be artificially manufactured to replicate the expected conditions of impacted sediment. For example, to accurately mimic the chronic effect of decommissioning of oil as gas platforms, incubations could be spiked with environmentally relevant level of concentration of contaminants such as hydrocarbons or heavy metals. While artificially constructing these scenarios requires careful validation, it would significantly increase the ecological relevance and predictive power of future experimental designs, allowing researchers to accurately constrain organic carbon mineralisation across a broader range of anthropogenic impacts. This will also have implications for seabed management within a future changing climate.

5.5. Conclusion

Marine subtidal sediments contain vast amounts of organic carbon (Atwood et al., 2020; Legge et al., 2020; Smeaton, Hunt, et al., 2021) which are subject to a range of disturbance events (De Borger, Tiano, et al., 2021; Eigaard et al., 2017; Sciberras et al., 2016). There are growing calls for these interactions to be managed, however the effect of disturbance on organic carbon remains unclear (Chen et al., 2024; Epstein et al., 2022; Epstein & Roberts, 2022; Woodward-Rowe et al., 2025) Few experimental or in situ measurements have been conducted

to constrain the organic carbon degradation risk, leading many impact assessments to rely on predictive modelling (Atwood et al., 2024), thereby leaving a considerable research gap.

Initial results from this pilot study indicate that sediment type, temperature and depth in sediment play a key role in organic carbon mineralisation in disturbed sediment. Mixed sediments showed greater oxygen consumption rate (used a proxy for OC mineralisation) compared to muddy (coarse grained) sediments at 12 ºC. However, the interpretation of these findings must be considered alongside the study's methodological constraints, specifically the reliance on oxygen consumption as a proxy without complementary direct quantification of DIC changes and a lack of additional organic carbon reactivity measurement.

This study provides a baseline experimental attempt at constraining how disturbance across differing depths might affect organic carbon mineralisation at differing temperatures. This approach can be used to inform future applied investigations into the carbon impacts of multiple anthropogenic disturbance events, particularly those associated with bottom trawling and the installation, operation, and decommissioning of offshore infrastructure.

Chapter 6: General Discussion

6.1. Key findings

This thesis quantified and explored several aspects of blue carbon dynamics in shelf sediments influenced by offshore infrastructure including organic carbon stocks, accumulation rates, source identification, vulnerability and mineralisation. These parameters were primarily quantified in sediments impacted by two decommissioned oil and gas platforms in the North Sea: North West Hutton and Miller. Crucially, the relationship between these OC variables to offshore oil and gas platforms has not been previously studied. The initial rationale for this thesis focused on the effect of the 500 m exclusion zone around these sites, as it represents an undisturbed area of seabed during operation of the platform, offering a baseline in a shelf sea subjected to physical pressures such as bottom trawling (Eigaard et al., 2017). Contaminant analysis (heavy metals, hydrocarbons and radionuclides) revealed a chemical pressure gradient on sediment extending to approximately 200 m from the platforms (Chapter 2). Overall carbon dynamics in these areas were highly site specific with sediment type being a primary control on organic carbon stocks, but the contamination affecting the accuracy of traditional sediment dating techniques (Chapter 3). The characterisation of the carbon stocks around these sites also revealed a contribution from hydrocarbons closer to the platforms (Chapter 4), in greater quantities than found in chapter 2. Finally, the impact of decommissioning of infrastructure and therefore sediment disturbance was explored. To contribute to the knowledge gap of disturbance (through infrastructure interaction) on sedimentary organic carbon dynamics, the effect of sediment type, depth, organic carbon content and temperature was explored through a novel pilot study (Chapter 5).

6.1.1. Sedimentary blue carbon around decommissioned oil and gas platforms in the North Sea

Chapter 2 established the carbon dynamics in sediments at both decommissioned platforms, North West Hutton and Miller by measuring total organic carbon content and stock, initial organic carbon accumulation rates (OCARs) and characterising sediment type. Carbon stock varied distinctly between sites. At Miller, organic carbon stocks were highest close to the platform (50 m) and decreased sharply at 100 m and remained low and consistent throughout to the control site. Conversely, there was no relationship between distance and organic carbon stock at North West Hutton with highest values being exhibited at cores at greater distances (800, 1600 and 3200 m), outside of the 500 m exclusion zone designation. Although sediment type varied between the sites, spatial patterns relative to the platform were similar between the two sites, suggesting a local influence of the platforms on the seabed. Sediment at Miller was sandy at nearly all distances from the site (100 m – 3200 m) however, close to the platform (50 m) there was significantly higher mud content, likely a contribution from the drilling muds expelled near the platform (Ball et al., 2012; CNR International, 2013). Sediment type at North West Hutton was consistently muddier than those at Miller, although a similar trend of finer sediment particles were located at 50 m and 100 m from the platform. Finally, OCARs were calculated from sediments cores at 400 and 3200 m away from North West Hutton. Due to this large spatial separation these values were averaged across the whole site to give an estimate of background OCAR (0.003 to 0.009 $gC/cm^{-2}/y^{-1}$).

OC content at Miller generally adhered to hypothesised trend with particle size, exhibiting a strong positive correlation with mud content (finer particles) throughout sediment cores, consistent with typical shelf sea sediments (Diesing et al., 2017). The highest mud and organic carbon stocks found at 50 m were hypothesised to come from either, or a combination of both, natural OC enrichment from attached epifauna (Krone et al., 2013) or anthropogenic

enrichment of hydrocarbons (Breuer et al., 2004) within drills cuttings piles. As, at this time, quantifying hydrocarbons was not within the scope of this chapter, the UK Benthos Database was used (Offshore Energies, 2015) to estimate total hydrocarbon content (THC) (< 8%). In contrast, sediments at North West Hutton site did not display a typical strong correlation between mud and organic content, nor were elevated levels observed at 50 m. This deviation was attributed to a 'shadow' effect whereby the predominant current (SE/NW) move faeces and detritus produced by attached epifauna to greater distances from the site (Klunder et al., 2018).

These initial findings describe the total carbon stock and accumulation rates which provide a baseline for subsequent chapters. However, the data immediately presented two research challenges. Firstly, sediment cores close to North West Hutton (50, 100, 200 m) were found to be chemically contaminated with elevated levels of radium-226 (^{226}Ra) (Ahmad et al., 2021) and heavy metals (Olsgard & Gray, 1995). This contamination interfered with the traditional, direct measurement of lead-210 (^{210}Pb) required for geochronological dating and subsequent OCARs (Arias-Ortiz et al., 2018). This issue provided the rationale for chapter 3, which focused on adjusting these rates using correction values and additional analytical techniques. Secondly, a significant knowledge gap remained regarding the specific source of the organic carbon found at both sites, considering the hydrocarbon inputs to the seabed that may have occurred during construction and operation of the platform. This prompted chapter 4 to characterise the organic carbon stock and determine its origin. A key conclusion in this study is that, accounting for carbon stock only provides a temporal snapshot of how much organic carbon there is at the point of sampling (2021), which was after decommissioning of both sites, and missing the potential changes during platform operation, and pre construction. Without pre-construction and pre-decommissioning baseline carbon stocks, this research was fundamentally constrained in its ability to definitively disentangle the effects of

decommissioning on the blue carbon dynamics but is the first study to highlight the legacy contaminants (heavy metals, hydrocarbons, radionuclides) on sedimentary carbon post O&G decommissioning. This study also led onto a small project investigation the radiological impacts on benthic fauna around this site (Dal Molin et al., 2025)

6.1.2. Correcting organic carbon accumulation rates in contaminated shelf sediments

After the work in Chapter 2 on carbon stocks unable to confidently determine OCARs in heavily contaminated sediments, particularly those close to North West Hutton, Chapter 3 aimed to correct for these methodological constraints using two distinct techniques. The primary problem stemmed from heavy metal contamination attenuating gamma waves measured by gamma spectrometry (Dal Molin et al., 2018), which inhibited the accurate determination of ^{210}Pb activity that provide the basis data for calculation OCARs. To resolve this, correction factors were created for these samples, which accounted for heavy metal contamination, and alpha spectrometric techniques were used to measure polonium-210 (^{210}Po) as a proxy for traditional ^{210}Pb. Heavy metal contamination close to North West Hutton was quantified using ICP-MS. These concentrations in combination with partial chemical analysis of samples were used to create correction factors to apply to initial ^{210}Pb data from chapter 2, thereby accounting for this attenuation. Secondly, to validate these corrections, ^{210}Po, a decay product of ^{210}Pb, was measured via alpha spectrometry on the same samples. This technique involved the complete dissolution of the sediment matrix through hydrofluoric (HF) acid digestion, which effectively eliminated the heavy metal contamination and its effect on the measurement of the emitted alpha particles. This was the first time that two complementary techniques have been used to correct OCARs in legacy O&G sediments.

It is worth noting that OCAR values presented in Chapter 3 are extremely high for shelf sediment, greater than values estimated in the Norwegian trench (Diesing et al., 2021) and even

the Western Irish Sea Mud Belt(Ward et al., 2025). Radionuclide and carbon content analysis has been validated however this maybe due to sampling inaccuracies, such as on board sampling and core slicing for later analysis including Dry Bulk Density.

However, results from this study showed that without these corrective approaches OCARs could have been severely overestimated by up to 149.99 % at 100 m due to the contamination of samples primarily from heavy metals such as Pb, Sr and Ba, which had the highest elemental mass attenuation. This is important, as there are so few direct OCAR measurements across the North Sea, that this could provide a bias in overestimating carbon accumulation (and carbon stocks) in the North Sea. The corrected ^{210}Pb results were in relatively good agreement with the ^{210}Po results acquired from alpha spectrometric analysis. However, activity concentrations derived from uncorrected gamma spectrometry showed significantly lower activity concentrations of ^{210}Pb compared to both alpha spectrometry (^{210}Po) and corrected gamma spectrometry. Heavy metals were concentrated at 50 and 100 m from North West Hutton with highest concentrations of all three heavy metals (Barium, Strontium and Lead) in the top 5 cm at 50 m on the northern transect. A plausible explanation for this localised pollution is the presence of drills cuttings piles nearby the platform which contain higher than background levels of heavy metals, and often remain in piles, largely undisturbed by hydrodynamics (Ball et al., 2012; Breuer et al., 2004; Olsgard & Gray, 1995).

Typically, shelf sediments do not have high accumulation rates unless in depositional environments such as glacial troughs (Diesing et al., 2024) or muddy depocenters (Ward et al., 2025). Specifically for localised contamination O&G platforms in the shelf seas this represents a relatively small area compared to the entire North Sea shelf. Crucially, the issue of contamination-induced miscalculation of OCARs has wider implications, particularly for coastal sediments. Coastal zones naturally exhibit higher OCARs than shelf sediment due to higher primary productivity (McLeod et al., 2011) and greater sedimentation rates (from

terrestrial and riverine inputs, as well as marine) (Smeaton & Austin, 2022b; Smeaton, Yang, et al., 2021). However, similar to the shelf sites investigated here, coastal zones are also frequently subjected to heavy metal contamination from industrial activities, including iron, steel, aluminum, thorium, uranium, titanium dioxide production and China clay extraction sites (SEPA, 2014). These findings highlight the critical need for a more comprehensive approach to blue carbon assessments in environments impacted by infrastructure (either offshore or onshore) which produce these contaminants to ensure the accuracy and reliability of carbon budget estimations. Identification of areas of potential contamination could highlight where this approach may be better suited for alternative OCAR measurements to avoid overestimation.

6.1.3. Source Identification of Sedimentary Organic Carbon at Decommissioned North Sea Platforms

Building on the quantification of organic carbon stocks in chapter 2, chapter 4 aimed to determine the source of the organic carbon found at both North West Hutton and Miller through stable isotope ($\delta^{13}C_{org}$) and Total Hydrocarbon (THC) analysis. Furthermore, vulnerability of this organic carbon was measured through thermogravimetric analysis (TGA) to determine if the altered composition influenced its lability (susceptibility to degradation). The necessity of direct measurement arose as initial attempts to constrain the proportion of hydrocarbons using the UK benthos database were limited to measurements starting at 100 m from both sites. Therefore, it was essential to determine THC within the same samples in which total organic carbon stock was measured. This study used a novel adaptation of a binary mixing model (Thornton & Mcmanus, 1994), which are typically used to determine proportion of terrestrial and marine sources (Smeaton & Austin, 2022b), to instead determine the proportion from anthropogenic sources versus marine sources. This was achieved by using an anthropogenic

end member, from North West Hutton crude oil (Sofer, 1984) and a marine end member, averaged from North Sea marine species dataset by Smeaton et al., (2022).

The binary mixing model revealed distinct spatial patterns in the fraction of anthropogenic carbon (F_{anthro}) at both sites. The mean fraction of anthropogenic carbon across the site at Miller was 0.06 with a range 0 to 0.21 (so up to 21% of the carbon was hydrocarbon derived) with significantly higher values found close to the site at 50 m and 100 m (0.09 ± 0.05) at shallow depths compared to 200 m and 3200 m (0.01 ± 0.01). The same pattern was seen at North West Hutton, mean F_{anthro} was 0.05 with a range of 0 to 0.20 with significantly higher values at 50 m and 100 m (0.11 ± 0.04) compared to all other distances (200 m, 400 m and 3200 m) (0.02 ± 0.02). Furthermore, organic carbon stock did show some contribution from hydrocarbons at North West Hutton with hydrocarbon contribution to total organic carbon (%) at 50 m ranges from 0.02 to 42.99%. At the control sites from North West Hutton (3200 m), THC was negligible with a range between 0.0008% to 0.001%, reflecting natural background pyrogenic hydrocarbons. Both THC and F_{anthro} showed a strong correlation indicating that this enrichment, especially close to the platforms, are from petroleum hydrocarbon sources, linked to oil extraction activities. However, at North West Hutton this did not correlate with OC content, showing that this oil source might not actually be a driver in carbon stock increases. Values of carbon lability from these same samples, using TGA, were analysed through a carbon reactivity index (CRI) (Smeaton & Austin, 2022a). Generally, CRI was high (less reactive) for all sediments with a range of 0.64 to 0.85 (between a range of 0-1, with 0 for very labile and 1 for refractory) and did not vary greatly with distance from each site. Nevertheless, this chapter specifically highlighted methodological concerns, suggesting that TGA may not be the most suitable descriptor of OC lability in this specific context, as discussed in the reactivity chapter (Chapter 5).

However, this carbon characterisation study did reveal that local near-site contamination can alter the typical organic carbon pool, particularly in shallower sediments where these anthropogenic deposits are made. As typical stock estimates are constrained to 10 cm (Graves et al., 2022), these results indicate that the organic carbon stocks in shelf sediments are not exclusively marine/terrestrially derived (so potentially not 'blue carbon') and therefore their contribution to climate change mitigation may be overestimated if the non-natural, anthropogenic component is included. It should be noted however, that this footprint of sediment this inputted anthropogenic carbon resides within represents a small area compared to the entire North Sea shelf.

This chapter changes the initial rationale from chapter 2, specifically that THC in sediments around these platforms was insignificant. THC contribution to total organic carbon stock described here show near 2-fold increase from 8% in chapter 2 to 15.90%. This highlights that samples such as those found in the UK Benthos Database at greater distances from platforms (100 m) may mask how much THC content is near these sites. However, THC did not correlate with organic carbon content, which suggests that elevated levels of hydrocarbons are not drivers of an increase in organic carbon at 50 m or at greater distances. Furthermore, despite having high levels of THC at 50 m from North West Hutton, chapter 2 highlighted that carbon content increases with distance with highest levels found at greater distances. This suggests that hydrocarbon content does not drive organic carbon content in these sediments as it only explains up to 15.90% of total stock at 50 m and instead may be linked to other activities or pressures that occur within or interact with the sediments.

6.1.4. Organic carbon mineralisation of temperature controlled disturbed subtidal sediments

The final data chapter (chapter 5) is primarily a methodological exploration to quantify how organic carbon remineralisation rates, measured via sediment oxygen consumption, are influenced by sediment type, core depth, and temperature, measuring the microbial degradation as an alternative to the TGA approach typically used for measuring reactivity (see Chapter 4). This chapter aimed to develop an experimental design which could be implemented to investigate the effect on acute anthropogenic activities (including decommissioning) on carbon stocks under changing temperature conditions. This builds on a two key research gaps in blue carbon science: carbon vulnerability (Black et al., 2022; Porz et al., 2024), and carbon remineralisation (Epstein et al., 2022; Sciberras et al., 2016; Smeaton & Austin, 2022a). A key question remains about the fate of OC which is suspended as a result of disturbance, from either trawling or the activities of offshore infrastructure.

Organic carbon mineralisation rates were tested in subtidal sediments from the coast of Mersea, Essex, United Kingdom. Two sediment types were targeted, fine-grained muddy sediments and coarse-grained mixed sediments, using different depths from each sediment (0 - 2 cm, 2 – 5 cm and 5 – 10 cm). The sediments were placed into a mesocosm set up to measure oxygen consumption over time whilst being constantly resuspended, and subject to three temperatures (8 ºC, 12 ºC, 16 ºC). Oxygen concentration was measured in each chamber throughout a 24 h period, and oxygen consumption rates calculated from 20,000 to 40,000 seconds to only measure organic carbon mineralisation rather than chemical oxygen demand.

Initial results from this pilot study indicate that sediment type, temperature and depth play a key role in organic carbon mineralisation in disturbed sediment. Mixed sediments showed a greater oxygen consumption rate (used a proxy for OC mineralisation) compared to muddy (fine grained) sediments at 12 ºC. However, the interpretation of these findings must be considered alongside the study's methodological constraints, specifically the reliance on oxygen consumption as a proxy without complementary direct quantification of DIC changes

and a lack of supporting organic carbon reactivity measurement. Despite this, the proof of concept experiment shows that this set up does indeed work for measuring oxygen consumption (as a proxy for remineralisation), and this approach can now be fine-tuned and improved.

As explored in chapter 4, TGA analysis described lability through temperature degradation of organic compounds, which might not be the most accurate way to describe how likely OC is to undergo microbial mediated mineralisation. Combining the experimental mesocosm approach, with TGA and other organic carbon dynamic measurements shown in previous chapters such as source identification, could be used to improve understanding of carbon vulnerability in shelf sediments. This will fill a vital research gap around the carbon impacts of multiple anthropogenic disturbance events, particularly those associated with bottom trawling and the installation, operation, and decommissioning of offshore infrastructure.

6.1.5. Concluding remarks

All four of these data chapters explore various carbon measurements from subtidal sediments, particularly in the context of offshore infrastructure. Chapter 2 established the sediment type, organic carbon stock and initial OCARs in sediments around the decommissioned platforms North West Hutton and Miller. These OCARs were refined in chapter 3 to account for the heavy metal pollution and highlight how this might affect other sediments and impact blue carbon assessments. Chapter 4 determined the relative contribution to the OC stock (measured in Chapter 2) from anthropogenic sources, with a specific focus on hydrocarbon addition. Finally, chapter 5 attempted to determine how organic carbon mineralisation rates might change due to disturbance by testing multiple factors (sediment type, temperature, depth and OC amount), trialling a new experimental approach. The presented thesis contributed novel information to the fields blue carbon science and marine biogeochemistry, including the first publication on the impact of legacy O&G activity on

sedimentary carbon (Woodward-Rowe et al., 2025), and an associated radioecological publication (Dal Molin et al., 2025).

The key knowledge gap that highlighted throughout this thesis is the uncertainty of organic carbon vulnerability to remineralisation from disturbance events. With governments (national and international) looking to increase the amount of offshore infrastructure to meet rising energy demand (Bugnot et al., 2021) and net zero targets, the amount of disturbance in shelf seas is likely to increase (Heinatz & Scheffold, 2023), against a background of intensive fishing activity. Therefore, constraining the potential effect of disturbance on carbon stocks from these activities is vital for protecting the climate mitigation potential of shelf sediments. Going forward, this thesis provides a methodology framework determining organic carbon accumulation rates as part blue carbon assessment in contaminated sediments. This work also highlights the need to determine the source of organic carbon in shelf sediment to determine its climate relevance. Finally, to fully untangle the effects of offshore infrastructure from construction, operation and decommissioning, these measures of carbon dynamics must be taken throughout each process, and this requires close engagement with the offshore industry sector.

References

Abbasian, F., Lockington, R., Mallavarapu, M., & Naidu, R. (2015). A Comprehensive Review of Aliphatic Hydrocarbon Biodegradation by Bacteria. *Applied Biochemistry and Biotechnology*, *176*(3), 670–699. https://doi.org/10.1007/s12010-015-1603-5

Abril-Hernández, J. M. (2025). Assessment of the Performance of Pb-Based Dating Models with a Challenging Sediment History in Maryport Harbour (UK). *Journal of Marine Science and Engineering*, *13*(1). https://doi.org/https://doi.org/10.3390/jmse13010144

Ahiaga-Dagbui, D. D., Love, P. E. D., Whyte, A., & Boateng, P. (2017). Costing and Technological Challenges of Offshore Oil and Gas Decommissioning in the UK North Sea. *Journal of Construction Engineering and Management*, *143*(7). https://doi.org/https://doi.org/10.1061/(ASCE)CO.1943-7862.0001317

Ahmad, F., Morris, K., Law, G. T. W., Taylor, K. G., & Shaw, S. (2021). Fate of radium on the discharge of oil and gas produced water to the marine environment. *Chemosphere*, *273*. https://doi.org/ARTN 129550

10.1016/j.chemosphere.2021.129550

Aller, R. C., Hannides, A., Heilbrun, C., & Panzeca, C. (2004). Coupling of early diagenetic processes and sedimentary dynamics in tropical shelf environments: the Gulf of Papua deltaic complex. *Continental Shelf Research*, *24*(19), 2455–2486. https://doi.org/10.1016/j.csr.2004.07.018

Alongi, D. M. (2012). Carbon sequestration in mangrove forests. *Carbon Management*, *3*(3), 313–322. https://doi.org/10.4155/cmt.12.20

Alongi, D. M. (2020). Global Significance of Mangrove Blue Carbon in Climate Change Mitigation. *Sci*, *2*(67), 1–15. https://doi.org/10.3390/sci2030057

Alt-Epping, U., Mil-Homens, M., Hebbeln, D., Abrantes, F., & Schneider, R. R. (2007). Provenance of organic matter and nutrient conditions on a river- and upwelling influenced shelf: A case study from the Portuguese Margin. *Marine Geology*, *243*(1-4), 169–179. https://doi.org/10.1016/j.margeo.2007.04.016

Appleby, P. G., & Oldfield, F. (1978). The calculation of lead-210 dates assuming a constant rate of supply of unsupported 210Pb to the sediment. *Catena*, *5*, 1–8. https://doi.org/https://doi.org/10.1016/S0341-8162(78)80002-2

Aquatera, L. (2007). *Initial screening assessment of BP's UKCS cuttings piles*.

Arias-Ortiz, A., Masqué, P., Garcia-Orellana, J., Serrano, O., Mazarrasa, I., Marbá, N., Lovelock, C. E., Lavery, P. S., & Duarte, C. M. (2018). Reviews and syntheses: 210Pb-derived sediment and carbon accumulation rates in vegetated coastal ecosystems - Setting the record straight. *Biogeosciences*, *15*(22), 6791–6818. https://doi.org/10.5194/bg-15-6791-2018

Arndt, S., Jørgensen, B. B., LaRowe, D. E., Middelburg, J. J., Pancost, R. D., & Regnier, P. (2013). Quantifying the degradation of organic matter in marine sediments: A review and synthesis. *Earth-Science Reviews*, *123*, 53–86. https://doi.org/10.1016/j.earscirev.2013.02.008

Arnosti, C., Jorgensen, B. B., Sagemann, J., & Thamdrup, B. (1998). Temperature dependence of microbial degradation of organic matter in marine sediments: polysaccharide hydrolysis, oxygen consumption, and sulfate reduction. *Marine Ecology Progress Series*, *165*, 59–70. https://doi.org/https://doi.org/10.3354/meps165059

Ashley, M. C., Mangi, S. C., & Rodwell, L. D. (2014). The potential of offshore windfarms to act as marine protected areas - A systematic review of current evidence. *Marine Policy*, *45*, 301–309. https://doi.org/10.1016/j.marpol.2013.09.002

Atlas, R. M. (1981). Microbial-Degradation of Petroleum-Hydrocarbons - an Environmental Perspective. *Microbiological Reviews*, *45*(1), 180–209. https://doi.org/DOI: 10.1128/mr.45.1.180-209.1981

Atwood, T. B., Romanou, A., DeVries, T., Lerner, P. E., Mayorga, J. S., Bradley, D., Cabral, R. B., Schmidt, G. A., & Sala, E. (2024). Atmospheric CO2 emissions and ocean acidification from bottom-trawling. *Frontiers in Marine Science*, *10*. https://doi.org/10.3389/fmars.2023.1125137

Atwood, T. B., Witt, A., Mayorga, J., Hammill, E., & Sala, E. (2020). Global Patterns in Marine Sediment Carbon Stocks. *Frontiers in Marine Science*, *7*(165), 1–9. https://doi.org/10.3389/fmars.2020.00165

Ausín, B., Bruni, E., Haghipour, N., Welte, C., Bernasconi, S. M., & Eglinton, T. I. (2021). Controls on the abundance, provenance and age of organic carbon buried in continental margin sediments. *Earth and Planetary Science Letters*, *558*. https://doi.org/10.1016/j.epsl.2021.116759

Azam, F., Smith, D. C., Steward, G. F., & Hagstrom, A. (1993). Bacteria-organic matter coupling and its significance for oceanic carbon cycling. *Microbial Ecology*, *28*, 167–179.

Bailey, H., Brookes, K. L., & Thompson, P. M. (2014). Assessing environmental impacts of offshore wind farms: Lessons learned and recommendations for the future. *Aquatic Biosystems*, *10*(1). https://doi.org/10.1186/2046-9063-10-8

Bakke, T., Klungsøyr, J., & Sanni, S. (2013). Environmental impacts of produced water and drilling waste discharges from the Norwegian offshore petroleum industry. *Marine Environmental Research*, *92*, 154–169. https://doi.org/10.1016/j.marenvres.2013.09.012

Ball, A. S., Stewart, R. J., & Schliephake, K. (2012). A review of the current options for the treatment and safe disposal of drill cuttings. In *Waste Management and Research* (Vol. 30, pp. 457–473).

Barsanti, M., Garcia-Tenorio, R., Schirone, A., Rozmaric, M., Ruiz-Fernández, A. C., Sanchez-Cabeza, J. A., Delbono, I., Conte, F., Godoy, J. M. D., Heijnis, H., Eriksson, M., Hatje, V., Laissaoui, A., Nguyen, H. Q., Okuku, E., Al-Rousan, S. A., Uddin, S., Yii, M. W., & Osvath, I. (2020). Challenges and limitations of the Pb sediment dating method: Results from an IAEA modelling interlaboratory comparison exercise. *Quaternary Geochronology*, *59*. https://doi.org/https://doi.org/10.1016/j.quageo.2020.101093

Bartlett, M. S. (1937). Properties of Sufficiency and Statistical Tests. *Proc. R. Soc. London. Ser. A - Math. Phys. Sci.*, *160*, 268–282. https://doi.org/https://doi.org/10.1098/rspa.1937.0109

Bauer, J. E., Cai, W. J., Raymond, P. A., Bianchi, T. S., Hopkinson, C. S., & Regnier, P. A. G. (2013). The changing carbon cycle of the coastal ocean. *Nature*, *504*, 61–70. https://doi.org/10.1038/nature12857

Benjamini, Y., & Hochberg, Y. (1995). Controlling the False Discovery Rate: A Practical and Powerful Approach to Multiple Testing. *Journal of the Royal Statistical Society. Series B (Methodological)*, *57*(1), 289–300. https://doi.org/https://doi.org/10.1111/j.2517-6161.1995.tb02031.x

Bertram, C., Quaas, M., Reusch, T. B. H., Vafeidis, A. T., Wolff, C., & Rickels, W. (2021). The blue carbon wealth of nations. *Nature Climate Change*, *11*(8), 704–709. https://doi.org/10.1038/s41558-021-01089-4

Bianchi, T. S., Aller, R. C., Atwood, T. B., Brown, C. J., Buatois, L. A., Levin, L. A., Levinton, J. S., Middelburg, J. J., Morrison, E. S., Regnier, P., Shields, M. R., Snelgrove, P. V. R., Sotka, E. E., & Stanley, R. R. E. (2021). What global

biogeochemical consequences will marine animal-sediment interactions have during climate change? *Elementa*, *9*(1). https://doi.org/10.1525/elementa.2020.00180

Bianchi, T. S., Cui, X., Blair, N. E., Burdige, D. J., Eglinton, T. I., & Galy, V. (2018). Centers of organic carbon burial and oxidation at the land-ocean interface. *Organic Geochemistry*, *115*, 138–155. https://doi.org/https://doi.org/10.1016/j.orggeochem.2017.09.008

Bianchi, T. S., Mitra, S., & McKee, B. A. (2002). Sources of terrestrially-derived organic carbon in lower Mississippi River and Louisiana shelf sediments: implications for differential sedimentation and transport at the coastal margin. *Marine Chemistry*, *77*(2-3), 211–223. https://doi.org/https://doi.org/10.1016/S0304-4203(01)00088-3

Birchenough, S. N. R., & Degraer, S. (2020). Science in support of ecologically sound decommissioning strategies for offshore man-made structures: Taking stock of current knowledge and considering future challenges. *ICES Journal of Marine Science*, *77*(3), 1075–1078. https://doi.org/10.1093/icesjms/fsaa039

Black, K. E., Smeaton, C., Turrell, W. R., & Austin, W. E. N. (2022). Assessing the potential vulnerability of sedimentary carbon stores to bottom trawling disturbance within the UK EEZ. *Frontiers in Marine Science*, *9*. https://doi.org/https://doi.org/10.3389/fmars.2022.892892

Blacklaws, J., & Johnston, D. (2013). *North West Hutton Decommissioning Programme Close-out Report*.

Blott, S. J., & Pye, K. (2001). GRADISTAT: a grain size distribution and statistics package for the analysis of unconsolidated sediments. *Earth Surface Processes and Landforms*, *26*(11), 1237–1248. https://doi.org/10.1002/esp.261

Bonferroni, C. (1936). Teoria statistica delle classi e calcolo delle probabilita. *Pubbl. del R Ist. Super. di Sci. Econ. e Commericiali di Firenze*, 3–62.

BP. (2005). *North West Hutton Decommissioning Programme*.

BP. (2011). *Miller Decommissioning Programme*.

Branch, T. A., Jensen, O. P., Ricard, D., Ye, Y., & Hilborn, R. (2011). Contrasting global trends in marine fishery status obtained from catches and from stock assessments. *Conservation Biology*, *25*(4), 777–786. https://doi.org/10.1111/j.1523-1739.2011.01687.x

Breimann, S. A., O'Neill, F. G., Summerbell, K., & Mayor, D. J. (2022). Quantifying the resuspension of nutrients and sediment by demersal trawling. *Continental Shelf Research*, *233*. https://doi.org/10.1016/j.csr.2021.104628

Breuer, E., Stevenson, A. G., Howe, J. A., Carroll, J., & Shimmield, G. B. (2004). Drill cutting accumulations in the Northern and Central North Sea: A review of environmental interactions and chemical fate. *Marine Pollution Bulletin*, *48*(1-2), 12–25. https://doi.org/10.1016/j.marpolbul.2003.08.009

Brickhill, M. J., Lee, S. Y., & Connolly, R. M. (2005). Fishes associated with artificial reefs: attributing changes to attraction or production using novel approaches. *Journal of Fish Biology*, *67*, 53–71. https://doi.org/10.1111/j.1095-8649.2005.00915.x

Brosschot, S. (2022). *Comparing hydrogen networks and electricity grids for transporting offshore wind energy to shore in the North Sea region. A spatial network optimisation approach.* Universiteit Utrech].

Bugnot, A. B., Mayer-Pinto, M., Airoldi, L., Heery, E. C., Johnston, E. L., Critchley, L. P., Strain, E. M. A., Morris, R. L., Loke, L. H. L., Bishop, M. J., Sheehan, E. V., Coleman, R. A., & Dafforn, K. A. (2021). Current and projected global extent of marine built structures. *Nature Sustainability*, *4*(1), 33–41. https://doi.org/10.1038/s41893-020-00595-1

Bull, A. S., & Love, M. S. (2019). Worldwide oil and gas platform decommissioning: A review of practices and reefing options. *Ocean and Coastal Management*, *168*, 274–306. https://doi.org/https://doi.org/10.1016/j.ocecoaman.2018.10.024

Burdige, D. J. (2007). Preservation of organic matter in marine sediments: Controls, mechanisms, and an imbalance in sediment organic carbon budgets? *Chemical Reviews*, *107*(2), 467–485. https://doi.org/10.1021/cr050347q

Burrows, M. T., Moore, P., Sugden, H., Fitzsimmons, C., Smeaton, C., Austin, W., Parker, R., Kroger, S., Powell, C., Gregory, L., Procter, W., & Brook, T. (2021). *Assessment of Carbon Capture and Storage in Natural Systems within the English North Sea (Including within Marine Protected Areas)*.

Capel, E. L., de la Rosa Arranz, J. M., González-Vila, F. J., González-Perez, J. A., & Manning, D. A. C. (2006). Elucidation of different forms of organic carbon in marine sediments from the Atlantic coast of Spain using thermal analysis coupled to isotope ratio and quadrupole mass spectrometry. *Organic Geochemistry*, *37*(12), 1983–1994. https://doi.org/10.1016/j.orggeochem.2006.07.025

Champely, S. (2020). *R package 'pwr'*. In

Chen, Z., Cameron, T. C., Couce, E., Garcia, C., Hicks, N., Thomas, G. E., Thompson, M. S. A., Whitby, C., & O'Gorman, E. J. (2024). Oil and gas platforms degrade benthic invertebrate diversity and food web structure. *Science of the Total Environment*, *929*. https://doi.org/10.1016/j.scitotenv.2024.172536

Cliff, N. (1996). *Ordinal Methods for Behavioral Data Analysis*. Lawrence Erlbaum Associates. https://doi.org/https://doi.org/10.4324/9781315806730

CNR International. (2013). *Murchison Facilities Decommissioning Environmental Statement*.

CNR International. (2017). *Ninian Northern Platfrom late life & decommissioning project*.

Coates, D. A., Deschutter, Y., Vincx, M., & Vanaverbeke, J. (2014). Enrichment and shifts in macrobenthic assemblages in an offshore wind farm area in the Belgian part of the North Sea. *Marine Environmental Research*, *95*, 1–12. https://doi.org/10.1016/j.marenvres.2013.12.008

Cohen, J. (1988). *Statistical Power Analysis for the Behavioral Science*. https://doi.org/https://doi.org/10.4324/9780203771587

Coolen, J. W. P. (2017). North Sea Reefs. In (pp. 1–203).

Coolen, J. W. P., Boon, A. R., Crooijmans, R., van Pelt, H., Kleissen, F., Gerla, D., Beermann, J., Birchenough, S. N. R., Becking, L. E., & Luttikhuizen, P. C. (2020). Marine stepping-stones: Connectivity of Mytilus edulis populations between offshore energy installations. *Molecular Ecology*, *29*(4), 686–703. https://doi.org/10.1111/mec.15364

Coolen, J. W. P., Lengkeek, W., Degraer, S., Kerckhof, F., Kirkwood, R. J., & Lindeboom, H. J. (2016). Distribution of the invasive Caprella mutica Schurin, 1935 and native Caprella linearis (Linnaeus, 1767) on artificial hard substrates in the North Sea: Separation by habitat. *Aquatic Invasions*, *11*(4), 437–449. https://doi.org/10.3391/ai.2016.11.4.08

Coolen, J. W. P., Van Der Weide, B., Cuperus, J., Blomberg, M., Van Moorsel, G. W. N. M., Faasse, M. A., Bos, O. G., Degraer, S., & Lindeboom, H. J. (2020). Benthic biodiversity on old platforms, young wind farms, and rocky reefs. *ICES Journal of Marine Science*, *77*(3), 1250–1265. https://doi.org/10.1093/icesjms/fsy092

Coughlan, M., Guerrini, M., Creane, S., O'Shea, M., Ward, S. L., Van Landeghem, K. J. J., Murphy, J., & Doherty, P. (2021). A new seabed mobility index for the Irish Sea: Modelling seabed shear stress and classifying sediment mobilisation to help predict erosion, deposition, and sediment distribution. *Continental Shelf Research*, *229*. https://doi.org/https://doi.org/10.1016/j.csr.2021.104574

Coulon, F., McKew, B. A., Osborn, A. M., McGenity, T. J., & Timmis, K. N. (2007). Effects of temperature and biostimulation on oil-degrading microbial communities in temperate estuarine waters. *Environ Microbiol*, *9*(1), 177–186. https://doi.org/10.1111/j.1462-2920.2006.01126.x

Craig, H. (1953). The geochemistry of the stable carbon isotopes. *Geochimica et Cosmochlimica Acta*, *3*, 53–92. https://doi.org/https://doi.org/10.1016/0016-7037(53)90001-5

D'Hondt, S., Inagaki, F., Zarikian, C. A., Abrams, L. J., Dubois, N., Engelhardt, T., Evans, H., Ferdelman, T., Gribsholt, B., Harris, R. N., Hoppie, B. W., Hyun, J. H., Kallmeyer, J., Kim, J., Lynch, J. E., McKinley, C. C., Mitsunobu, S., Morono, Y., Murray, R. W.,…Ziebis, W. (2015). Presence of oxygen and aerobic communities from sea floor to basement in deep-sea sediments. *Nature Geoscience*, *8*(4), 299–304. https://doi.org/10.1038/ngeo2387

Dal Molin, F., Blowers, P., Brady, D., Brown, N., Cogan, S., Davis, T., Hamstead, P., Huk, M., Limbach, H., & Smedley, P. (2023). Determination of Blue Carbon sequestration rates in the UK North Sea using lead-210 and complementary fingerprinting tools. In. https://doi.org/https://doi.org/10.1039/9781837670758

Dal Molin, F., Hunt, D., Dewar, A., Lozach, S., Phillips, C., Thomas, B., Warford, L., Parker, J. E., Walker, J., Chocholek, M., Paterson, D. M., Woodward-Rowe, H., & Hicks, N. (2025). A new approach for assessing the radioecological risk associated with the legacy discharge of oil derived natural radioactivity in the UK North Sea. *Mar Pollut Bull*, *212*, 117585. https://doi.org/10.1016/j.marpolbul.2025.117585

Dal Molin, F., Warwick, P. E., & Read, D. (2018). Under-estimation of 210Pb in industrial radioactive scales. *Analytica Chimica Acta*, *1000*, 67–74. https://doi.org/10.1016/j.aca.2017.08.037

Dannheim, J., Beermann, J., Lacroix, G., De Mesel, I., Kerckhof, F., Schön, I., Degraer, S., Birchenough, S., Garcia, C., Coolen, J. W. P., Lindeboom, H. J., & Wegener, A. (2018). *Understanding the influence of man-made structures on the ecosystem functions of the North Sea (UNDINE)*.

Dannheim, J., Bergström, L., Birchenough, S. N. R., Brzana, R., Boon, A. R., Coolen, J. W. P., Dauvin, J. C., De Mesel, I., Derweduwen, J., Gill, A. B., Hutchison, Z. L., Jackson, A. C., Janas, U., Martin, G., Raoux, A., Reubens, J., Rostin, L., Vanaverbeke, J., Wilding, T. A.,…Degraer, S. (2020). Benthic effects of offshore renewables: Identification of knowledge gaps and urgently needed research. *ICES Journal of Marine Science*, *77*(3), 1092–1108. https://doi.org/https://doi.org/10.1093/icesjms/fsz018

Dauwe, B., Middelburg, J. J., & Herman, P. M. J. (2001). Effect of oxygen on the degradability of organic matter in subtidal and intertidal sediments of the North Sea area. *Marine Ecology Progress Series*, *215*, 13–22. https://doi.org/https://doi.org/10.3354/meps215013

De Borger, E., Ivanov, E., Capet, A., Braeckman, U., Vanaverbeke, J., Grégoire, M., & Soetaert, K. (2021). Offshore Windfarm Footprint of Sediment Organic Matter Mineralization Processes. *Frontiers in Marine Science*, *8*. https://doi.org/10.3389/fmars.2021.632243

De Borger, E., Tiano, J., Braeckman, U., Rijnsdorp, A. D., & Soetaert, K. (2021). Impact of bottom trawling on sediment biogeochemistry: A modelling approach. *Biogeosciences*, *18*(8), 2539–2557. https://doi.org/10.5194/bg-18-2539-2021

De Dominicis, M., O'Hara-Murray, R., & Gallego, A. (2018). *The Scottish Shelf Model 1990 – 2014 climatology version 2.01*.

De Falco, G., Magni, P., Teräsvuori, L. M. H., & Matteucci, G. (2004). Sediment grain size and organic carbon distribution in the cabras lagoon (Sardinia, Western Mediterranean). *Chemistry and Ecology*, *20*(SUPPL. 1). https://doi.org/10.1080/02757540310001629189

De Haas, H. (1997). Transport, preservation and accumulation of organic carbon in the North Sea. In (pp. 1–149): Univ.

de Haas, H., van Weering, T. C. E., & de Stieger, H. (2002). Organic carbon in shelf seas: sinks or sources, processes and products. *Continental Shelf Research*, *22*(5), 691–717. https://doi.org/https://doi.org/10.1016/S0278-4343(01)00093-0

De La Rocha, C. L., & Passow, U. (2007). Factors influencing the sinking of POC and the efficiency of the biological carbon pump. *Deep-Sea Research Part Ii-Topical Studies in Oceanography*, *54*(5-7), 639–658. https://doi.org/10.1016/j.dsr2.2007.01.004

De Mendiburu, F. (2020). *R package: 'agricolae'*.

Denny, M., Baskaran, M., Walsh, C., & Ibrahim, V. (2022). Investigation of self-attenuation of Pb (46 keV) gamma ray in sediment, certified reference material and high-density minerals: Implication to precise measurement of Pb. *Journal of Environmental Radioactivity*, *249*. https://doi.org/https://doi.org/10.1016/j.jenvrad.2022.106888

Depestele, J., Ivanović, A., Degrendele, K., Esmaeili, M., Polet, H., Roche, M., Summerbell, K., Teal, L. R., Vanelslander, B., & O'Neill, F. G. (2016). Measuring and assessing the physical impact of beam trawling. *ICES Journal of Marine Science*, *73*, i15–i26. https://doi.org/10.1093/icesjms/fsv056

Diesing, M., Kroger, S., Parker, R., Jenkins, C., Mason, C., & Weston, K. (2017). Predicting the standing stock of organic carbon in surface sediments of the North-West European continental shelf. *Biogeochemistry*(135), 183–200. https://doi.org/10.1594/PANGAEA.871584

Diesing, M., Paradis, S., Jensen, H., Thorsnes, T., Bjarnadóttir, L. R., & Knies, J. (2024). Glacial troughs as centres of organic carbon accumulation on the Norwegian continental margin. *Communications Earth and Environment*, *5*(1). https://doi.org/10.1038/s43247-024-01502-8

Diesing, M., Thorsnes, T., & Rún Bjarnadóttir, L. (2021). Organic carbon densities and accumulation rates in surface sediments of the North Sea and Skagerrak. *Biogeosciences*, *18*(6), 2139–2160. https://doi.org/10.5194/bg-18-2139-2021

Dinsley, J. M., Gowing, C. J. B., & Marriott, A. L. (2019). *Natural and anthropogenic influences on atmospheric Pb-210 deposition and activity in sediments*

Dounas, C., Davies, I., Triantafyllou, G., Koulouri, P., Petihakis, G., Arvanitidis, C., Sourlatzis, G., & Eleftheriou, A. (2007). Large-scale impacts of bottom trawling on shelf primary productivity. *Continental Shelf Research*, *27*(17), 2198–2210. https://doi.org/10.1016/j.csr.2007.05.006

Duarte, C. M., Losada, I. J., Hendriks, I. E., Mazarrasa, I., & Marbà, N. (2013). The role of coastal plant communities for climate change mitigation and adaptation. *Nature Climate Change*, *3*(11), 961–968. https://doi.org/10.1038/nclimate1970

Ducrotoy, J.-P., Elliottà, M., & De Jonge, V. N. (2000). The North Sea. *Marine Pollution Bulletin*, *41*, 5–23. https://doi.org/https://doi.org/10.1016/S0025-326X(00)00099-0

Dunn, O. J. (1964). Multiple Comparisons Using Rank Sums. *Technometrics*, *6*(3), 241–252. https://doi.org/https://doi.org/10.1080/00401706.1964.10490181

Dunne, J. P., Sarmiento, J. L., & Gnanadesikan, A. (2007). A synthesis of global particle export from the surface ocean and cycling through the ocean interior and on the seafloor. *Global Biogeochemical Cycles*, *21*(4). https://doi.org/https://doi.org/10.1029/2006GB002907

Eigaard, O. R., Bastardie, F., Hintzen, N. T., Buhl-Mortensen, L., Buhl-Mortensen, P., Catarino, R., Dinesen, G. E., Egekvist, J., Fock, H. O., Geitner, K., Gerritsen, H. D., González, M. M., Jonsson, P., Kavadas, S., Laffargue, P., Lundy, M., Gonzalez-Mirelis, G., Nielsen, J. R., Papadopoulou, N.,…Rijnsdorp, A. D. (2017). The footprint of bottom trawling in European waters: Distribution, intensity, and seabed integrity. *ICES Journal of Marine Science*, *74*(3), 847–865. https://doi.org/10.1093/icesjms/fsw194

Ellingsen, K. E. (2001). Biodiversity of a continental shelf soft-sediment macrobenthos community. *Marine Ecology Progress Series*, *218*, 1–15. https://doi.org/https://doi.org/10.3354/meps218001

Ellingsen, K. E. (2002). Soft-sediment benthic biodiversity on the continental shelf in relation to environmental variability. *Marine Ecology Progress Series*, *232*, 15–27. https://doi.org/https://doi.org/10.3354/meps232015

Elrick-Barr, C. E., Zimmerhackel, J. S., Hill, G., Clifton, J., Ackermann, F., Burton, M., & Harvey, E. S. (2022). Man-made structures in the marine environment: A review of stakeholders' social and economic values and perceptions. *Environmental Science and Policy*, *129*, 12–18. https://doi.org/10.1016/j.envsci.2021.12.006

Emery, K. O. (1969). The continental shelves *Scientific American 3*, 106–125. https://doi.org/https://www.jstor.org/stable/26069611

Engelhard, G. H., Righton, D. A., & Pinnegar, J. K. (2014). Climate change and fishing: A century of shifting distribution in North Sea cod. *Global Change Biology*, *20*(8), 2473–2483. https://doi.org/10.1111/gcb.12513

Epstein, G., Middelburg, J. J., Hawkins, J. P., Norris, C. R., & Roberts, C. M. (2022). The impact of mobile demersal fishing on carbon storage in seabed sediments. *Global Change Biology*, *28*, 2875–2894. https://doi.org/https://doi.org/10.1111/gcb.16105Digital

Epstein, G., & Roberts, C. M. (2022). Identifying priority areas to manage mobile bottom fishing on seabed carbon in the UK. *PLOS Climate*, *1*(9), e0000059–e0000059. https://doi.org/https://doi.org/10.1371/journal.pclm.0000059

Falkowski, P., Scholes, R. J., Boyle, E., Canadell, J., Canfield, D., Elser, J., Gruber, N., Hibbard, K., Högberg, P., Linder, S., Mackenzie, F. T., Iii, B. M., Pedersen, T., Rosenthal, Y., Seitzinger, S., Smetacek, V., & Steffen, W. (2000). The Global Carbon Cycle: A Test of Our Knowledge of Earth as a System. *Science*, *290*, 291–296. https://doi.org/10.1126/science.290.5490.291

Falkowski, P. G., Katz, M. E., Knoll, A. H., Quigg, A., Raven, J. A., Schofield, O., & Taylor, F. J. R. (2004). The Evolution of Modern Eukaryotic Phytoplankton. *Science*, *305*, 354–360. https://doi.org/10.1126/science.1095964

Findlay, A. J., Pellerin, A., Laufer, K., & Jørgensen, B. B. (2020). Quantification of sulphide oxidation rates in marine sediment. *Geochimica et Cosmochimica Acta*, *280*, 441–452. https://doi.org/10.1016/j.gca.2020.04.007

Folk, R. L. (1954). The Distinction between Grain Size and Mineral Composition in Sedimentary-Rock Nomenclature. *The Journal of Geology*, *62*(4), 344–359. https://doi.org/https://doi.org/10.1086/626171

Fontugne, M. R., & Duplessy, J. C. (1981). Organic carbon isotopic fractionation by marine phytoplankton in the temperature range - 1 to 31C. *Oceanologica Acta*, *4*(1), 85–90.

Fortune, I. S., & Paterson, D. M. (2020). Ecological best practice in decommissioning: A review of scientific research. *ICES Journal of Marine Science*, *77*(3), 1079–1091. https://doi.org/10.1093/icesjms/fsy130

Fowler, A. M., Jørgensen, A. M., Coolen, J. W. P., Jones, D. O. B., Svendsen, J. C., Brabant, R., Rumes, B., & Degraer, S. (2020). The ecology of infrastructure decommissioning

in the North Sea: What we need to know and how to achieve it. *ICES Journal of Marine Science*, *77*(3), 1109–1126. https://doi.org/10.1093/icesjms/fsz143

Fowler, A. M., Macreadie, P. I., Jones, D. O. B., & Booth, D. J. (2014). A multi-criteria decision approach to decommissioning of offshore oil and gas infrastructure. *Ocean and Coastal Management*, *87*, 20–29. https://doi.org/10.1016/j.ocecoaman.2013.10.019

Fujii, T., & Jamieson, A. J. (2016). Fine-scale monitoring of fish movements and multiple environmental parameters around a decommissioned offshore oil platform: A pilot study in the North Sea. *Ocean Engineering*, *126*, 481–487. https://doi.org/10.1016/j.oceaneng.2016.09.003

G.W.E.C. (2023). *Global Offshore Wind report*. www.gwec.net

Glanemann, N., Willner, S. N., & Levermann, A. (2020). Paris Climate Agreement passes the cost-benefit test. *Nature Communications*, *11*(1). https://doi.org/https://doi.org/10.1038/s41467-019-13961-1

Glud, R. N., Berg, P., Stahl, H., Hume, A., Larsen, M., Eyre, B. D., & Cook, P. L. M. (2016). Benthic Carbon Mineralization and Nutrient Turnover in a Scottish Sea Loch: An Integrative In Situ Study. *Aquatic Geochemistry*, *22*(5-6), 443–467. https://doi.org/10.1007/s10498-016-9300-8

Gore, C., Gehrels, W. R., Smeaton, C., Andrews, L., Mcmahon, L., Hibbert, F., Austin, W. E. N., Nolte, S., & Garrett, E. (2024). Saltmarsh blue carbon accumulation rates and their relationship with sea-level rise on a multi-decadal timescale in northern England. *Estuarine Coastal and Shelf Science*, *299*. https://doi.org/https://doi.org/10.1016/j.ecss.2024.108665

Graves, C. A., Benson, L., Aldridge, J., Austin, W. E. N., Dal Molin, F., Fonseca, V. G., Hicks, N., Hynes, C., Kröger, S., Lamb, P. D., Mason, C., Powell, C., Smeaton, C., Wexler, S. K., Woulds, C., & Parker, R. (2022). Sedimentary carbon on the continental shelf: Emerging capabilities and research priorities for Blue Carbon. *Frontiers in Marine Science*, *9*. https://doi.org/10.3389/fmars.2022.926215

Gray, J., Jones, S. R., & Smith, A. D. (1995). Discharges to the environment from the Sellafield Site, 1951-1992. *J. Radiol. Prot*, *15*, 99–131. https://doi.org/10.1088/0952-4746/15/2/001

Greiner, J. T., McGlathery, K. J., Gunnell, J., & McKee, B. A. (2013). Seagrass Restoration Enhances "Blue Carbon" Sequestration in Coastal Waters. *PLoS ONE*, *8*(8). https://doi.org/10.1371/journal.pone.0072469

Grossman, G. D., Jones, G. P., & Seaman, W. J. (1997). Do artificial reefs increase regional fish production? A review of existing data. *Artificial Reef Management*, 1–7. https://doi.org/10.1577/1548-8446(1997)022

Guo, Y., Wang, H., & Lian, J. (2022). Review of integrated installation technologies for offshore wind turbines: Current progress and future development trends. *Energy Conversion and Management*, *255*. https://doi.org/https://doi.org/10.1016/j.enconman.2022.115319

Haanes, H., Jensen, H. K. B., Lepland, A., & Heldal, H. E. (2023). Increased barium levels in recent marine sediments from the Norwegian and Barents Seas suggest impact of hydrocarbon drilling and production. *Marine Pollution Bulletin*, *186*. https://doi.org/10.1016/j.marpolbul.2022.114478

Hale, R., Godbold, J. A., Sciberras, M., Dwight, J., Wood, C., Hiddink, J. G., & Solan, M. (2017). Mediation of macronutrients and carbon by post-disturbance shelf sea sediment communities. *Biogeochemistry*, *135*(1-2), 121–133. https://doi.org/10.1007/s10533-017-0350-9

Hall, R., Topham, E., & João, E. (2022). Environmental Impact Assessment for the decommissioning of offshore wind farms. *Renewable and Sustainable Energy Reviews*, *165*. https://doi.org/10.1016/j.rser.2022.112580

Harmelin-Vivien, M., Le Diréach, L., Bayle-Sempere, J., Charbonnel, E., García-Charton, J. A., Ody, D., Pérez-Ruzafa, A., Reñones, O., Sánchez-Jerez, P., & Valle, C. (2008). Gradients of abundance and biomass across reserve boundaries in six Mediterranean marine protected areas: Evidence of fish spillover? *Biological Conservation*, *141*(7), 1829–1839. https://doi.org/10.1016/j.biocon.2008.04.029

Hartnett, H. E., Keil, R. G., Hedges, J. I., & Devol, A. H. (1998). Influence of oxygen exposure time on organic carbon preservation in continental margin sediments. *Nature*, *391*, 572–574.

Hatcher, C., Shah, S., Clyde, & Co, L. L. P. (2021). *Could rigs to reefs contribute to the UK's net zero target?*

Hedges, J. I., & Keil, R. G. (1995). Sedimentary organic matter preservation: an assessment and speculative synthesis. *Marine Chemistry*, *49*, 81–115. https://doi.org/https://doi.org/10.1016/0304-4203(95)00008-F

Hedges, J. I., Keil, R. G., & Benner, R. (1997). What happens to terrestrial organic matter in the ocean? *Organic Geochemistry*, *27*(5-6), 195–212. https://doi.org/10.1016/s0146-6380(97)00066-1

Heinatz, K., & Scheffold, M. I. E. (2023). A first estimate of the effect of offshore wind farms on sedimentary organic carbon stocks in the Southern North Sea. *Frontiers in Marine Science*, *9*. https://doi.org/10.3389/fmars.2022.1068967

Heip, C., & Craeymeersch, J. A. (1995). Benthic community structures in the North Sea. *Helgoländer Meeresuntersuchungen*, *49*, 313–328. https://doi.org/https://doi.org/10.1007/BF02368359

Herr, D., von Unger, M., Laffoley, D., & McGivern, A. (2017). Pathways for implementation of blue carbon initiatives. *Aquatic Conservation: Marine and Freshwater Ecosystems*, *27*, 116–129. https://doi.org/10.1002/aqc.2793

Hicks, N., Ubbara, G. R., Silburn, B., Smith, H. E. K., Kröger, S., Parker, E. R., Sivyer, D., Kitidis, V., Hatton, A., Mayor, D. J., & Stahl, H. (2017). Oxygen dynamics in shelf seas sediments incorporating seasonal variability. *Biogeochemistry*, *135*(1-2), 35–47. https://doi.org/10.1007/s10533-017-0326-9

Hiddink, J. G., Burrows, M. T., & García Molinos, J. (2015). Temperature tracking by North Sea benthic invertebrates in response to climate change. *Global Change Biology*, *21*(1), 117–129. https://doi.org/10.1111/gcb.12726

Hiddink, J. G., Jennings, S., Sciberras, M., Szostek, C. L., Hughes, K. M., Ellis, N., Rijnsdorp, A. D., McConnaughey, R. A., Mazor, T., Hilborn, R., Collie, J. S., Pitcher, C. R., Amoroso, R. O., Parma, A. M., Suuronen, P., & Kaiser, M. J. (2017). Global analysis of depletion and recovery of seabed biota after bottom trawling disturbance. *Proceedings of the National Academy of Sciences of the United States of America*, *114*(31), 8301–8306. https://doi.org/10.1073/pnas.1618858114

Hiddink, J. G., van de Velde, S. J., McConnaughey, R. A., De Borger, E., Tiano, J., Kaiser, M. J., Sweetman, A. K., & Sciberras, M. (2023). Quantifying the carbon benefits of ending bottom trawling. *Nature*, *617*, 397–402. https://doi.org/10.1038/s41586-021-03371-z

Hinzmann, N., Stein, P., & Gattermann, J. (2018). Decommissioning of offshore monopiles occuring problems and alternative solutions. Proceedings of the ASME 2018 37th International Conference on Ocean, Offshore and Arctic Engineering,

Hoshino, T., Doi, H., Uramoto, G.-I., Wörmer, L., Adhikari, R. R., Xiao, N., Morono, Y., D'Hondt, S., Hinrichs, K.-U., & Inagaki, F. (2020). Global diversity of microbial

communities in marine sediment. *PNAS*, *117*(44), 27587–27597. https://doi.org/10.1073/pnas.1919139117/-/DCSupplemental

Howard, J., Sutton-Grier, A. E., Smart, L. S., Lopes, C. C., Hamilton, J., Kleypas, J., Simpson, S., McGowan, J., Pessarrodona, A., Alleway, H. K., & Landis, E. (2023). Blue carbon pathways for climate mitigation: Known, emerging and unlikely. *Marine Policy*, *156*. https://doi.org/10.1016/j.marpol.2023.105788

Howard, J. L., Lopes, C. C., Wilson, S. S., McGee-Absten, V., Carrión, C. I., & Fourqurean, J. W. (2020). Decomposition Rates of Surficial and Buried Organic Matter and the Lability of Soil Carbon Stocks Across a Large Tropical Seagrass Landscape. *Estuaries and Coasts*, *44*(3), 846–866. https://doi.org/10.1007/s12237-020-00817-x

Huettel, M., Berg, P., & Kostka, J. E. (2014). Benthic exchange and biogeochemical cycling in permeable sediments. *Annual Review of Marine Science*, *6*, 23–51. https://doi.org/10.1146/annurev-marine-051413-012706

Hulthe, G., Hulth, S., & Hall, P. O. J. (1998). Effect of oxygen on degradation rate of refractory and labile organic matter in continental margin sediments. *Geochimica et Cosmochimica Acta*, *62*(8). https://doi.org/https://doi.org/10.1016/S0016-7037(98)00044-1

Hunter, E. M., Mills, H. J., & Kostka, J. E. (2006). Microbial community diversity associated with carbon and nitrogen cycling in permeable shelf sediments. *Applied and Environmental Microbiology*, *72*(9), 5689–5701. https://doi.org/10.1128/AEM.03007-05

Huppert, A., Blasius, B., & Stone, L. (2002). A model of phytoplankton blooms. *American Naturalist*, *159*(2), 156–171. https://doi.org/https://doi.org/10.1086/324789Doi 10.1086/324789

International Atomic Energy, A. (2021). Certification of Activity Concentration of Radionuclides in IAEA-465 Baltic Sea Sediment. *IAEA Analytical Quality in Nuclear Applications Series*(65), 1–60.

Jagerroos, S., & Krause, P. R. (2016). Rigs-To-Reef; Impact or Enhancement on Marine Biodiversity. *Journal of Ecosystem & Ecography*, *6*(2). https://doi.org/10.4172/2157-7625.1000187

Jia, G., & Jia, J. (2012). Determination of radium isotopes in environmental samples by gamma spectrometry, liquid scintillation counting and alpha spectrometry: A review of analytical methodology. *Journal of Environmental Radioactivity*, *106*, 98–119. https://doi.org/10.1016/j.jenvrad.2011.12.003

Jørgensen, B. B., Wenzhöfer, F., Egger, M., & Glud, R. N. (2022). Sediment oxygen consumption: Role in the global marine carbon cycle. *Earth-Science Reviews*, *228*. https://doi.org/https://doi.org/10.1016/j.earscirev.2022.103987

Jørgensen, D. (2012). OSPAR's exclusion of rigs-to-reefs in the North Sea. *Ocean and Coastal Management*, *58*, 57–61. https://doi.org/10.1016/j.ocecoaman.2011.12.012

Kelly, C. A., Law, R. J., & Emerson, H. S. (2000). *Methods for analysis for hydrocarbons and polycyclic aromatic hydrocarbons (PAH) in marine samples, Science series, aquatic environment protection: analytical methods.*

Klunder, L., Lavaleye, M. S. S., Filippidi, A., Van Bleijswijk, J. D. L., Reichart, G. J., Van Der Veer, H. W., Duineveld, G. C. A., & Mienis, F. (2018). Impact of an artificial structure on the benthic community composition in the southern North Sea: Assessed by a morphological and molecular approach. *ICES Journal of Marine Science*, *77*(3), 1167–1177. https://doi.org/10.1093/icesjms/fsy114

Koide, M., Soutar, A., & Goldberg, E. D. (1972). Marine Geochronology with Pb-210. *Earth and Planetary Science Letters*, *14*(3), 442–&. https://doi.org/10.1016/0012-821x(72)90146-X

Krause, J. R., Hinojosa-Corona, A., Gray, A. B., Herguera, J. C., McDonnell, J., Schaefer, M. V., Ying, S. C., & Watson, E. B. (2022). Beyond habitat boundaries: Organic matter cycling requires a system-wide approach for accurate blue carbon accounting. *Limnology and Oceanography*. https://doi.org/10.1002/lno.12071

Krishnaswamy, S., Lal, D., Martin, J. M., & Meybeck, M. (1972). Geochronology of lake sediments. *Earth and Planetary Science Letters*, *11*(1-5), 407–414. https://doi.org/https://doi.org/10.1016/0012-821X(71)90202-0

Kristensen, E. (2000). Organic matter diagenesis at the oxic/anoxic interface in coastal marine sediments, with emphasis on the role of burrowing animals. *Hydrobiologia*, *426*, 1–24. https://doi.org/https://doi.org/10.1023/A:1003980226194

Kristensen, E., & Blackburn, T. H. (1987). The fate of organic carbon and nitrogen in experimental marine sediment systems: Influence of bioturbation and anoxia. *Journal of Marine Research*, *45*, 231–257.

Krone, R., Gutow, L., Joschko, T. J., & Schröder, A. (2013). Epifauna dynamics at an offshore foundation - Implications of future wind power farming in the North Sea. *Marine Environmental Research*, *85*, 1–12. https://doi.org/10.1016/j.marenvres.2012.12.004

LaRowe, D. E., Arndt, S., Bradley, J. A., Estes, E. R., Hoarfrost, A., Lang, S. Q., Lloyd, K. G., Mahmoudi, N., Orsi, W. D., Shah Walter, S. R., Steen, A. D., & Zhao, R. (2020). The fate of organic carbon in marine sediments - New insights from recent data and analysis. *Earth-Science Reviews*, *204*. https://doi.org/10.1016/j.earscirev.2020.103146

Laruelle, G. G., Cai, W. J., Hu, X., Gruber, N., Mackenzie, F. T., & Regnier, P. (2018). Continental shelves as a variable but increasing global sink for atmospheric carbon dioxide. *Nature Communications*, *9*(1). https://doi.org/10.1038/s41467-017-02738-z

Le Moigne, F. A. C. (2019). Pathways of Organic Carbon Downward Transport by the Oceanic Biological Carbon Pump. *Frontiers in Marine Science*, *6*. https://doi.org/https://doi.org/10.3389/fmars.2019.00634

Leahy, J. G., & Colwell, R. R. (1990). Microbial-Degradation of Hydrocarbons in the Environment. *Microbiological Reviews*, *54*(3), 305–315. https://doi.org/https://doi.org/10.1128/mr.54.3.305-315.1990

Lee, T. R., Wood, W. T., & Phrampus, B. J. (2019). A Machine Learning (kNN) Approach to Predicting Global Seafloor Total Organic Carbon. *Global Biogeochemical Cycles*, *33*(1), 37–46. https://doi.org/10.1029/2018GB005992

Legendre, L., Rivkin, R. B., Weinbauer, M. G., Guidi, L., & Uitz, J. (2015). The microbial carbon pump concept: Potential biogeochemical significance in the globally changing ocean. *Progress in Oceanography*, *134*, 432–450. https://doi.org/10.1016/j.pocean.2015.01.008

Legge, O., Johnson, M., Hicks, N., Jickells, T., Diesing, M., Aldridge, J., Andrews, J., Artioli, Y., Bakker, D. C. E., Burrows, M. T., Carr, N., Cripps, G., Felgate, S. L., Fernand, L., Greenwood, N., Hartman, S., Kröger, S., Lessin, G., Mahaffey, C.,…Williamson, P. (2020). Carbon on the Northwest European Shelf: Contemporary Budget and Future Influences. *Frontiers in Marine Science*, *7*. https://doi.org/10.3389/fmars.2020.00143

Leipe, T., Tauber, F., Vallius, H., Virtasalo, J., Uścinowicz, S., Kowalski, N., Hille, S., Lindgren, S., & Myllyvirta, T. (2011). Particulate organic carbon (POC) in surface sediments of the Baltic Sea. *Geo-Marine Letters*, *31*(3), 175–188. https://doi.org/10.1007/s00367-010-0223-x

Lérida Toro, V., Abascal, U., Villa Alfageme, M., Klar, J., Hicks, N., & López Gutiérrez, J. M. (2022). 129I in sediment cores from the Celtic Sea by AMS through a microwave digestion process. *Nuclear Instruments and Methods in Physics Research B*, *529*, 61–67. https://doi.org/10.1016/j.nimb.2022.08.016

Li, C., Wang, H., Liao, X., Xiao, R., Liu, K., Bai, J., Li, B., & He, Q. (2022). Heavy metal pollution in coastal wetlands: A systematic review of studies globally over the past three decades. *Journal of Hazardous Materials*, *424*. https://doi.org/10.1016/j.jhazmat.2021.127312

Lohse, L., Epping, E. H. G., Helder, W., & Van Raaphorst, W. (1996). Oxygen pore water profiles in continental shelf sediments of the North Sea: turbulent versus molecular diffusion. *Marine Ecology Progress Series*, 63–75. https://doi.org/https://doi.org/10.3354/meps145063

Lovelock, C. E., & Duarte, C. M. (2019). Dimensions of blue carbon and emerging perspectives. *Biology Letters*, *15*. https://doi.org/10.1098/rsbl.2018.0781

Luisetti, T., Ferrini, S., Grilli, G., Jickells, T. D., Kennedy, H., Kröger, S., Lorenzoni, I., Milligan, B., van der Molen, J., Parker, R., Pryce, T., Turner, R. K., & Tyllianakis, E. (2020). Climate action requires new accounting guidance and governance frameworks to manage carbon in shelf seas. *Nature Communications*, *11*(1). https://doi.org/10.1038/s41467-020-18242-w

Luisetti, T., Turner, R. K., Andrews, J. E., Jickells, T. D., Kröger, S., Diesing, M., Paltriguera, L., Johnson, M. T., Parker, E. R., Bakker, D. C. E., & Weston, K. (2019). Quantifying and valuing carbon flows and stores in coastal and shelf ecosystems in the UK. *Ecosystem Services*, *35*, 67–76. https://doi.org/10.1016/j.ecoser.2018.10.013

Lynch-Stieglitz, J., Stocker, T. F., Broecker, W. S., & Fairbanks, R. G. (1995). The influence of air-sea exchange on the isotopic composition of oceanic carbon: Observations and modeling. *Global Biogeochemical Cycles*, *9*(4), 653–665. https://doi.org/10.1029/95GB02574

Lytle, T. F., & Lytle, J. S. (1979). Sediment Hydrocarbons Near an Oil Rig. *Estuarine and Coastal Marine Science*, *9*, 319–330. https://doi.org/https://doi.org/10.1016/0302-3524(79)90044-6

Maar, M., Bolding, K., Petersen, J. K., Hansen, J. L. S., & Timmermann, K. (2009). Local effects of blue mussels around turbine foundations in an ecosystem model of Nysted off-shore wind farm, Denmark. *Journal of Sea Research*, *62*(2-3), 159–174. https://doi.org/10.1016/j.seares.2009.01.008

Macreadie, P. I., Anton, A., Raven, J. A., Beaumont, N., Connolly, R. M., Friess, D. A., Kelleway, J. J., Kennedy, H., Kuwae, T., Lavery, P. S., Lovelock, C. E., Smale, D. A., Apostolaki, E. T., Atwood, T. B., Baldock, J., Bianchi, T. S., Chmura, G. L., Eyre, B. D., Fourqurean, J. W.,…Duarte, C. M. (2019). The future of Blue Carbon science. *Nature Communications*, *10*. https://doi.org/10.1038/s41467-019-11693-w

Macreadie, P. I., Fowler, A. M., & Booth, D. J. (2011). Rigs-to-reefs: Will the deep sea benefit from artificial habitat? *Frontiers in Ecology and the Environment*, *9*, 455–461. https://doi.org/10.1890/100112

Macreadie, P. I., Nielsen, D. A., Kelleway, J. J., Atwood, T. B., Seymour, J. R., Petrou, K., Connolly, R. M., Thomson, A. C. G., Trevathan-Tackett, S. M., & Ralph, P. J. (2017). Can we manage coastal ecosystems to sequester more blue carbon? *Frontiers in Ecology and the Environment*, *15*(4), 206–213. https://doi.org/10.1002/fee.1484

Malinverno, A., & Martinez, E. A. (2015). The effect of temperature on organic carbon degradation in marine sediments. *Scientific Reports*, *5*. https://doi.org/https://doi.org/10.1038/srep17861

Mangiafico, & Salvatore, S. (2023). *R package: 'rcompanion'*. In

Mariani, G., Cheung, W. W. L., Lyet, A., Sala, E., Mayorga, J., Velez, L., Gaines, S. D., Dejean, T., Troussellier, M., & Mouillot, D. (2020). Let more big fish sink: Fisheries prevent blue carbon sequestration-half in unprofitable areas. *Sci. Adv*, *6*. https://doi.org/10.1126/sciadv.abb4848

Martins, M. C. I., Carter, M. I. D., Rouse, S., & Russell, D. J. F. (2023). Offshore energy structures in the North Sea: Past, present and future. *Marine Policy*, *152*. https://doi.org/10.1016/j.marpol.2023.105629

Mason, C. (2022). *NMBAQC's Best Practice Guidance. Particle Size Analysis (PSA) for Supporting Biological Analysis. National Marine Biological AQC Coordinating Committee*.

Masque, P., Isla, E., Sanchez-Cabeza, J. A., Palanques, A., Bruach, J. M., Puig, P., & Guillen, J. (2002). Sediment accumulation rates and carbon fluxes to bottom sediments at the Western Bransfield Strait (Antarctica). *Deep-Sea Research II: Topical Studies in Oceanography*, *49*(4-5), 921–933. https://doi.org/https://doi.org/10.1016/S0967-0645(01)00131-X

Mayer, L. M. (1994). Relationships between mineral surfaces and organic carbon concentrations in soils and sediments. *Chemical Geology*, *114*, 347–363. https://doi.org/https://doi.org/10.1016/0009-2541(94)90063-9

McCartney, M., Kershaw, P. J., & Allington, D. J. (1990). The Behavior of Pb-210 and Ra-226 in the Eastern Irish Sea. *Journal of Environmental Radioactivity*, *12*(3), 243–265. https://doi.org/10.1016/0265-931x(90)90025-Q

McLeod, E., Chmura, G. L., Bouillon, S., Salm, R., Björk, M., Duarte, C. M., Lovelock, C. E., Schlesinger, W. H., & Silliman, B. R. (2011). A blueprint for blue carbon: Toward an improved understanding of the role of vegetated coastal habitats in sequestering CO2. *Frontiers in Ecology and the Environment*, *9*, 552–560. https://doi.org/10.1890/110004

McLeod, E., Salm, R., Green, A., & Almany, J. (2009). Designing marine protected area networks to address the impacts of climate change. *Frontiers in Ecology and the Environment*, *7*(7), 362–370. https://doi.org/10.1890/070211

McMahon, L., Ladd, C. J. T., Burden, A., Garrett, E., Redeker, K. R., Lawrence, P., & Gehrels, R. (2023). Maximizing blue carbon stocks through saltmarsh restoration. *Frontiers in Marine Science*, *10*. https://doi.org/10.3389/fmars.2023.1106607

Michaud, E., Desrosiers, G., Mermillod-Blondin, F., Sundby, B., & Stora, G. (2006). The functional group approach to bioturbation: II. The effects of the Macoma balthica community on fluxes of nutrients and dissolved organic carbon across the sediment-water interface. *Journal of Experimental Marine Biology and Ecology*, *337*(2), 178–189. https://doi.org/10.1016/j.jembe.2006.06.025

Middelburg, J. J. (2018). Reviews and syntheses: To the bottom of carbon processing at the seafloor. In *Biogeosciences* (Vol. 15, pp. 413–427): Copernicus GmbH.

Middelburg, J. J. (2019). Carbon Processing at the Seafloor. In *Marine carbon biogeochemistry: A primer for Earth system scientists* (pp. 57–75). https://doi.org/10.1007/978-3-030-10822-9_4

Middelburg, J. J., & Nieuwenhuize, J. (1998). Carbon and nitrogen stable isotopes in suspended matter and sediments from the Schelde Estuary. *Marine Chemistry*, *60*, 217–225. https://doi.org/https://doi.org/10.1016/S0304-4203(97)00104-7

Mitchell, C., Hu, C., Bowler, B., Drapeau, D., & Balch, W. M. (2017). Estimating Particulate Inorganic Carbon Concentrations of the Global Ocean From Ocean Color Measurements Using a Reflectance Difference Approach. *Journal of Geophysical Research: Oceans*, *122*(11), 8707–8720. https://doi.org/10.1002/2017JC013146

Molen, J. v. d., García-García, L. M., Whomersley, P., Callaway, A., Posen, P. E., & Hyder, K. (2018). Connectivity of larval stages of sedentary marine communities between hard substrates and offshore structures in the North Sea. *Scientific Reports*, *8*(1). https://doi.org/10.1038/s41598-018-32912-2

Mori, F., Umezawa, Y., Kondo, R., Nishihara, G. N., & Wada, M. (2021). Potential oxygen consumption and community composition of sediment bacteria in a seasonally hypoxic enclosed bay. *PeerJ*, *9*. https://doi.org/10.7717/peerj.11836

Moritsch, M. M., Gallagher, A. J., Harris, S. D., Howe, W., Fu, C., Bervoets, T., & Duarte, C. M. (2025). Carbon dynamics under loss and restoration scenarios in the world's largest seagrass meadow. *Scientific Reports*, *15*(1), 1–12. https://doi.org/https://doi.org/10.1038/s41598-025-01993-1

Moritsch, M. M., Young, M., Carnell, P., Macreadie, P. I., Lovelock, C., Nicholson, E., Raimondi, P. T., Wedding, L. M., & Ierodiaconou, D. (2021). Estimating blue carbon sequestration under coastal management scenarios. *Science of the Total Environment*, *777*. https://doi.org/10.1016/j.scitotenv.2021.145962

Mucci, A., Sundby, B., Gehlen, M., Arakaki, T., Zhong, S., & Silverberg, N. (2000). The fate of carbon in continental shelf sediments of eastern Canada: a case study. *Deep-Sea Research II*, *47*, 733–760. https://doi.org/https://doi.org/10.1016/S0967-0645(99)00124-1

Nellemann, C., Corcoran, E., Duarte, C. M., Valdes, L., De Young, C., Fonseca, L., & Grimsditch, G. (2009). *Blue carbon : the role of healthy oceans in binding carbon : a rapid response assessment* (9788277010601).

O'Neill, F. G., & Summerbell, K. (2011). The mobilisation of sediment by demersal otter trawls. *Marine Pollution Bulletin*, *62*(5), 1088–1097. https://doi.org/10.1016/j.marpolbul.2011.01.038

Offshore Energies UK. (2015). *UK Benthos Database 5.1.7* (

Ogle, D., Wheeler, P., & Dinno, A. (2020). *R package 'FSA'*.

Olsgard, F., & Gray, J. S. (1995). A comprehensive analysis of the effects of offshore oil and gas exploration and production on the benthic communities of the Norwegian continental shelf. *Marine Ecology Progress Series*, *122*, 277–306. https://doi.org/https://doi.org/10.3354/meps122277

OSPAR. (1998). *OSPAR Commission Ministerial Meeting of the OSPAR Commission Sintra, Programmes and Measures* (0946955778).

Otto, L., Zimmerman, J. T. E., Furnes, G. K., Mork, M., Saetre, R., & Becker, G. (1990). Review of the physical oceanography of the North Sea. *Netherlands Journal of Sea Research*, *26*, 161–238. https://doi.org/https://doi.org/10.1016/0077-7579(90)90091-T

Oueslati, W., Jlassi, A., Ben Mna, H., Mesnage, V., Rahmouni, R., Added, A., Trabelsi, L., & Aleya, L. (2025). Blue carbon stock in Tunisian coastal sediments: First assessment and implications for ecosystem conservation and climate change mitigation. *Marine Pollution Bulletin*, *215*. https://doi.org/10.1016/j.marpolbul.2025.117909

Ounanian, K., van Tatenhove, J. P. M., & Ramírez-Monsalve, P. (2020). Midnight at the oasis: does restoration change the rigs-to-reefs debate in the North Sea? *Journal of Environmental Policy and Planning*, *22*(2), 211–225. https://doi.org/10.1080/1523908X.2019.1697657

Ouyang, X., & Lee, S. Y. (2014). Updated estimates of carbon accumulation rates in coastal marsh sediments. *Biogeosciences*, *11*(18), 5057–5071. https://doi.org/10.5194/bg-11-5057-2014

Palanques, A., Puig, P., Guillén, J., Demestre, M., & Martín, J. (2014). Effects of bottom trawling on the Ebro continental shelf sedimentary system (NW Mediterranean). *Continental Shelf Research*, *72*, 83–98. https://doi.org/10.1016/j.csr.2013.10.008

Paradis, S., Goñi, M., Masqué, P., Durán, R., Arjona-Camas, M., Palanques, A., & Puig, P. (2021). Persistence of Biogeochemical Alterations of Deep-Sea Sediments by Bottom Trawling. *Geophysical Research Letters*, *48*. https://doi.org/10.1029/2020GL091279

Paradis, S., Pusceddu, A., Masqué, P., Puig, P., Moccia, D., Russo, T., & Iacono, C. L. (2019). Organic matter contents and degradation in a highly trawled area during fresh particle inputs (Gulf of Castellammare, southwestern Mediterranean). *Biogeosciences*, *16*(21), 4307–4320. https://doi.org/10.5194/bg-16-4307-2019

Patterson, W., & Tarnecki, J. (2016). Reef Fish Community Structure at Natural versus Artificial Reefs in the Northern Gulf of Mexico. Proceedings of the 66th Gulf and Caribbean Fisheries Institute,

Paxton, A. B., Newton, E. A., Adler, A. M., van Hoeck, R. V., Iversen, E. S., Christopher Taylor, J., Peterson, C. H., & Silliman, B. R. (2020). Artificial habitats host elevated densities of large reef-associated predators. *PLoS ONE*, *15*(9). https://doi.org/10.1371/journal.pone.0237374

Peng, R. H., Xiong, A. S., Xue, Y., Fu, X. Y., Gao, F., Zhao, W., Tian, Y. S., & Yao, Q. H. (2008). Microbial biodegradation of polyaromatic hydrocarbons. *Fems Microbiology Reviews*, *32*(6), 927–955. https://doi.org/10.1111/j.1574-6976.2008.00127.x

Perera, N., Lokupitiya, E., Halwatura, D., & Udagedara, S. (2022). Quantification of blue carbon in tropical salt marshes and their role in climate change mitigation. *Science of the Total Environment*, *820*. https://doi.org/10.1016/j.scitotenv.2022.153313

Perkol-Finkel, S., Shashar, N., & Benayahu, Y. (2006). Can artificial reefs mimic natural reef communities? The roles of structural features and age. *Marine Environmental Research*, *61*(2), 121–135. https://doi.org/10.1016/j.marenvres.2005.08.001

Pham, M. K., Aust, M. O., Bartocci, J., Blinova, O., Carvalho, F. P., Chamizo, E., Cook, M., Degering, D., Fujak, M., Gascó, C., Gurriaran, R., Jobbágy, V., Herrmann, J., Hult, M., Ilchmann, C., La Rosa, J., Laubenstein, M., Lee, S. H., Levy, I.,…Zalewska, T. (2024). A new certified reference material IAEA-465 for radionuclides in Baltic Sea sediment. *Journal of Environmental Radioactivity*, *278*. https://doi.org/10.1016/j.jenvrad.2024.107499

Phillipson, J., & Symes, D. (2018). 'A sea of troubles': Brexit and the fisheries question. *Marine Policy*, *90*, 168–173. https://doi.org/10.1016/j.marpol.2017.12.016

Pickering, H., & Whitmarsh, D. (1997). Artificial reefs and fisheries exploitation: a review of the 'attraction versus production' debate, the influence of design and its significance for policy. *Fisheries Research*, *31*, 39–59.

Porz, L., Zhang, W., Christiansen, N., Kossack, J., Daewel, U., & Schrum, C. (2024). Quantification and mitigation of bottom-trawling impacts on sedimentary organic carbon stocks in the North Sea. *Biogeosciences*, *21*(10), 2547–2570. https://doi.org/10.5194/bg-21-2547-2024

Porz, L., Zhang, W., Hanebuth, T. J. J., & Schrum, C. (2021). Physical processes controlling mud depocenter development on continental shelves – Geological, oceanographic, and modeling concepts. *Marine Geology*, *432*. https://doi.org/10.1016/j.margeo.2020.106402

Potts, L. D., Calderon, L. J. P., Gubry-Rangin, C., Witte, U., & Anderson, J. A. (2019). Characterisation of microbial communities of drill cuttings piles from offshore oil and gas installations. *Marine Pollution Bulletin*, *142*, 169–177. https://doi.org/10.1016/j.marpolbul.2019.03.014

Povinec, P. P., Bailly Du Bois, P., Kershaw, P. J., Nies, H., & Scotto, P. (2003). Temporal and spatial trends in the distribution of 137Cs in surface waters of Northern European Seas - A record of 40 years of investigations. *Deep-Sea Research Part II: Topical Studies in Oceanography*, *50*(17-21), 2785–2801. https://doi.org/10.1016/S0967-0645(03)00148-6

Pusceddu, A., Fiordelmondo, C., Polymenakou, P., Polychronaki, T., Tselepides, A., & Danovaro, R. (2005). Effects of bottom trawling on the quantity and biochemical

composition of organic matter in coastal marine sediments (Thermaikos Gulf, northwestern Aegean Sea). *Continental Shelf Research*, *25*(19-20), 2491–2505. https://doi.org/10.1016/j.csr.2005.08.013

Putuhena, H., White, D., Gourvenec, S., & Sturt, F. (2023). Finding space for offshore wind to support net zero: A methodology to assess spatial constraints and future scenarios, illustrated by a UK case study. *Renewable and Sustainable Energy Reviews*, *182*. https://doi.org/10.1016/j.rser.2023.113358

Quante, M., & Colijn, F. (2016). *North Sea region climate change assessment*. Spinger Nature https://doi.org/https://doi.org/10.1007/978-3-319-39745-0

Rastelli, E., Corinaldesi, C., Dell'Anno, A., Amaro, T., Greco, S., Lo Martire, M., Carugati, L., Queirós, A. M., Widdicombe, S., & Danovaro, R. (2016). CO2 leakage from carbon dioxide capture and storage (CCS) systems affects organic matter cycling in surface marine sediments. *Marine Environmental Research*, *122*, 158–168. https://doi.org/10.1016/j.marenvres.2016.10.007

Richard, D., Sundby, B., & Mucci, A. (2013). Kinetics of manganese adsorption, desorption, and oxidation in coastal marine sediments. *Limnology and Oceanography*, *58*(3), 987–996. https://doi.org/10.4319/lo.2013.58.3.0987

Roberts, C. (2007). *Unnatural History of the Sea*. Island Press.

Robinson, J. E., Newell, R. C., Seiderer, L. J., & Simpson, N. M. (2005). Impacts of aggregate dredging on sediment composition and associated benthic fauna at an offshore dredge site in the southern North Sea. *Marine Environmental Research*, *60*(1), 51–68. https://doi.org/10.1016/j.marenvres.2004.09.001

Ronconi, R. A., Allard, K. A., & Taylor, P. D. (2015). Bird interactions with offshore oil and gas platforms: Review of impacts and monitoring techniques. In *Journal of Environmental Management* (Vol. 147, pp. 34–45): Academic Press.

Rusch, A., Huettel, M., Wild, C., & Reimers, C. E. (2006). Benthic oxygen consumption and organic matter turnover in organic-poor, permeable shelf sands. *Aquatic Geochemistry*, *12*(1), 1–19. https://doi.org/10.1007/s10498-005-0784-x

Rutherford, P. M., Dudas, M. J., & Samek, R. A. (1994). Environmental Impacts of Phosphogypsum. *Science of the Total Environment*, *149*(1-2), 1–38. https://doi.org/10.1016/0048-9697(94)90002-7

Sabine, C. L., Feely, R. A., Gruber, N., Key, R. M., Lee, K., Bullister, J. L., Wanninkhof, R., Wong, C. S., Wallace, D. W. R., Tilbrook, B., Millero, F. J., Peng, T. H., Kozyr, A., Ono, T., & Rios, A. F. (2004). The oceanic sink for anthropogenic CO2. *Science*, *305*(5682), 367–371. https://doi.org/10.1126/science.1097403

Sala, E., Mayorga, J., Bradley, D., Cabral, R. B., Atwood, T. B., Auber, A., Cheung, W., Costello, C., Ferretti, F., Friedlander, A. M., Gaines, S. D., Garilao, C., Goodell, W., Halpern, B. S., Hinson, A., Kaschner, K., Kesner-Reyes, K., Leprieur, F., McGowan, J.,…Lubchenco, J. (2021). Protecting the global ocean for biodiversity, food and climate. *Nature*, *592*(7854), 397–402. https://doi.org/10.1038/s41586-021-03371-z

Salm, R. V., Done, T., & McLeod, E. (2011). Marine protected area planning in a changing climate. In *Coral Reefs and Climate Change: Science and Management* (pp. 207–222). https://doi.org/10.1029/61ce12

Sanchez-Cabeza, J. A., & Ruiz-Fernández, A. C. (2012). Pb sediment radiochronology: An integrated formulation and classification of dating models. *Geochimica et Cosmochimica Acta*, *82*, 183–200. https://doi.org/10.1016/j.gca.2010.12.024

Schneider, J. A., & Senders, M. (2010). Foundation design: A comparison of oil and gas platforms with offshore wind turbines. *Marine Technology Society Journal*, *44*(1), 32–51. https://doi.org/10.4031/MTSJ.44.1.5

Schutter, M., Dorenbosch, M., Driessen, F. M. F., Lengkeek, W., Bos, O. G., & Coolen, J. W. P. (2019). Oil and gas platforms as artificial substrates for epibenthic North Sea fauna: Effects of location and depth. *Journal of Sea Research*, *153*. https://doi.org/10.1016/j.seares.2019.101782

Sciberras, M., Parker, R., Powell, C., Robertson, C., Kröger, S., Bolam, S., & Geert Hiddink, J. (2016). Impacts of bottom fishing on the sediment infaunal community and biogeochemistry of cohesive and non-cohesive sediments. *Limnology and Oceanography*, *61*(6), 2076–2089. https://doi.org/10.1002/lno.10354

SEPA. (2014). *Strategy for the management of Naturally Occurring Radioactive Material (NORM) waste in the United Kingdom*.

Shapiro, S. S., & Wilk, M. B. (1965). An Analysis of Variance Test for Normality (Complete Samples) An analysis of variance test for normality (complete samples)t. *Biometrika*, *52*(3 and 4), 591–611. https://doi.org/https://doi.org/10.1093/biomet/52.3-4.591

Slavik, K., Lemmen, C., Zhang, W., Kerimoglu, O., Klingbeil, K., & Wirtz, K. W. (2017). The large scale impact of offshore wind farm structures on pelagic primary productivity in the southern North Sea. *Hydrobiologia*, *845*, 35–53. https://doi.org/https://doi.org/10.1007/s10750-018-3653-5

Smeaton, C., & Austin, W. E. N. (2022a). Quality Not Quantity: Prioritizing the Management of Sedimentary Organic Matter Across Continental Shelf Seas. *Geophysical Research Letters*, *49*(5). https://doi.org/10.1029/2021GL097481

Smeaton, C., & Austin, W. E. N. (2022b). Understanding the Role of Terrestrial and Marine Carbon in the Mid-Latitude Fjords of scotland. *Global Biogeochemical Cycles*, *36*(11). https://doi.org/10.1029/2022GB007434

Smeaton, C., Hunt, C. A., Turrell, W. R., & Austin, W. E. N. (2021). Marine Sedimentary Carbon Stocks of the United Kingdom's Exclusive Economic Zone. *Frontiers in Earth Science*, *9*. https://doi.org/10.3389/feart.2021.593324

Smeaton, C., Yang, H., & Austin, W. E. N. (2021). Carbon burial in the mid-latitude fjords of Scotland. *Marine Geology*, *441*. https://doi.org/10.1016/j.margeo.2021.106618

Soetaert, K., Herman, P. M. J., & Middelburg, J. J. (1996). A model of early diagenetic processes from the shelf to abyssal depths. *Ceochimica et Cosmochimica Acta*, *60*(6), 1019–1040. https://doi.org/https://doi.org/10.1016/0016-7037(96)00013-0

Soetaert, K., Middelburg, J. J., Herman, P. M. J., & Buis, K. (2000). On the coupling of benthic and pelagic biogeochemical models. *Earth-Science Reviews*, *51*, 173–201. https://doi.org/https://doi.org/10.1016/S0012-8252(00)00004-0

Sofer, Z. (1984). Stable Carbon Isotope Compositions of Crude Oils: Application to Source Depositional Environments and Petroleum Alteration. *The American Association of Petroleum Geologists Bulletin*, *68*(1), 31–49. https://doi.org/https://doi.org/10.1306/AD460963-16F7-11D7-8645000102C1865D

Sommer, B., Fowler, A. M., Macreadie, P. I., Palandro, D. A., Aziz, A. C., & Booth, D. J. (2019). Decommissioning of offshore oil and gas structures – Environmental opportunities and challenges. *Science of the Total Environment*, *658*, 973–981. https://doi.org/10.1016/j.scitotenv.2018.12.193

Stephens, D., & Diesing, M. (2015). Towards quantitative spatial models of seabed sediment composition. *PLoS ONE*, *10*(11). https://doi.org/10.1371/journal.pone.0142502

Talin, F., Tolla, C., Rabouille, C., & Poggiale, J. C. (2002). Relations between bacterial biomass and carbon cycle in marine sediments: an early diagenetic model. *Acta Biotheoretica*, *51*, 295–315. https://doi.org/https://doi.org/10.1023/B:ACBI.0000003985.11896.b4

Tamborski, J. J., Cai, P., Eagle, M., Henderson, P., & Charette, M. A. (2022). Revisiting 228Th as a tool for determining sedimentation and mass accumulation rates. *Chemical Geology*, *607*. https://doi.org/10.1016/j.chemgeo.2022.121006

Techera, E. J., & Chandler, J. (2015). Offshore installations, decommissioning and artificial reefs: Do current legal frameworks best serve the marine environment? *Marine Policy*, *59*, 53–60. https://doi.org/10.1016/j.marpol.2015.04.021

Tesi, T., Miserocchi, S., Goñi, M. A., Langone, L., Boldrin, A., & Turchetto, M. (2007). Organic matter origin and distribution in suspended particulate materials and surficial sediments from the western Adriatic Sea (Italy). *Estuarine, Coastal and Shelf Science*, *73*(3-4), 431–446. https://doi.org/10.1016/j.ecss.2007.02.008

The Crown Estate. (2022). *Offshore Wind Report*.

Thomas, H., Bozec, Y., De Baar, H. J. W., Elkalay, K., Frankignoulle, M., Schiettecatte, L. S., Kattner, G., & Borges, A. V. (2005). The carbon budget of the North Sea. *Biogeosciences*, *2*, 87–96. https://doi.org/https://doi.org/10.5194/bg-2-87-2005

Thomas, H., Bozec, Y., Elkalay, K., & de Baar, H. J. W. (2004). Enhanced open ocean storage of CO2 from Shelf Sea pumping. *Science*, *304*(5673), 1005–1008. https://doi.org/10.1126/science.1096033

Thompson, C. E. L., Couceiro, F., Fones, G. R., Helsby, R., Amos, C. L., Black, K., Parker, E. R., Greenwood, N., Statham, P. J., & Kelly-Gerreyn, B. A. (2011). In situ flume measurements of resuspension in the North Sea. *Estuarine, Coastal and Shelf Science*, *94*(1), 77–88. https://doi.org/10.1016/j.ecss.2011.05.026

Thornton, S. F., & Mcmanus, J. (1994). Application of Organic-Carbon and Nitrogen Stable-Isotope and C/N Ratios as Source Indicators of Organic-Matter Provenance in Estuarine Systems - Evidence from the Tay Estuary, Scotland. *Estuarine Coastal and Shelf Science*, *38*(3), 219–233. https://doi.org/10.1006/ecss.1994.1015

Thurstan, R. H., Brockington, S., & Roberts, C. M. (2010). The effects of 118 years of industrial fishing on UK bottom trawl fisheries. *Nature Communications*, *1*(15). https://doi.org/10.1038/ncomms1013

Tiano, J., De Borger, E., Paradis, S., Bradshaw, C., Morys, C., Pusceddu, A., Ennas, C., Soetaert, K., Puig, P., Masqué, P., & Sciberras, M. (2024). Global meta-analysis of demersal fishing impacts on organic carbon and associated biogeochemistry. *Fish and Fisheries*, *25*(6), 936–950. https://doi.org/10.1111/faf.12855

Tiano, J., De Borger, E., Paradis, S., Bradshaw, C., Morys, C., Pusceddu, A., Ennas, C., Soetaert, K., Puig, P., Masqué, P., & Sciberras, M. (2024). Global meta-analysis of demersal fishing impacts on organic carbon and associated biogeochemistry. *Fish and Fisheries*. https://doi.org/10.1111/faf.12855

Tidbury, H., Taylor, N., van der Molen, J., Garcia, L., Posen, P., Gill, A., Lincoln, S., Judd, A., & Hyder, K. (2020). Social network analysis as a tool for marine spatial planning: Impacts of decommissioning on connectivity in the North Sea. *Journal of Applied Ecology*, *57*(3), 566–577. https://doi.org/10.1111/1365-2664.13551

Todd, V. L. G., Lavallin, E. W., & Macreadie, P. I. (2018). Quantitative analysis of fish and invertebrate assemblage dynamics in association with a North Sea oil and gas installation complex. *Marine Environmental Research*, 69–79. https://doi.org/10.1016/j.marenvres.2018.09.018

Torchiano, M. (2020). *R package: 'effsize'*. In

Tukey, J. W. (1953). Some selected quick and easy methods of statistical analysis. *Transactions of the New York Academy of Sciences*, *16*(2), 88–97. https://doi.org/10.1111/j.2164-0947.1953.tb01326.x

van der Molin, J., Aldridge, J. N., Coughlan, C., Parker, E. R., Stephens, D., & Ruardij, P. (2013). Modelling marine ecosystem response to climate change and trawling in the

north sea. *Biogeochemistry*, *113*, 213–236. https://doi.org/https://doi.org/10.1007/s10533-012-9763-7

Van Der Stap, T., Coolen, J. W. P., & Lindeboom, H. J. (2016). Marine fouling assemblages on offshore gas platforms in the southern North Sea: Effects of depth and distance from shore on biodiversity. *PLoS ONE*, *11*(1). https://doi.org/10.1371/journal.pone.0146324

Vidal, P. d. C. J., González, M. O. A., Vasconcelos, R. M. d., Melo, D. C. d., Ferreira, P. d. O., Sampaio, P. G. V., & Silva, D. R. d. (2022). Decommissioning of offshore oil and gas platforms: A systematic literature review of factors involved in the process. *Ocean Engineering*, *255*. https://doi.org/10.1016/j.oceaneng.2022.111428

Wang, W. P., Wang, L., & Shao, Z. Z. (2018). Polycyclic Aromatic Hydrocarbon (PAH) Degradation Pathways of the Obligate Marine PAH Degrader Cycloclasticus sp. Strain P1. *Applied and Environmental Microbiology*, *84*(21). https://doi.org/10.1128/AEM.01261-18

Ward, S. L., Bradley, S. L., Roseby, Z. A., Wilmes, S. B., Vosper, D. F., Roberts, C. M., & Scourse, J. D. (2025). The Role of Long-Term Hydrodynamic Evolution in the Accumulation and Preservation of Organic Carbon-Rich Shelf Sea Deposits. *Journal of Geophysical Research: Oceans*, *130*(4). https://doi.org/10.1029/2024jc022092

Wei, T., & Simko, V. (2021). Package 'corrplot': Visualization of a Correlation Matrix. *(Version 0.92)*. https://doi.org/https://github.com/taiyun/corrplot

Wei, X., & Zhou, J. (2024). Multi-Criteria Decision Analysis for Sustainable Oil and Gas Infrastructure Decommissioning: A Systematic Review of Criteria Involved in the Process. *Sustainability*, *16*. https://doi.org/10.3390/su16167205

Weinert, M., Mathis, M., Kröncke, I., Pohlmann, T., & Reiss, H. (2021). Climate change effects on marine protected areas: Projected decline of benthic species in the North Sea. *Marine Environmental Research*, *163*. https://doi.org/10.1016/j.marenvres.2020.105230

Wickham, H. (2010). ggplot2 : elegant graphics for data analysis. *Journal of Statistical Software*, *35*(1), 1–1.

Wilk, C. (2020). *R package 'cowplot'*. https://cran.r-project.org/web/packages/cowplot/index.html

Wilkinson, G. M., Besterman, A., Buelo, C., Gephart, J., & Pace, M. L. (2018). A synthesis of modern organic carbon accumulation rates in coastal and aquatic inland ecosystems. *Scientific Reports*, *8*(1), 1–9. https://doi.org/10.1038/s41598-018-34126-y

Williamson, P., & Gattuso, J.-P. (2022). Carbon Removal Using Coastal Blue Carbon Ecosystems Is Uncertain and Unreliable, With Questionable Climatic Cost-Effectiveness. *Frontiers in Climate*, *4*. https://doi.org/10.3389/fclim.2022.853666

Wilson, R. J., Speirs, D. C., Sabatino, A., & Heath, M. R. (2018). A synthetic map of the north-west European Shelf sedimentary environment for applications in marine science. *Earth System Science Data*, *10*(1), 109–130. https://doi.org/10.5194/essd-10-109-2018

Winther, N. G., & Johannessen, J. A. (2006). North Sea circulation: Atlantic inflow and its destination. *Journal of Geophysical Research: Oceans*, *111*(12). https://doi.org/10.1029/2005JC003310

Woodward-Rowe, H., Dal Molin, F., Gregson, B. H., Mason, C., Parker, R., & Hicks, N. (2025). Sedimentary blue carbon around decommissioned oil and gas platforms in the North Sea. *Marine Pollution Bulletin*, *219*. https://doi.org/10.1016/j.marpolbul.2025.118250

Woulds, C., Cowie, G. L., Levin, L. A., Andersson, J. H., Middelburg, J. J., Vandewiele, S., Lamont, P. A., Larkin, K. E., Gooday, A. J., Schumacher, S., Whitcraft, C., Jeffreys,

R. M., & Schwartz, M. (2007). Oxygen as a control on seafloor biological communities and their roles in sedimentary carbon cycling. *Limnology and Oceanography*, *52*(4), 1698–1709. https://doi.org/10.4319/lo.2007.52.4.1698

Wright, S. R., Lynam, C. P., Righton, D. A., Metcalfe, J., Hunter, E., Riley, A., Garcia, L., Posen, P., & Hyder, K. (2020). Structure in a sea of sand: Fish abundance in relation to man-made structures in the North Sea. *ICES Journal of Marine Science*, *77*(3), 1206–1218. https://doi.org/10.1093/icesjms/fsy142

Wu, X., Hu, Y., Li, Y., Yang, J., Duan, L., Wang, T., Adcock, T., Jiang, Z., Gao, Z., Lin, Z., Borthwick, A., & Liao, S. (2019). Foundations of offshore wind turbines: A review. *Renewable and Sustainable Energy Reviews*, *104*, 379–393. https://doi.org/10.1016/j.rser.2019.01.012

Zawawi, N. A. W. A., Liew, M. S., & Na, K. L. (2012). Decommissioning of offshore platform: A sustainable framework. *2012 IEEE Colloquium on Humanities, Science and Engineering (CHUSER)*, 26–31. https://doi.org/10.1109/CHUSER.2012.6504275

Appendices

Appendix figures

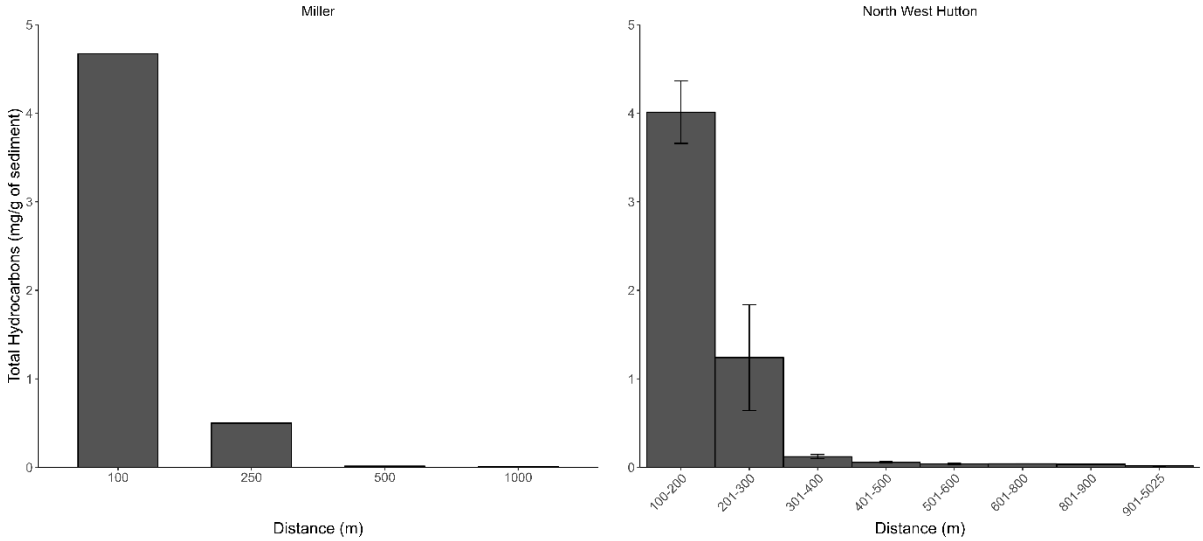

Appendix figure 1: Total hydrocarbon content (mg/g) of sediment at increasing distances from Miller and North West Hutton. Sampling distance from Miller where 100, 250, 500 and 1000m and 100-200, 201-300, 301-400, 401-500, 501-600, 601-800,801-900,901-5025m. This data was taken from the UK Benthos database v5.17 (Offshore Energies UK, 2015).

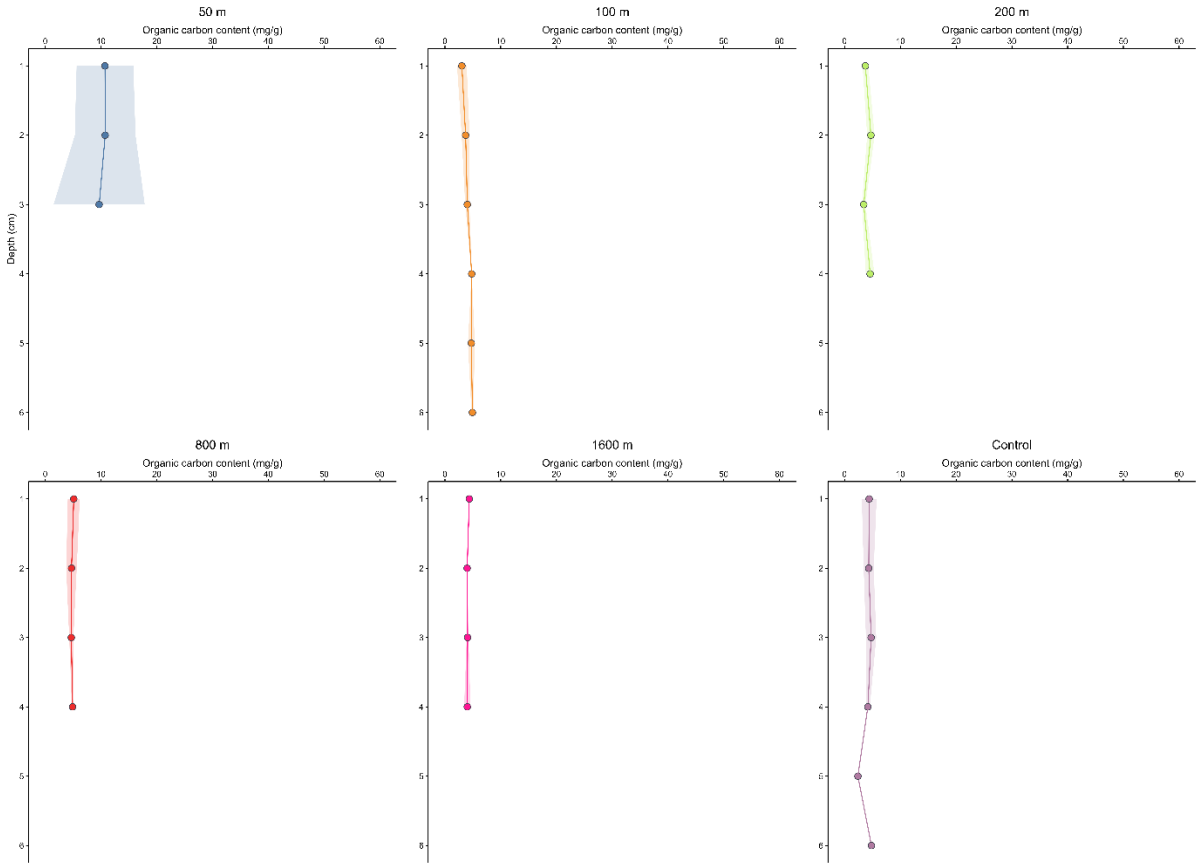

Appendix figure 2: Averaged organic carbon content (mg/g of sediment) depth profiles at the decommissioned Miller platform, along the northern transect. Where possible, three cores were averaged; shaded areas represent standard deviation.. Three cores were used for 50m and 800m and two cores were used for 100 m, 1600 m and control (3200 m).

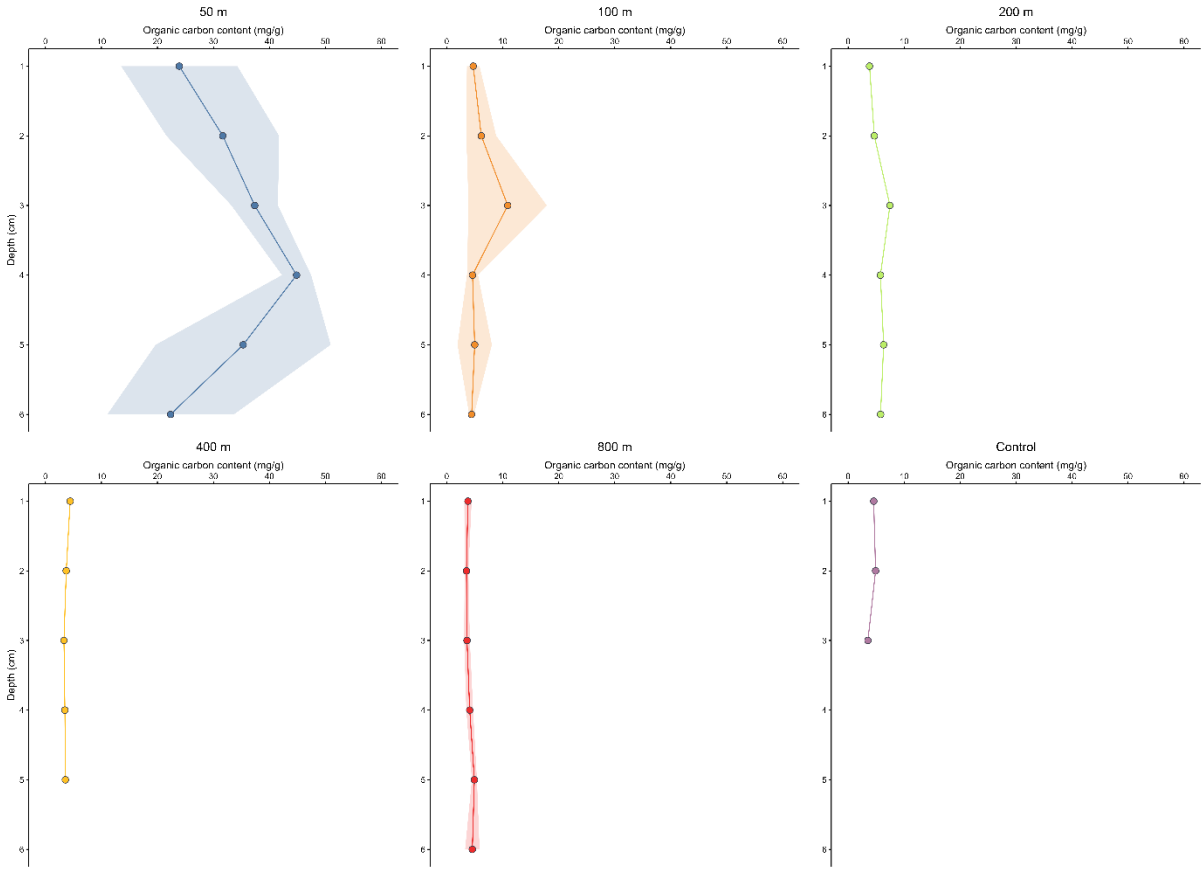

Appendix figure 3: Averaged organic carbon content (mg/g of sediment) depth profiles at the decommissioned Miller platform, along the southern transect. Where possible, three cores were averaged; shaded areas represent standard deviation. Three cores were used for 50m and 100m and two cores were used for 800m. Only one core was available for 200, 400 and control (3200m).

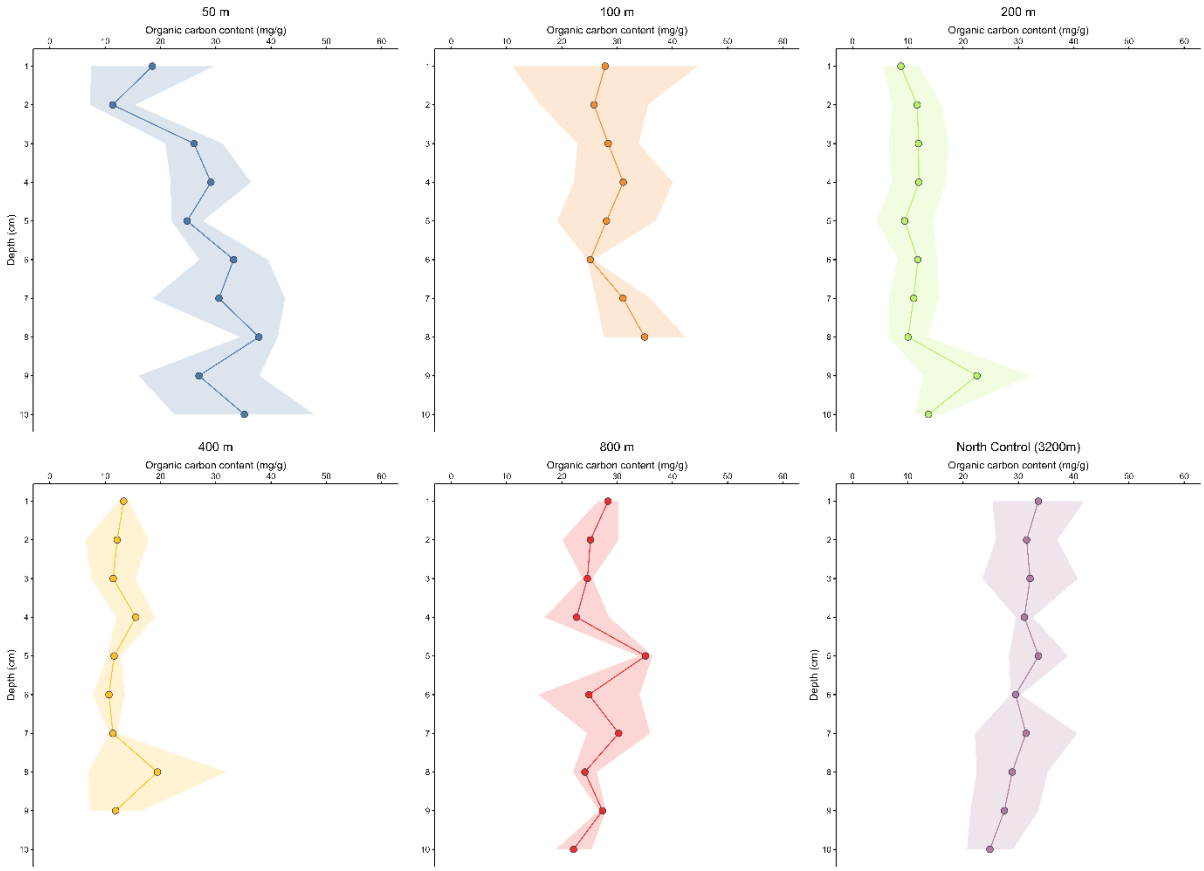

Appendix figure 4: Averaged organic carbon content (mg/g of sediment) depth profiles at North West Hutton decommissioned platform along the northern transect. Where possible, three cores were averaged; shaded areas represent standard deviation. Three cores were used for 50m, 100m, 200m, 400m, 800m and control (3200m).

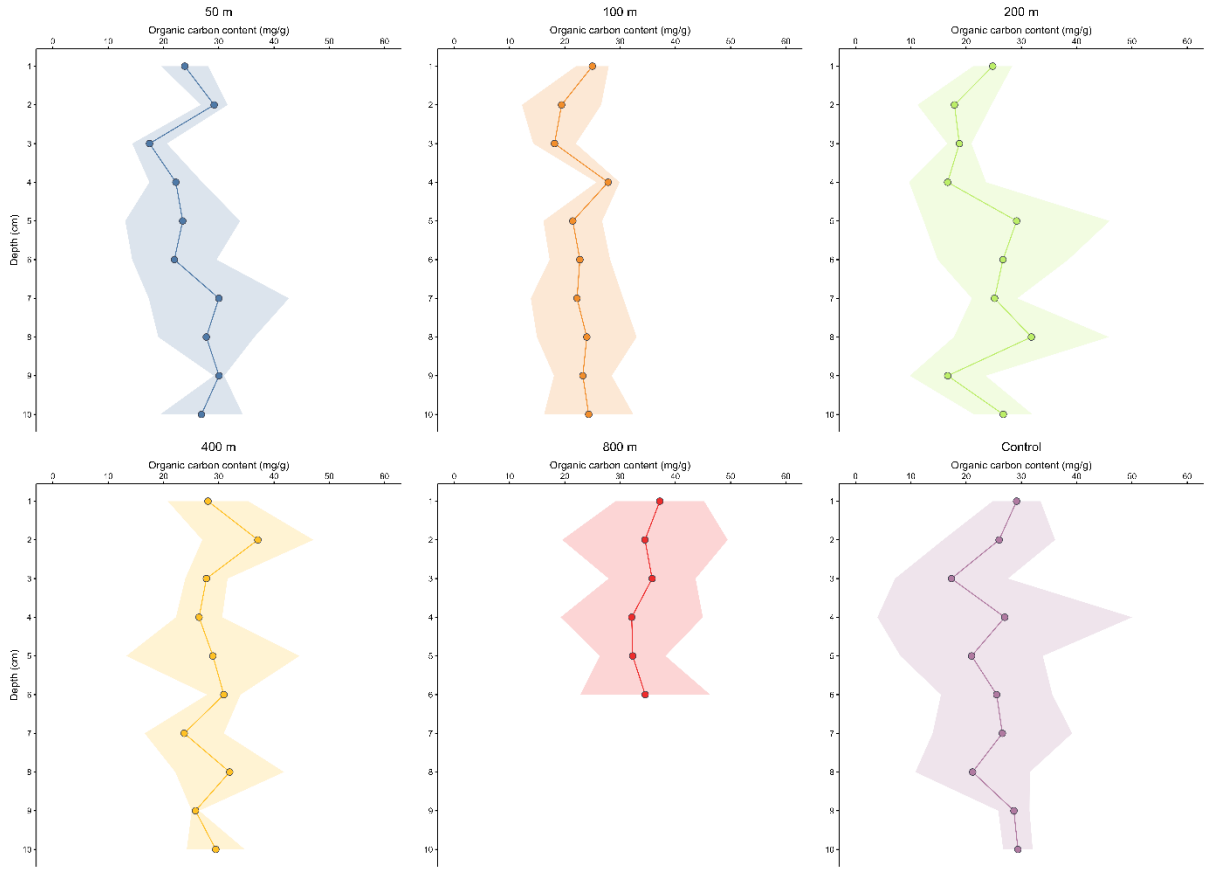

Appendix figure 5: Averaged organic carbon content (mg/g of sediment) depth profiles at the decommissioned North West Hutton platform along the southern transect. Where possible, three cores were averaged; shaded areas represent standard deviation. Three cores were used for 50m, 100m, 200m, 400m, 800m, and control (3200m).

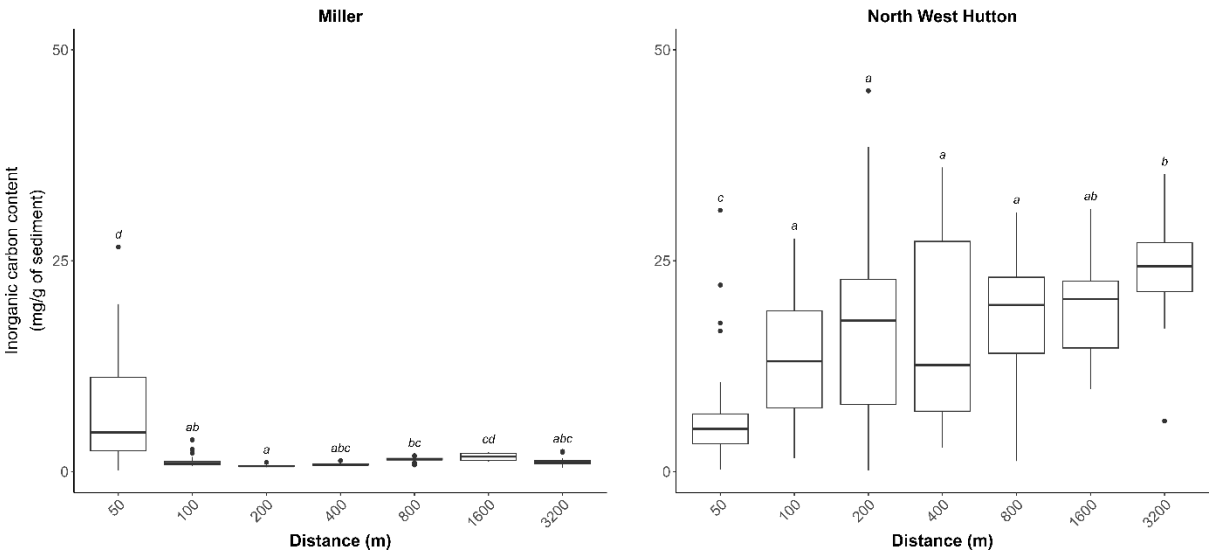

Appendix figure 6: Inorganic carbon content (mg/g of sediment) of 1 cm sediment core slices collected at increasing distances (50- 3200 m) away from two decommissioned oil and gas platforms, Miller and North West Hutton. Sediment was analysed to 10 cm depth at North West Hutton and 6 cm at Miller. Letters above boxes (a,b,c) indicate significant difference in inorganic carbon content between sampling distance ($P < 0.05$ Kruskal-Wallis test followed by Dunn's post hoc test) with differing letters indicating significant differences.

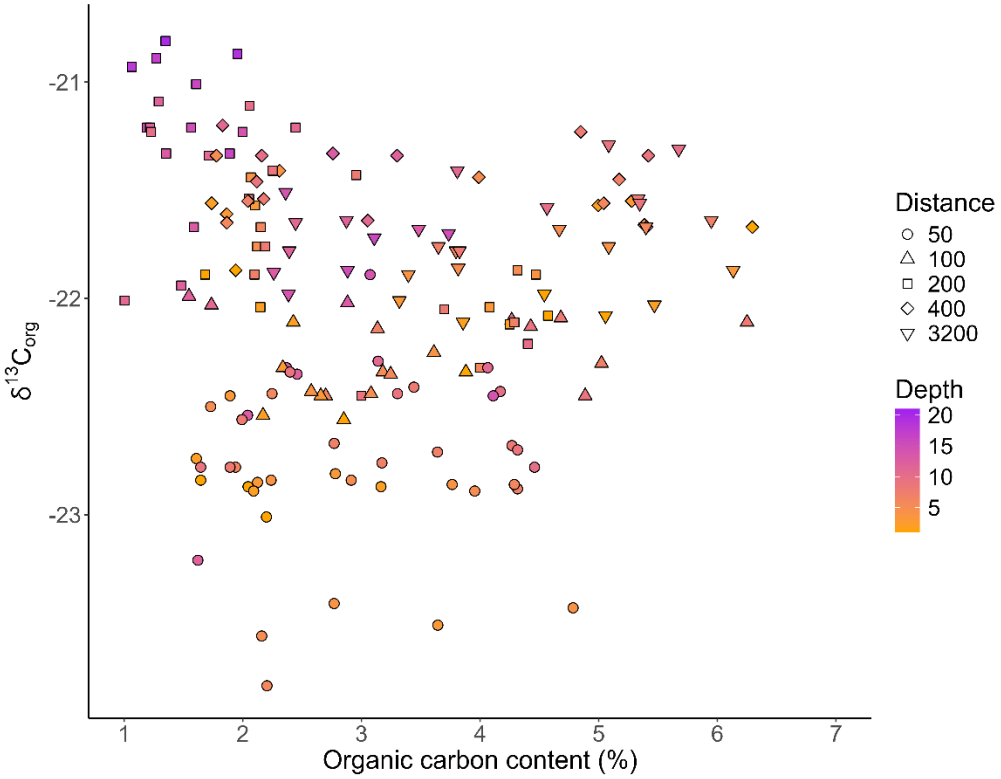

Appendix figure 7: Comparison of $\delta^{13}C_{org}$ and organic carbon content (%) of sediment slices from sediment cores at varying distances (50 – 3200 m) from two decommissioned oil and gas platforms, Miller and North West Hutton in the North Sea. Distance is determined by shape of points and depth of the slice is determined with a colour gradient with orange being shallower depths and purple being deeper depths.

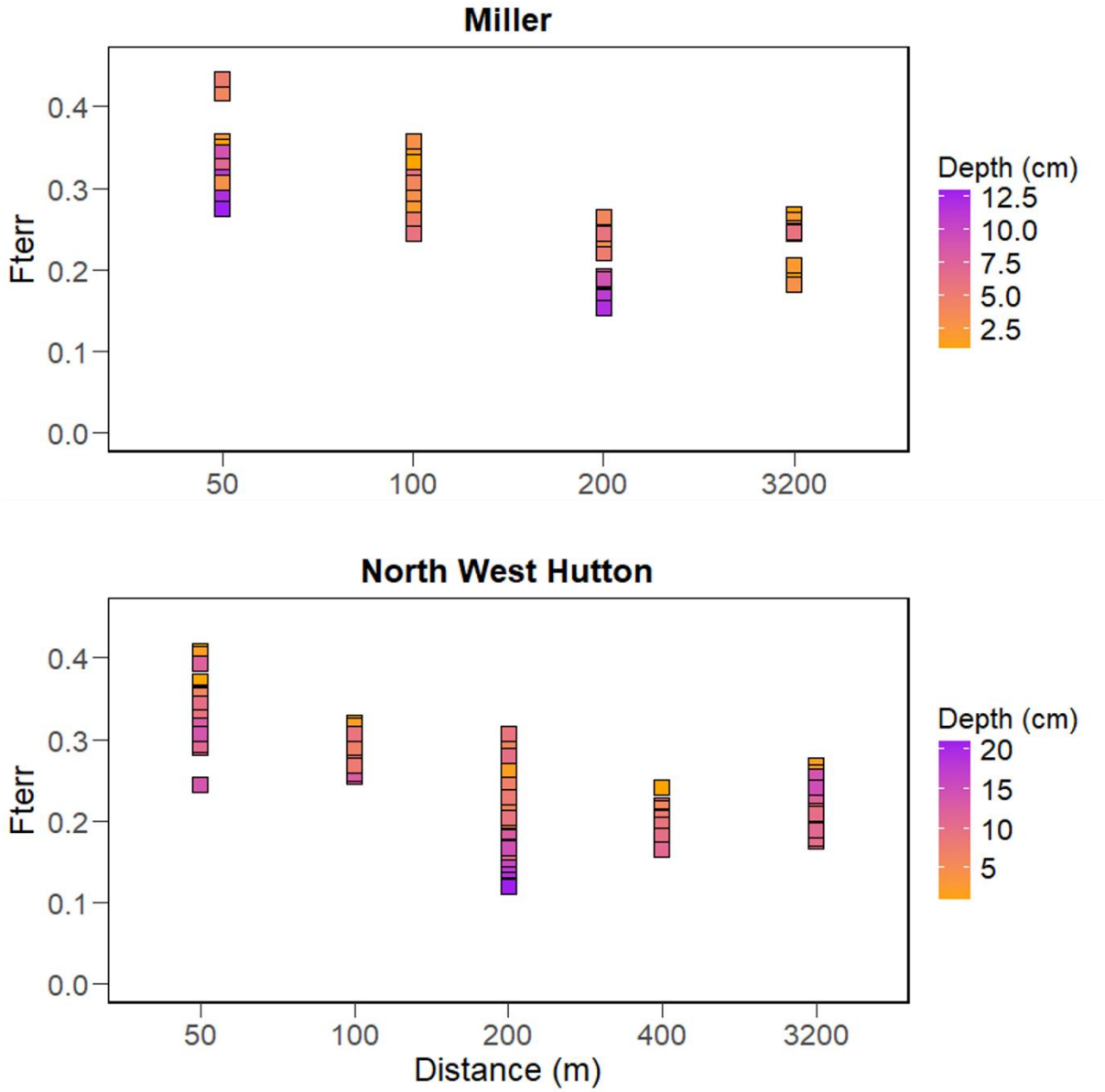

Appendix figure 8: Calculated fraction of organic carbon content from terrestrial sources (F_{terr}) from sediment cores from varying distances (m) from two decommissioned O&G platforms, Miller and North West Hutton.

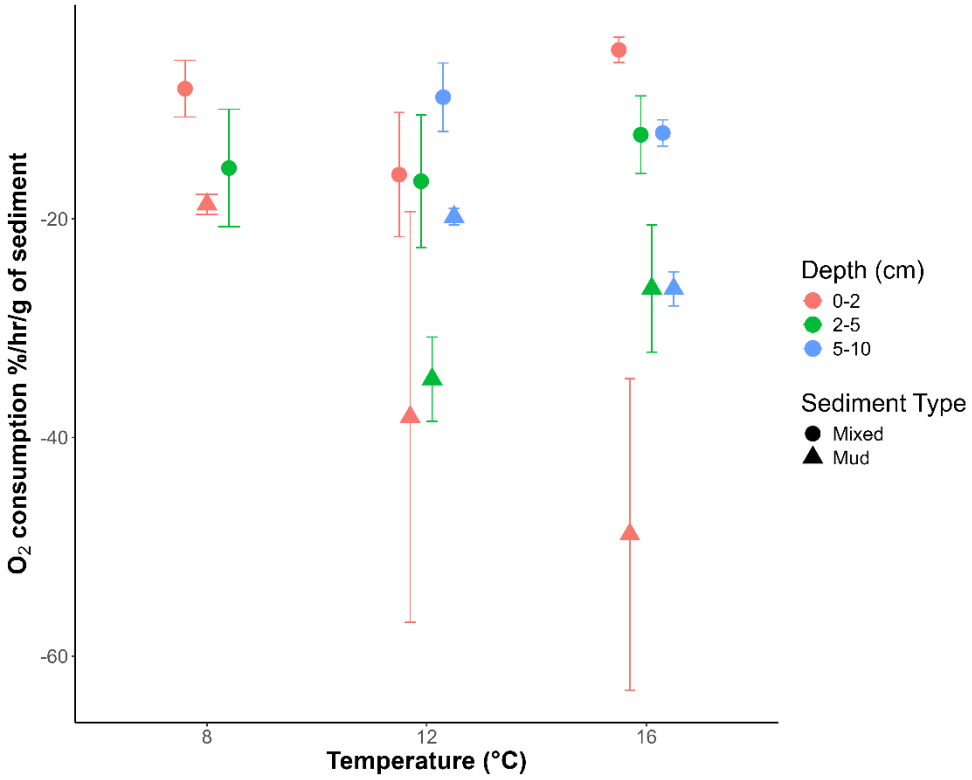

Appendix figure 9: Previous comparison of oxygen consumption rate normalised to the amount of sediment in each incubation rather than per gram of organic carbon.

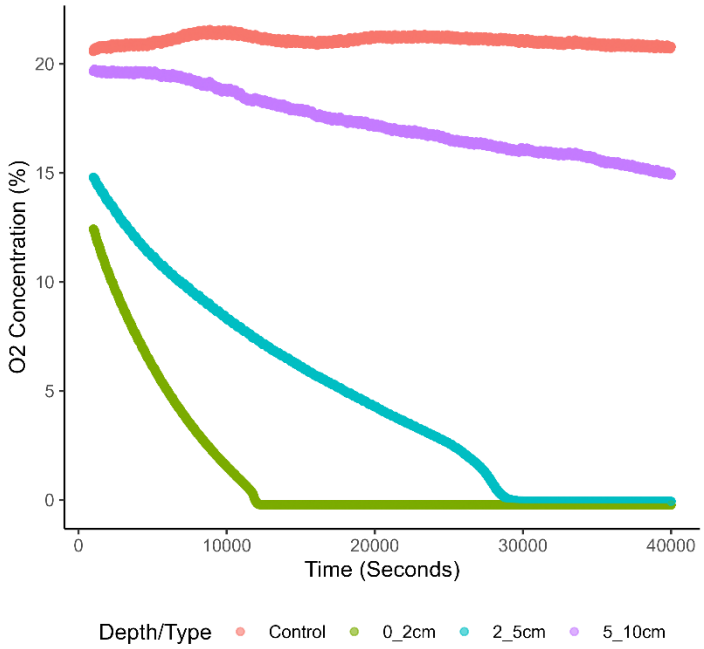

Appendix figure 10: Example of incubation where 0 – 2 cm and 2 – 5 cm sediment segments dropped to 0% oxygen consumption before window of organic carbon mineralisation.

Appendix tables

Appendix Table 1: Sampling information of sediment cores collected from the decommissioned Miller and North West Hutton platforms including, distance from site (m), direction of transect from site (North/South), core type, water depth (m), modal sediment classification and mean porosity.

Site	Distance (m)	Direction	Core Type	Depth (m)	Modal Sediment Classification	Mean Porosity
Miller	50	North	Grab	104.3	Muddy Sand	0.55
Miller	50	North	Grab	104.3	Muddy Sand	0.49
Miller	50	North	Grab	104.1	Muddy Sand	0.49
Miller	50	South	Grab	104.5	Sandy Mud	0.58
Miller	50	South	Grab	102.4	Sandy Mud	0.58
Miller	50	South	Grab	103.9	Sandy Mud	0.57
Miller	100	North	Grab	105.7	Sand	0.42
Miller	100	North	Grab	105.4	Sand	0.43
Miller	100	South	Multi corer	103.2	Sand	0.45
Miller	100	South	Multi corer	103.4	Sand	0.42
Miller	100	South	Multi corer	103.4	Sand	0.46
Miller	200	North	Grab	105.2	Sand	0.40
Miller	200	North	Grab	105.2	Sand	0.40
Miller	200	South	Multi corer	104	Sand	0.44
Miller	400	South	Multi corer	105.2	Sand	0.41
Miller	800	North	Grab	109.2	Muddy Sand	0.46
Miller	800	North	Grab	107.2	Muddy Sand	0.43
Miller	800	North	Grab	107.5	Sand	0.43
Miller	800	South	Multi corer	108.1	Sand	0.40
Miller	800	South	Multi corer	108	Sand	0.41
Miller	1600	North	Grab	108.7	Sand	0.43

Miller	1600	North	Grab	109.2	Sand	0.43
Miller	1600	South	Multi corer	110.3	Sand	0.42
Miller	1600	South	Multi corer	110.3	Muddy Sand	0.44
Miller	1600	South	Multi corer	110.3	Muddy Sand	0.43
Miller	3200	North	Grab	107.1	Sand	0.43
Miller	3200	North	Grab	106.6	Sand	0.43
Miller	3200	South	Multi corer	109.2	Sand	0.45
Hutton	50	North	Grab	104.3	Sandy Mud	0.64
Hutton	50	North	Grab	104.3	Sandy Mud	0.65
Hutton	50	North	Grab	104.1	Sandy Mud	0.67
Hutton	50	South	Multi corer	104.5	Sandy Mud	0.66
Hutton	50	South	Multi corer	102.4	Sandy Mud	0.66
Hutton	50	South	Multi corer	103.9	Sandy Mud	0.67
Hutton	100	North	Multi corer	144.5	Muddy Sand	0.60
Hutton	100	North	Multi corer	144.4	Muddy Sand	0.59
Hutton	100	North	Multi corer	144.4	Muddy Sand	0.61
Hutton	100	South	Multi corer	145.3	Muddy Sand	0.64
Hutton	100	South	Multi corer	144.8	Muddy Sand	0.65
Hutton	100	South	Multi corer	145.5	Muddy Sand	0.58
Hutton	200	North	Multi corer	145.2	Muddy Sand	0.57
Hutton	200	North	Multi corer	144.8	Muddy Sand	0.58

Hutton	200	North	Multi corer	144.7	Muddy Sand	0.57
Hutton	200	South	Multi corer	145	Muddy Sand	0.55
Hutton	200	South	Multi corer	145	Muddy Sand	0.54
Hutton	200	South	Multi corer	145.5	Muddy Sand	0.56
Hutton	400	North	Multi corer	145.9	Muddy Sand	0.53
Hutton	400	North	Multi corer	145.2	Muddy Sand	0.55
Hutton	400	North	Multi corer	145.5	Muddy Sand	0.56
Hutton	400	South	Multi corer	147	Muddy Sand	0.54
Hutton	400	South	Multi corer	144.3	Muddy Sand	0.52
Hutton	400	South	Multi corer	144.3	Muddy Sand	0.55
Hutton	800	North	Multi corer	144.8	Muddy Sand	0.54
Hutton	800	North	Multi corer	145.3	Muddy Sand	0.53
Hutton	800	North	Multi corer	145.1	Muddy Sand	0.53
Hutton	800	South	Multi corer	144.1	Muddy Sand	0.54
Hutton	800	South	Multi corer	143.8	Muddy Sand	0.51
Hutton	800	South	Multi corer	144.3	Muddy Sand	0.54
Hutton	1600	South	Multi corer	145.5	Muddy Sand	0.53
Hutton	1600	South	Multi corer	145.5	Muddy Sand	0.53
Hutton	1600	South	Multi corer	145.1	Muddy Sand	0.54

Hutton	3200	North	Multi corer	147.9	Muddy Sand	0.52
Hutton	3200	North	Multi corer	147.1	Muddy Sand	0.51
Hutton	3200	North	Multi corer	147.1	Muddy Sand	0.52
Hutton	3200	South	Multi corer	147.4	Muddy Sand	0.52
Hutton	3200	South	Multi corer	147.4	Muddy Sand	0.52
Hutton	3200	South	Multi corer	147.9	Muddy Sand	0.52

Appendix 2: Pairwise comparisons of organic carbon (OC) content between distance groups at North West Hutton and Miller decommissioned platforms. Effect size metrics include Cliff's Delta (δ), Cohen's d, and statistical power (1- β) for each comparison. Cliff's Delta values indicate the direction and magnitude of difference, where positive values reflect higher OC in the first group of the pair. Power estimates reflect the probability of detecting the observed effect given the sample sizes and $\alpha = 0.05$. Large effect sizes and high power values (≥ 0.8) indicate strong evidence for differences in OC between distance categories.

Site	Distance (G1)	Distance (G2)	Cliff's Delta	Cohen's D	Power
Miller	100	50	-0.88602	-3.82199	1
Miller	200	50	-0.92339	-4.81093	1
Miller	400	50	-0.96129	-6.97756	1
Miller	1600	50	-0.92396	-4.83141	1
Miller	3200	50	-0.93118	-5.10863	1
Miller	100	200	0.083333	0.167248	0.082571
Miller	1600	200	0.013393	0.026788	0.0508
Miller	100	400	0.56	1.351853	0.775293
Miller	200	400	0.475	1.079563	0.516051
Miller	1600	400	0.742857	2.219306	0.993159
Miller	3200	400	0.52	1.217562	0.606792
Miller	50	800	0.930876	5.095992	1
Miller	100	800	0.090476	0.181698	0.104372
Miller	200	800	$1.39e^{-17}$	$2.78e^{-17}$	0.05

Miller	400	800	-0.62857	-1.61638	0.896983
Miller	1600	800	-0.0051	-0.0102	0.050161
Miller	3200	800	-0.0619	-0.12405	0.066584
Miller	100	1600	0.078571	0.15763	0.090687
Miller	100	3200	0.115556	0.2367	0.11108
Miller	200	3200	0.05	0.100125	0.05836
Miller	1600	3200	0.057143	0.114473	0.064104
Hutton	3200	50	0.151111	0.305733	0.382608
Hutton	1600	50	0.37931	0.819892	0.947915
Hutton	400	50	-0.31525	-0.66439	0.948851
Hutton	200	50	-0.52778	-1.24273	0.999999
Hutton	100	50	-0.03631	-0.07267	0.0674
Hutton	1600	200	0.787356	2.554286	1
Hutton	100	200	0.544048	1.296811	1
Hutton	3200	400	0.374576	0.807976	0.992033
Hutton	1600	400	0.603741	1.514689	0.999998
Hutton	200	400	-0.1904	-0.38789	0.555002
Hutton	100	400	0.308717	0.649141	0.931857
Hutton	3200	800	-0.018	-0.03601	0.053988
Hutton	1600	800	0.222069	0.455512	0.486959
Hutton	400	800	-0.46373	-1.04682	0.999705
Hutton	200	800	-0.70667	-1.99751	1
Hutton	100	800	-0.20643	-0.42195	0.574815
Hutton	50	800	-0.18733	-0.38142	0.505709
Hutton	100	1600	-0.45074	-1.00988	0.991862
Hutton	1600	3200	0.283908	0.592184	0.735471
Hutton	200	3200	-0.59611	-1.48489	1
Hutton	100	3200	-0.20536	-0.41966	0.610108

Appendix material

Appendix material 1: Methods provided by Gregson et al (in prep) for GC-MS analysis for total hydrocarbon content.

Hydrocarbons were solvent extracted from 2 g of dried (20°C) and milled sediment in 10 mL of 1:1 hexane:dichloromethane (>99% HPLC Grade). Extraction occurred by vigorously shaking the sediment and solvent mixture, in new sterile borosilicate glass bottles with PTFE-lined silicon septa lids, at 2000 rpm for 16 hours on Multi-Reax desktop orbital shakers (Radleys, UK). Samples were subsequently centrifuged at 3,500 rpm for 30 minutes, filtered through a 0.20 µM PTFE syringe filter, and concentrated using nitrogen gas via a TurboVap® (Biotage, Sweden). Deuterated alkanes ($nonadecane_{d40}$ and $triacontane_{d62}$ at 10 µg ml^{-1}) and PAH ($naphthalene_{d8}$ and $anthrancene_{d10}$ at 10 µg ml^{-1}) internal standards were added to each sample and quantification was performed on an Agilent 7890A Gas Chromatography system coupled with a Triple-Axis detector, operating at 70 eV in positive ion mode, using conditions as previously described (Coulon et al., 2007). For quality control, a calibration check (10 µg ml^{-1}) and a blank were analysed every 20 samples. Quantification of alkanes and PAHs was performed using surrogate standards and five calibrations levels (range 25 – 500 ng ml^{-1}). We quantified alkanes between C_{10} and C_{40} in chain length, and the following PAHs: flourene, phenanthrene, antracene, pyrene, benz[a]anthracene, chrysene, benzo[b]fluoranthene, benzo[k]fluoranthene, benzo[a]pyrene, ideno[1,2,3-cd]pyrene, dibenz[a,h]anthracene, benzo[g,h,i]perylene.